INTERNATIONAL TELECOMMUNICATION UNION

CCIR

INTERNATIONAL
RADIO CONSULTATIVE
COMMITTEE

REPORT 322-2

CHARACTERISTICS AND APPLICATIONS OF ATMOSPHERIC RADIO NOISE DATA

Geneva, 1983

ISBN 92-61-01741-X

CONTENTS

		Page
List of symbols		1
1.	Introduction	2
2.	Radio noise predictions	2
3.	Description of the parameters used	3
4.	Methods used to obtain predictions	5
5.	The noise data or predictions	5
6.	Application of noise data to system evaluation	7
7.	The influence of the directivity and polarization of antennas	11

REPORT 322-2

CHARACTERISTICS AND APPLICATIONS OF ATMOSPHERIC RADIO NOISE DATA

(Study Programme 29B/6)

(1963-1974-1982)

LIST OF SYMBOLS

Where a symbol is shown in both lower case and capital letters, the capital letter is used to represent the equivalent, in decibels, of the quantity denoted by the lower case letter.

A Instantaneous amplitude of the noise envelope (dB)

$A_{r.m.s.}$ Root-mean-square value of the noise envelope voltage (dB)

APD Cumulative amplitude-probability distribution function of the noise envelope

b, B Effective receiver noise bandwidth (Hz) ($B = 10 \log b$)

C A protection factor (dB) necessary to provide the required carrier-to-noise ratio for a given percentage of time within the time block

C_u Protection factor (dB) required to provide the required carrier-to-noise ratio for 90% of the time block

D Deviation of an hourly value of F_a from the time block median F_{am} (dB)

D_l Value of the average noise power exceeded for 90% of the hours within a time block (dB below the median value for the time block)

D_s Value of the received signal power exceeded for 90% of the time (dB below the median value of the day-to-day variations in the hourly median)

D_u Value of the average noise power exceeded for 10% of the hours within a time block (dB above the time block median)

E_e Expected value of the signal field strength required for a given grade of service (dB(μV/m))

E_n Root-mean-square noise field strength for a 1 kHz bandwidth (dB(μV/m))

f, F Operating noise factor of a receiving system ($F = 10 \log f$)

f_a, F_a Effective antenna noise-factor which results from the external noise power available from a loss-free antenna ($F_a = 10 \log f_a$)

F_{am} Median of the hourly values of F_a within a time block

f_c Noise factor of the antenna circuit (its loss in available power)

f_{MHz} Frequency (MHz)

f_r Noise factor of the receiver

f_t Noise factor of the transmission line (its loss in available power)

k Boltzmann's constant = 1.38×10^{-23} J/K

P Received signal power available from an equivalent loss-free antenna (dB)

P_e Expected value of P

P_{me} Median value of P_e

p_n, P_n Noise power available from an equivalent loss-free antenna ($P_n = 10 \log p_n$)

p_s, P_s Received signal power required for a given signal-to-noise ratio, from a loss-free antenna ($P_s = 10 \log p_s$)

r, R Signal-to-noise power ratio required ($R = 10 \log r$)

R_h Carrier-to-noise ratio required for a given grade of service for some percentage of the hour (dB)

t Standard normal deviate

T_a Effective antenna temperature in the presence of external noise

T_0 Reference temperature, taken as 288 K

V_d Voltage deviation; the ratio (dB) of the root-mean-square to the average of the noise envelope voltage

V_{dm} Median value of V_d

Δ $A - A_{rms}$

σ_C Standard deviation of the required protection factor, C

σ_D Standard deviation of D

σ_{Dl} Standard deviation of D_l

σ_{Du} Standard deviation of D_u

σ_{Fam} Standard deviation of F_{am}

σ_P Standard deviation of estimates of the expected received signal power

σ_R Standard deviation of R

σ_T Total standard deviation; total uncertainty of P_e

σ_Δ Standard deviation of Δ

1. Introduction

The determination of the minimum signal level required for satisfactory radio reception in the absence of other unwanted radio signals necessitates a knowledge of the noise with which the wanted signal must compete. The whole problem involves a consideration of the type of modulation and the influence of the detailed characteristics of the noise on the recovery of the information contained in the transmitted signal.

There are a number of types of noise which may influence reception, although, with a particular circuit, usually only one type will predominate. Broadly, the noise can be divided into two categories depending on whether it originates in the receiving system or externally to the antenna. The internal noise is due to antenna and transmission line losses, or is generated in the receiver itself. It has the characteristics of thermal noise, and, in many cases, its effects on signal reception can be determined mathematically with a high degree of precision.

External noise can be divided into several types, each having its own characteristics. The most usual types are of atmospheric, galactic, and man-made origin. All these types are considered here, but since atmospheric noise usually predominates at frequencies below about 30 MHz, this Report deals primarily with this type and with its influence on the reception of signals.

The purpose of this Report is to present values of noise power and of other noise parameters, and to show, by example, the method of using these noise parameters and their statistical variations in the evaluation of the performance of a radio circuit. Additional examples of the use of the noise data in this Report and a summary of the effects of atmospheric radio noise (and similar forms of impulsive noise) on telecommunication systems performance is given in Spaulding [1981]. Also, recent results concerning atmospheric noise from lightning and means of developing appropriate communication systems to perform in this noise are summarized by URSI [1981], in Report 254 and in the references therein. Finally, Reports 258 and 670 give additional information concerning man-made and atmospheric noise, and Recommendation 339 gives required signal energy to noise power spectral density ratios for various systems operating in the presence of atmospheric noise.

The estimates for atmospheric noise levels given in this Report are for the average background noise level due to lightning in the absence of other signals, whether intentionally or unintentionally radiated. In addition, the noise due to local thunderstorms has not been included. In some areas of the world, the noise from local thunderstorms can be important for a significant percentage of the time. This local noise can also be significant at frequencies well above 30 MHz.

2. Radio noise predictions

This Report gives:

- predictions which take account of a major and reliable programme of noise measurements,
- statistical information on the accuracy of the predictions,
- a statistical description of the fine structure of the noise,
- methods of using the predictions in the estimation of system performance.

The data used were obtained mainly from the 16 stations shown in Fig. 1. These stations, with one exception, used standardized recording equipment, the ARN-2 Radio Noise Recorder, and were operated by a number of organizations in an international cooperative programme [URSI, 1962] (see Recommendation 174 (Warsaw, 1956)). Data collected from these stations during the period 1957 to 1961 [Crichlow *et al.*, 1959-1962] were used in the analysis.

The analysis was done, using a digital computer, by a technique which required that data from each station should be available for a number of frequencies, spread substantially over the whole range to be covered by the predictions. It was therefore not practicable to include data from other sources, where the frequency range was limited or where noise power values were not given. However, since it is desirable that the predictions finally take account of as much of the available information as possible, comparisons were made between the new predictions and data from sources not included in the analysis [Clarke, 1962; Lichter and Terina, 1960; Science Council of Japan, 1960]. Some modifications were made. The predictions should be reviewed and modified taking account of the additional data which are now available.

For these predictions, the data were grouped into four seasons of the year and six four-hour periods of the day in each season. The aggregate of corresponding four-hour periods of the day throughout a season was defined as a time block. Thus, there are in the year twenty-four time blocks, each consisting of about 360 hours (four hours in each day for about ninety days).

The division of the year into four seasons of three months each was made in the following way, although it was realized that the seasonal pattern of noise variations existing in temperate regions was not necessarily followed at lower latitudes.

Month	*Season*	
	Northern hemisphere	*Southern hemisphere*
December, January, February,	Winter	Summer
March, April, May,	Spring	Autumn
June, July, August,	Summer	Winter
September, October, November	Autumn	Spring

The main parameter presented is the median hourly value of the average noise power for each time block, and the variations in this parameter show systematic diurnal and seasonal variations of the noise. The variations of the hourly values within a time block have been treated statistically.

To facilitate the use of the noise data in this Report, a computer program is available from the CCIR Secretariat which gives a numerical representation of the noise power data contained in this Report (see Resolution 63). This is based on a numerical representation of 1 MHz atmospheric noise power contained in this Report [Zacharisen and Jones, 1970]. Maps for each hour of each month are given in terms of universal time by means of Fourier analyses performed separately of the periodic functions representing the longitudinal and diurnal variations of the original data. The dependence on frequency and the variability parameters are evaluated using the representations of Lucas and Harper [1965].

3. Description of the parameters used

It is generally agreed that no single noise parameter is a satisfactory index of interference for all types of radio service. Nevertheless it is desirable to adopt one parameter which can be used universally for comparing noise data from different sources, and to which other parameters can be related. The mean noise power seems the most generally useful and convenient for this purpose and is the basis of the predictions.

The noise power received from sources external to the antenna is conveniently expressed in terms of an effective antenna noise factor, f_a, which is defined by:

$$f_a = p_n / kT_0 b = T_a / T_0 \qquad (1)$$

where:

p_n: noise power available from an equivalent loss free antenna (W),

k: Boltzmann's constant = 1.38×10^{-23} J/K,

T_0: reference temperature, taken as 288 K,

b: effective receiver noise bandwidth (Hz),

T_a: effective antenna temperature in the presence of external noise.

Equations (1) illustrate two alternative methods of specifying the noise power, by the effective noise factor or the effective temperature of the antenna. The value of T_0 has been taken as 288 K so that 10 log kT_0 is equivalent to 204 dB below one Joule.

Both f_a and T_a are independent of bandwidth, because the available noise power from all sources may be assumed to be proportional to bandwidth, as is the reference power level.

The antenna noise factor, F_a, in decibels, in this Report is for a short vertical antenna over a perfectly conducting ground plane. Means of obtaining the appropriate antenna noise factor, F_a, for other types of antennas from the data in this Report are given in Report 670, and the references therein. This parameter is simply related to the r.m.s. noise field-strength along the antenna (a third way of specifying the noise level) by:

$$E_n = F_a - 65.5 + 20 \log f_{\text{MHz}} \qquad (2)$$

where:

E_n: r.m.s. noise field-strength for a 1 kHz bandwidth (dB(μV/m)),

F_a: noise factor for the frequency, f, in question,

f_{MHz}: frequency.

The value of the field strength for any bandwidth b Hz, other than 1 kHz, can be derived by adding (10 log b − 30) to E_n. For example, since Recommendation 339 gives required signal energy to noise power spectral density, the appropriate bandwidth there is 1 Hz. Figure 29 is a nomogram for the solution of equation (2) and may be used to derive E_n from F_a. It should be noted that E_n is the vertical component of the field at the antenna; the conformation of the incident waves may be complex, and cannot be deduced from measurements on a single vertical antenna.

Atmospheric radio noise is characterized by large, rapid fluctuations, but if the noise power is averaged over a period of several minutes, the average values are found to be nearly constant during a given hour, variations rarely exceeding ± 2 dB except near sunrise or sunset, or when there are local thunderstorms. The ARN-2 Radio Noise Recorder yields values of average power at each of eight frequencies for fifteen minutes each hour, and it is assumed that the resulting values of F_a used in the analysis were representative of the hourly values.

In predicting the expected noise level, the systematic trends, that is the trends with time of day, season, frequency, and geographical location, are taken into account explicitly. There are other variations which must be taken into account statistically. The value of F_a for a given hour of the day varies from day to day, because of random changes in thunderstorm activity and propagation conditions. The median of the hourly values within a time block (the time-block median), is designated as F_{am}. Variations of the hourly values during the time block can be represented by the values exceeded for 10% and 90% of the hours, expressed as deviations D_u and D_l from the time block median. When plotted on a normal probability graph (level in dB), the amplitude distribution of the deviations, D, above the median can be represented with reasonable accuracy by a straight line through the median and upper decile values, and a corresponding line through the median and lower decile values can be used to represent values below the median.

It is natural to expect some correlation of atmospheric radio noise with sunspot activity, since both propagation conditions and thunderstorm activity seem to be affected by the phase of the sunspot cycle. Some measurements at very low frequencies, made many years ago, did show such a correlation [Austin, 1932]. Although the data used in this revision were recorded only during a period of high sunspot activity, inspection of some data obtained over a longer period has not revealed any marked systematic variation of the noise with sunspot activity. A thorough examination of the data for such an effect, however, has not yet been made. The influence of sunspots is most likely to occur at high frequencies, but the incidence of galactic noise at times when the ionosphere fails to support the propagation of atmospheric noise tends to obscure the changes.

So far, we have dealt with the average power as represented by F_a. While this is a valuable parameter to use in determining the required signal-to-noise ratio for many types of communication circuits, other parameters give better correlation with character error-rate or message errors in some systems. For example, in determining the reliability of a radioteletype system, it is useful to have some knowledge of the amplitude-probability distribution (*APD*) of the noise. This shows the percentage time (time of occupation) for which any level is exceeded; usually it is the noise envelope which is so described. The *APD* is dependent upon the short-term characteristics of the noise, and, therefore, cannot be deduced from the hourly values of F_a alone.

A large number of *APD*'s have been measured in several countries, and reasonably consistent results have been obtained [URSI, 1962; Clarke, 1962; Science Council of Japan, 1960]. For presenting the data in an operationally useful form, it is convenient to construct a family of idealized curves, one of which can be chosen to represent a practical *APD* to a sufficient accuracy. This has been done by using a system of coordinates in which a Rayleigh distribution (representing the envelope of thermal-type noise), is a straight line with a slope of -0.5. The low amplitude parts of an atmospheric noise curve have this slope, the high amplitude parts are represented by a second straight line, with a greater slope, and the two lines are joined by an arc of a circle. The construction of these curves involved the use of quantities related to the r.m.s., average, and mean logarithmic values of the distribution, parameters which have been recorded in routine noise measurements [Crichlow *et al.*, 1960a, 1960b]. In practice, because the average voltage and mean logarithmic voltage are found to be closely correlated, the ratio of r.m.s. to average voltage, V_d (dB) is sufficient to specify the curve which can be used to represent the distribution [Spaulding *et al.*, 1962]. Some of the curves are reproduced in Fig. 27 in which are plotted the differences, Δ, between the instantaneous envelope amplitude, A, for any probability, and the r.m.s. value of A, $A_{r.m.s.}$, for a number of values of V_d, all quantities being in decibels. Data for intermediate values of V_d can be derived by interpolation. It should be noted that, if the r.m.s. value of the noise voltage itself is required, it is 3 dB lower than the r.m.s. envelope voltage. The curves can be used for a wide range of bandwidths, the effect of changing the bandwidth being to change the value of V_d and modify the *APD* correspondingly.

Estimates have also been made of the uncertainties in the derived *APD* curves. They are expressed as a standard deviation, σ_Δ, of the difference, Δ, as a function of probability and V_d (see § 5 and Fig. 28).

4. Methods used to obtain predictions

Values of F_{am}, collected from the network of stations previously mentioned, were edited to remove, as far as possible, the effects of man-made radio noise and unwanted signals. The values thus obtained were considered to represent actual atmospheric radio noise. The time block values at each frequency were compared with the predicted values from Report 65 (Los Angeles, 1959) and corrections derived. These were used in an electronic computer program to modify the world charts and frequency curves given in Report 65 (Los Angeles, 1959).

Computer techniques were also used to obtain a best estimate of the deviations, D_u and D_l, of the decile values of F_a from the median value F_{am}, for each time block. In a similar manner the median value, V_{dm}, of the voltage deviation, V_d, was obtained for each time block.

To obtain a measure of the variability of the noise with respect to the predicted values in each time block, all measured values were compared with the new predicted values. Standard deviations of F_{am}, D_u, and D_l, as functions of frequency, were found by a computer program. Uncertainties in the predicted amplitude-probability distributions were expressed in terms of σ_Δ, from a consideration of the variability of V_d. The results were determined for various values of V_d as a function of the percentage time of occupation.

5. The noise data or predictions

World charts, showing the expected median values of background atmospheric radio noise, F_{am} in dB above kT_0b, at 1 MHz for each time block, in local time, are shown in Figs. 2 to 25. Unlike the earlier Report, where only two sets of frequency curves were shown, one for day-time propagation conditions and one for night-time, a set of frequency curves is now given for each time block. This procedure is more flexible and is compatible with a more convenient arrangement, in which the noise grade charts for a given seasonal time block and the corresponding frequency curves are adjacent.

Galactic noise levels, extrapolated to 1 MHz from Cottony and Johler [1952] and verified using a vertical antenna, are shown on the frequency curves. Within a $\pm$ 2 dB temporal variation (neglecting ionospheric shielding), the values shown will be the upper limit of galactic noise, but in any given situation the received noise should be calculated considering critical frequencies and the directional properties of the antenna.

In many locations, man-made noise is a limiting factor in radiocommunication for at least part of the time. Although this type of noise depends on local conditions, a curve of expected values at a quiet receiving location has been added. The values plotted are the lowest of the man-made noise values recorded at sites chosen to ensure a minimum amount of man-made noise and lower values will seldom be found anywhere on the Earth's surface. Man-made noise levels, in terms of F_a, and their variations for various environmental categories (business, residential, rural and quiet rural, etc.) are given in Report 258. The noise levels for "quiet rural" locations given in Report 258 are taken from this Report. Additional information concerning man-made noise is summarized in Hagn [1981].

It will be observed that values of noise at 1 MHz are indicated which are below the expected levels of man-made and galactic noise. These values should be used with caution, as they represent only rough estimates of what atmospheric noise would be recorded if other types were not present. They are useful mainly as reference levels for low-noise locations, a 1 MHz noise value being assigned by plotting data at other frequencies on the noise curve.

Also included on the same set of figures are the estimated values of D_u, D_l, V_d, σ_{Fam}, σ_{Du} and σ_{Dl}. Thus, all values relating to one time block are to be found together. D_u will normally be used for assessing minimum required signal-strengths, but D_l may be needed to determine whether the internal noise of a receiving system is negligible under the quieter external noise conditions.

The values of σ_{Fam} have been derived by comparing actual observations with predictions for the same locations, and include such uncertainties as those due to the unpredictable variations from year to year and the errors introduced by the necessity of presenting a large volume of data in summarized and homogeneous form. Larger values may be expected at locations where no measurements have been made since there is an additional uncertainty in the process of geographical interpolation, but this cannot be assessed.

The curves of σ_{Fam} will be seen to extend only up to 10 MHz. At higher frequencies the predominant noise at many stations was often of galactic origin, and it was not considered practicable to try to derive estimates of the variability of the atmospheric noise alone.

Separate curves for D_u and σ_{Du} were derived using data from stations in temperate and tropical zones as defined in Nos. 406 to 411 of the Radio Regulations, Geneva, 1979. However, the variability of noise did not show a consistent pattern conforming with the defined zones, and, in consequence, the data from both zones were combined to obtain the curves used in this Report. The results of some work in India suggest that simplification of presentation may be possible. Further work may show that the variability is linked to some function of the noise intensity rather than geographical zones, though smaller variations would be expected over the oceans rather than at places near the main thunderstorm centres. The curves presented should be used with some caution, particularly during times of the day from 0800 to 1600 where the low values in the medium frequency range are known to have been influenced by man-made noise at most stations. No editing to minimize the effects of man-made noise was done in studying the variability, as was done with the values of F_{am}.

The figures are used in the following way. The value of F_{am} for 1 MHz is found directly from the noise charts for the time block (season and hour) under consideration. Using this value as the noise grade, the value of F_{am} for the required frequency is determined from the frequency curves. σ_{Fam}, D_u, and σ_{Du} are obtained for the required frequency from the variability curves. If the value of $D\ (= F_a - F_{am})$, or the value of σ_D is required for any percentage of time other than 10%, the values can be found by plotting D_u and σ_{Du} on a normal probability graph (with values in dB), and drawing straight lines through 0 dB at 50% and the 10% value as shown in Fig. 30. Values at percentages greater than 50% can be obtained in the same manner using D_l and σ_{Dl}.

The same cautionary note applies to the use of the curves of V_{dm} as mentioned in the discussion of D_u and σ_{Du}. The plotted values of V_{dm} are for a bandwidth of 200 Hz. Since V_d is not independent of the bandwidth as are F_a, D_u, and D_l, a method has been developed for converting a value of V_d, measured in one bandwidth, to the value that would have been measured in another [Spaulding *et al.*, 1962]. This conversion can be made by using the curves of Fig. 26, in which V_{dn} and V_{dw} are the values of V_d corresponding to the narrower bandwidth, b_n, and wider bandwidth, b_w, respectively. The corresponding values of V_{dn} and V_{dw} are read at the intersection of the lines defined by the bandwidth ratio, b_w/b_n, and the known value of V_d. The results given in Fig. 26 are based on ideal assumptions concerning filter impulse responses. Measurements have indicated that Fig. 26 gives the proper bandwidth conversion of V_d only for bandwidth ratios of the order of 20 or less and generally predicts too high a value of V_d for larger bandwidth ratios. Therefore, Fig. 26 should be used with caution for large bandwidth ratios.

APD curves corresponding to various values of V_d, are given in Fig. 27, in which the r.m.s. envelope voltage, $A_{r.m.s.}$, is taken as the reference. The measured values of V_d vary about the predicted median values. These variations are reflected in uncertainties in the precise shape of the *APD* curve, and these are shown in Fig. 28 in terms of the standard deviation, σ_Δ, of the amplitude deviations, Δ, corresponding to each percentage of time. Since each *APD* curve is specified relative to $A_{r.m.s.}$, the uncertainties in Δ near this value are small. Much larger values of σ_Δ occur at higher and lower percentages, with a constant value of σ_Δ over the Rayleigh portion of the curve. There will also be variations in the shape of actual *APD*'s for the same value of V_d; neglect of these is believed not to lead to appreciable errors. The validity of the idealized *APD* curves, in representing the actual distributions, and the way in which they vary with V_d and with bandwidth, have so far only been checked against limited data, and further verification is required. For the moment, therefore, the curves and bandwidth conversion factors should be used with caution.

6. Application of noise data to system evaluation

The treatment here is not intended to be comprehensive, since the subject, in its broad aspects, clearly involves many factors other than the atmospheric radio noise. However, it is considered desirable to give some indication of how the data may be used in the study of system performance. Additional examples and information are given in Spaulding [1981] and the references therein.

The assessment of the performance of a complete receiving system can be expressed in terms of its operating noise factor, f, which takes into account the external noise as well as noise generated within the receiving system. The factors involved and the techniques of evaluation are given in [Barsis *et al.*, 1961]. If it is assumed that the receiver is free from spurious responses and that all elements prior to the receiver are at the reference temperature T_0, then f is given by:

$$f = f_a - 1 + f_c f_t f_r \tag{3}$$

where:

f_c: the noise factor of the antenna circuit (its loss in available power);

f_t: the noise factor of the transmission line (its loss in available power);

f_r: the noise factor of the receiver.

The operating noise factor, f, is useful in determining the relation between the signal power, p_s, available from a loss-free antenna and the corresponding signal-to-noise ratio, r, at the intermediate frequency output of the receiver, since

$$p_s = f r k T_0 b \tag{4}$$

Putting $B = 10 \log b$, then P_s (dBW) becomes:

$$P_s = R + F + B - 204 \qquad \text{dBW} \tag{5}$$

In evaluating the operating noise factor, F, for use in equation (5), it is necessary to consider all of the parameters in equation (3). However, in many cases, one source of noise will predominate, and only one of the component noise factors will be important. At low frequencies, a receiving system with poor internal noise characteristics may often be used, since the values of f_a will be high, and will determine the value of f. In general, f_a will decrease with increasing frequency, and, at the higher frequencies, the antenna tends to become more efficient and f_c approaches unity. Under these conditions, f_t and/or f_r may become as important as f_a in the determination of f. The values of f_t and f_r can then be determined from calculations involving the design features of the transmission line and the receiver, or by direct measurement. When the antenna losses may be important, such as at the lower frequencies when a short vertical antenna near the ground is used, f_c must be obtained by indirect means. Frequently, an adequate estimation of these losses can be made from impedance measurements and the calculated value of the radiation resistance [Crichlow *et al.*, 1955].

Once the noise characteristics have been determined, the interfering effects to a given system must be deduced. In the past, the performance of a given type of service has been expressed in terms of the ratio of the required signal to a particular parameter of the noise, usually the mean noise power. For many types of service, use of the *APD*, involving more than one parameter and embodying information on the type of noise as well as the level, can result in more realistic estimates of the probable performance of the system, once the appropriate relationships have been established. The availability of information on the variations to be expected in the noise level also enables the probability of obtaining a required performance to be specified in more precise statistical terms.

It is convenient to define system performance statistically in terms of three independent component parts; grade of service, time availability, and service probability [Barsis *et al.*, 1961].

6.1 *Grade of service* refers to the degree of reliability over a short period of time (which is usually taken as one hour, but which may vary from a few minutes to more than an hour), during which the statistics of the signal-to-noise ratio may be considered to be stationary. It can be expressed, for example, as the percentage of error-free messages, the intelligibility achieved, or the percentage of satisfied observers.

6.2 *Time availability* refers to the percentage of the hours, or other short periods of time used in defining the grade of service, during which the specified grade of service or better is achieved. The time involved should include all of the expected variations and may be an entire sunspot cycle, a year, a particular season or month, or certain hours of the day during a specified longer period.

6.3 *Service probability* is defined as the probability that the specified grade of service or better will be achieved for the specified time availability. This combines statistically the uncertainties of the many parameters involved in the prediction of system performance.

When the desired performance of a system has been defined, it is necessary to evaluate the various factors affecting this performance. For the sake of clarity and simplicity, the performance will, in the following two examples, be evaluated in terms of the characteristics of the available signal and noise at the terminals of the equivalent loss-free receiving antenna. In both examples it has been assumed that a short vertical rod antenna is used and that the predominant noise is external to the antenna and of atmospheric origin. The seasons and time of day have been chosen so that the noise levels are at a maximum. In the first example, ground-wave propagation has been assumed, so that the signal level is steady and only the noise is variable. The calculations are based on the use of the *APD*, since the type of service is one for which the errors are amenable to reasonably precise mathematical evaluation, when the short term characteristics of the noise are known. The second example involves sky-wave propagation and thus both the signal and noise vary with time. The recommended values of signal-to-noise power ratios given in Recommendation 339, are introduced in this example. This is the procedure which must be followed for a large number of services, and particularly those involving subjective factors.

The determination of the service probability involves not only the uncertainties associated with the noise parameters but also the uncertainties of all values involved in the prediction process. Probably the most important of these are related to the prediction of the received signal and the required signal-to-noise ratio. Since the following examples are intended to show methods for using the noise information, values of σ for these other parameters are assumed values. While probably representative of the magnitude of the values of σ to be encountered, they should not be used unless it is impossible to obtain a better estimate. The determination of actual values to be used for any given circuit can usually be made by the use of information furnished by the CCIR in other publications.

6.4 *Example I*

Determine the performance of an FSK system with reception at Geneva, Switzerland, under the following conditions:

Frequency:	50 kHz
Time of day:	2000-2400 hours
Season:	summer
Bandwidth:	100 Hz
Propagation:	ground wave (resulting in a steady received signal)
Grade of service:	0.05% binary errors are permissible during a given hour. This corresponds approximately to 1% teletype errors in a five unit start-stop system [Watt *et al.*, 1958].

The problem is to assess the probability that a given received signal-power will provide the specified grade of service for any given percentage of the hours.

The expected value of received power, P_e, required for a particular grade of service during an hour when the antenna noise factor is F_a, is from equation (5),

$$P_e = F_a + R + B - 204 \qquad \text{dBW} \tag{6}$$

where R is the required pre-detection signal-to-noise power ratio (dB) for the given bandwidth.

When the receiving antenna is a short vertical rod, the corresponding field strength, E_e, is given by:

$$E_e = P_e + 20 \log f_{\text{MHz}} + 108.5 \qquad \text{dB}(\mu\text{V/m}) \tag{7}$$

Montgomery [1954] has shown that the probability of a binary error in a narrow-band frequency-modulation system is equal to one-half the probability that the noise envelope exceeds the carrier envelope at any instant. It is, therefore, necessary to determine the noise *APD* to determine the required signal-to-noise ratio. From Fig. 19 the value of V_{dm} at 50 kHz for 2000 to 2400 hours in the summer season is 8.5 dB for a bandwidth of 200 Hz. Converting to a bandwidth of 100 Hz by means of Fig. 26, V_{dm} becomes 6.4 dB. The corresponding *APD* can be plotted on Fig. 27 by connecting the ends of the curve $V_{dm} = 6$ and the curve $V_{dm} = 8$ to the corresponding crossing points on the ordinate and interpolating between the two lines at the proper percentage.

Using the criterion postulated by Montgomery, the required grade of service, with 0.05% binary errors, demands that the noise envelope will exceed the carrier envelope for only 0.1% of the time, and with the *APD* corresponding to $V_{dm} = 6.4$ dB, the carrier envelope must be 21.0 dB above $A_{r.m.s.}$ (from Fig. 27). The carrier power to mean noise-power ratio must therefore also be 21.0 dB, and this is the value to be taken for R in equation (6). The uncertainty in this value introduced by possible variations in the shape of the amplitude-probability distribution is 1.4 dB (from Fig. 28).

F_a must now be derived from the median value F_{am} plus a deviation D consistent with the percentage of hours during which a satisfactory service must be obtained. From Fig. 19, the 1 MHz value (noise grade) is 78 dB and the value of F_{am} at 50 kHz is 135 dB with a standard deviation, σ_{Fam}, of 3.4 dB. To allow for uncertainties in the value of the noise level, F_a, in a given hour, probability is required that a given deviation, $D = F_a - F_{am}$, will occur. The value of D_u (6.4 dB) is derived from Fig. 19c and from this, values of D are plotted on normal probability paper as in Fig. 30, it being assumed that the distribution of the decibel values above the median is normal. In a similar way σ_{Du} (1.9 dB) is derived from Fig. 19c and a curve for σ_D plotted in Fig. 30.

Equation (6) is next evaluated, by taking the percentage time availability as 100 minus the percentage time that D is exceeded, and P_e is plotted in Fig. 31. If required, the corresponding value of E_e can be derived from equation (7). From equation (6), $P_e = D - 30$ and this is the usual prediction of the power required to produce the specified grade of service as a function of time availability. But, since the prediction uncertainties have not been taken into account, only one-half of such circuits would be expected to meet the design criteria.

The uncertainties to consider are represented by the following standard deviations:

σ_P: the standard error of achieving the expected received signal power. This must be derived from propagation and other data and, for the purposes of this example, is assumed to be 2 dB;

σ_R: uncertainty in the required signal-to-noise ratio, standard deviation assumed to be 2 dB;

σ_Δ: 1.4 dB (from Fig. 28);

σ_{Fam}: 3.4 dB (from Fig. 19);

σ_D: standard deviation of D, which is a function of the required percentage time of operation (from Fig. 30).

The total uncertainty σ_T is deduced, on the assumption that the errors are uncorrelated, from:

$$\sigma_T^2 = \sigma_P^2 + \sigma_R^2 + \sigma_\Delta^2 + \sigma_{Fam}^2 + \sigma_D^2 \qquad (8)$$

σ_T has also been plotted in Fig. 31 and enables an estimate to be made of the service probability that the indicated time availability will be achieved, as follows.

For any given value of received power, P, the time availability can be determined as a function of the service probability from:

$$t = (P - P_e)/\sigma_T \qquad (9)$$

where t is a function (known as the standard normal deviate) of the service probability. Figure 32 gives the values of t as a function of service probability.

If a probability of only 0.5 is required that a specified time availability will be achieved, $t = 0$, $P = P_e$ and the required powers are given by Fig. 31; a power of -20 dBW would, for example, give a time availability of 94.6%. This situation is also represented by the point corresponding to 0.5 service probability on the curve $P = -20$ dBW plotted on Fig. 33. A higher time availability, say 99%, requires a higher value of P_e (-16.5 dBW with a standard deviation of 5.7 dB). With the same actual power of -20 dBW, the value of t is then -0.61 leading to a lower service probability of 0.27. In this way the relationship between the time availability and service probability can be plotted for $P = -20$ dBW, and for other power levels, as in Fig. 33.

From this figure, it can be seen that if P is taken as -30 dBW and a time availability of 99% is desired, there is a probability of less than 0.009 that the objective of less than 1% teletype errors will be achieved during 99% of the hours of operation. However, if $P = -10$ dBW, the probability would increase to better than 0.87. With $P = 0$ dBW, the chance of failing to achieve the required grade of service during 99% of the hours would be less than 0.002.

6.5 *Example II*

Determine the performance of an A3EJN telephony double-sideband system with reception at Geneva, Switzerland, under the following conditions:

Frequency:	5 MHz
Time of day :	2000-2400 hours
Season:	summer
Bandwidth:	6 kHz
Propagation:	ionospheric (resulting in a fading signal)
Grade of service:	marginally commercial for 95% of the hour.

Again the problem is to assess the probability that a given received signal power will provide the specified grade of service or better for any given percentage of the hours.

Equation (6) is not directly applicable here, since both the signal and the noise vary with time, and this must be taken into account. The value of R used in equation (6) is established for a given grade of service for steady-state signal conditions. Since the signal will vary within the hour due to interference fading, which can be represented by a Rayleigh distribution (Report 266), we can let R_h be the carrier-to-noise ratio required for the given grade of service for some percentage of the hour.

It has been found that the day-to-day variations of the hourly median received signal in dB are normally distributed (Report 266), and thus can be described by the median value and the deviation D_s, of the value exceeded 90% of the time, from the median. Since the values of F_a can also be considered to approximate to a normal distribution, a protection factor, C_u (dB), necessary to provide the required carrier-to-noise ratio for 90% of the time block, can be determined, assuming no correlation, from:

$$C_u^2 = D_u^2 + D_s^2 \tag{10}$$

By plotting C_u at the 10% point relative to 0 dB at the median value, using arithmetic probability coordinates, a value of C for any other percentage point can be found, since it will also have a normal distribution. With the values of R_h and C defined above, the equivalent of equation (6) can now be written as:

$$P_{me} = F_{am} + C + R_h + B - 204 \qquad \text{dBW} \tag{11}$$

where P_{me} is the median value of the expected required signal power.

From Fig. 19, the 1 MHz value (noise grade) for Geneva, Switzerland, is found to be 78, and the value of F_{am} at 5 MHz is 57 dB with a standard deviation, σ_{Fam}, of 4.1 dB. Also from Fig. 19, D_u is found to be 4.9 dB at 5 MHz, and the associated standard deviation, σ_{Du}, is 1.3 dB. Assuming values of D_s of 7 dB and σ_{Ds} of 1.5 dB, which are in fair agreement with values given in Report 266, the value of C_u can be found from equation (10) to be 8.54 dB. Also, a corresponding value of the standard deviation, σ_{Cu}, of C_u can be found, in a like manner, to be equal to 1.98 dB. Values of C and σ_C have been plotted on Fig. 34.

Recommended values of signal-to-noise ratios for steady signals are given for various services in Recommendation 339. The required peak radio-frequency signal-to-noise ratio in a 6 kHz bandwidth for double-sideband, marginally commercial A3EJN telephony is 27 dB for a steady signal, or 21 dB carrier-to-noise ratio. Since we are interested in the signal level exceeded 95% of the time for Rayleigh fading, then R_h must be 11.3 dB greater than for the steady signal, or 32.3 dB.

Equation (11) has been evaluated by taking the percentage time availability as 100 minus the percentage time that C is exceeded, and P_{me} is plotted on Fig. 35. E_c can be deduced from equation (7). As in Example I, P_c is

the expected power required to produce the specified grade of service as a function of time availability. Also, as in Example I, it is necessary to consider various prediction uncertainties. The total uncertainty, σ_T, is deduced, as before, on the assumption that the errors are uncorrelated, from:

$$\sigma_T^2 = \sigma_P^2 + \sigma_R^2 + \sigma_{Fam}^2 + \sigma_C^2 \qquad (12)$$

where:

σ_P: the standard deviation of estimates of the expected received signal power, assumed to be 5 dB;

σ_R: uncertainty in the required signal-to-noise ratio, the standard deviation assumed to be 2 dB;

σ_{Fam}: standard deviation of F_{am} about its predicted value, 4.1 dB (from Fig. 19);

σ_C: standard deviation of C, which is a function of the required percentage of time of operation (from Fig. 34).

The values of σ_T have also been plotted in Fig. 35.

Again, using equation (9), Fig. 32, and the values of σ_T from Fig. 35, Fig. 36 can be obtained.

7. The influence of the directivity and polarization of antennas

All the noise information presented in this Report, including the examples given in the last section, relates to a short vertical receiving antenna. Although such an antenna may be used in practice at low frequencies, long-distance communication at high frequencies is normally achieved by the use of a highly-directional antenna. Some allowance must therefore be made for the effects of directivity and polarization on the signal-to-noise ratio.

It is assumed that the signal gain is reasonably well-known, although it is dependent on the relative importance of the various propagation modes, which varies with time. The effective noise factor of the antenna, insofar as it is determined by atmospheric noise, may be influenced in several ways. If the noise sources were distributed isotropically, the noise factor would be independent of the directional properties. In practice, however, the azimuthal direction of the beam may coincide with the direction of an area where thunderstorms are prevalent, and the noise factor will be increased correspondingly, compared with the omnidirectional antenna. On the other hand, the converse may be true. The directivity in the vertical plane may be such as to differentiate in favour of, or against, the reception of noise from a strong source. The movement of storms in and out of the antenna beam may be expected to increase the variability of the noise, even if the average intensity is unchanged.

Experimental information on the effects of directivity is scarce, and in some respects conflicting. In an equatorial region (Singapore), the median value of F_a for certain directional antennas was found to be somewhat higher (about 4 dB on the average), than that for a vertical rod antenna over the same period. This figure is considerably lower than the maximum possible antenna gain, as would be expected from the widespread nature of the storms, but the fact that there was, on the average, some gain in noise in a wide range of storm conditions suggests that there was a tendency for the noise to be received more from the lower angles of elevation. In the Federal Republic of Germany also, directional antennas had, on the average, higher noise factors [Kronjäger and Vogt, 1959]. On the other hand, in experiments in Australia, the average noise factors of several antennas, beamed in different directions, were a few decibels lower than that of a vertical rod antenna, the interpretation being that there was significant noise incident at high angles. It appears therefore that, in general terms, the gain in signal-to-noise ratio is likely to be approximately that in the signal alone (which may, however, be less than the optimum gain), and that if more precise figures are needed, it is necessary to take into account the storm locations and the critical frequencies of the ionosphere in addition to the antenna polar diagram. More investigations are required before the allowances can be made reasonably precise, but it appears that the differences will usually be less than 6 dB.

Even less information is available on the effects of antenna polarization, but for a first approximation, it may be assumed that the received noise would be comparable with either polarization, provided the antenna height is large compared with the wavelength.

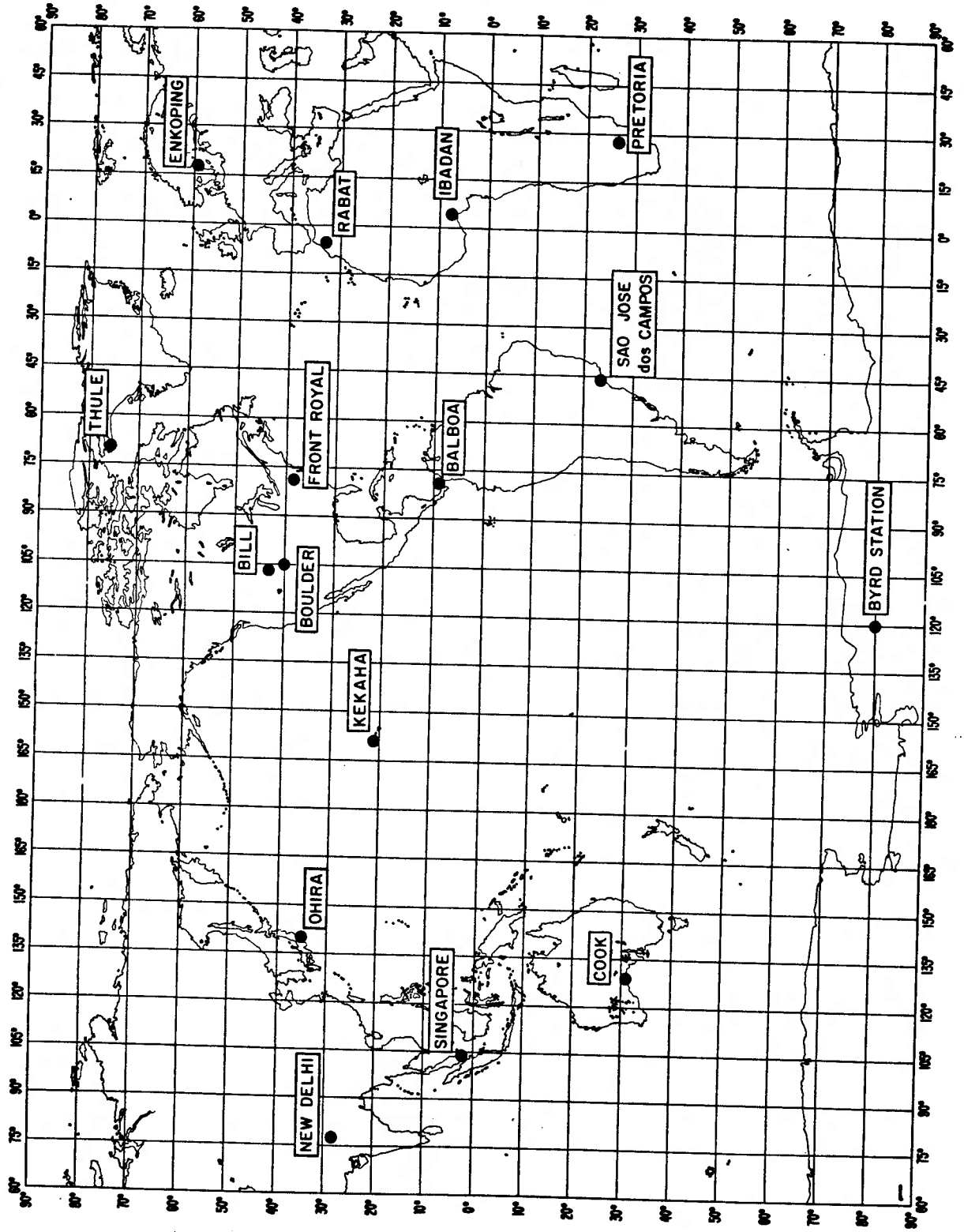

FIGURE 1 – *Stations which provided radio noise data*

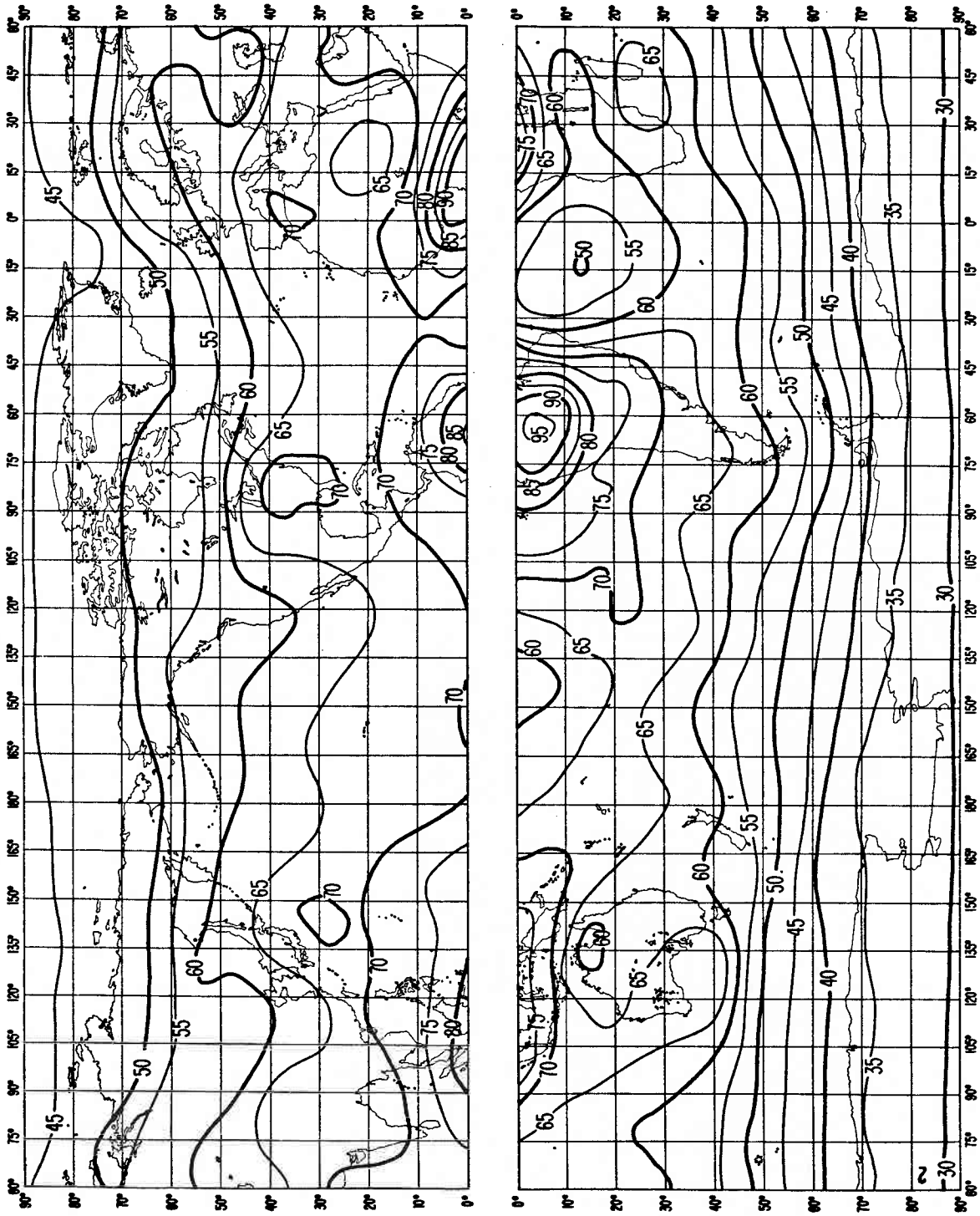

FIGURE 2a – *Expected values of atmospheric radio noise, F_{am} (dB above kT_0b at 1 MHz)*
(Winter; 0000-0400 h)

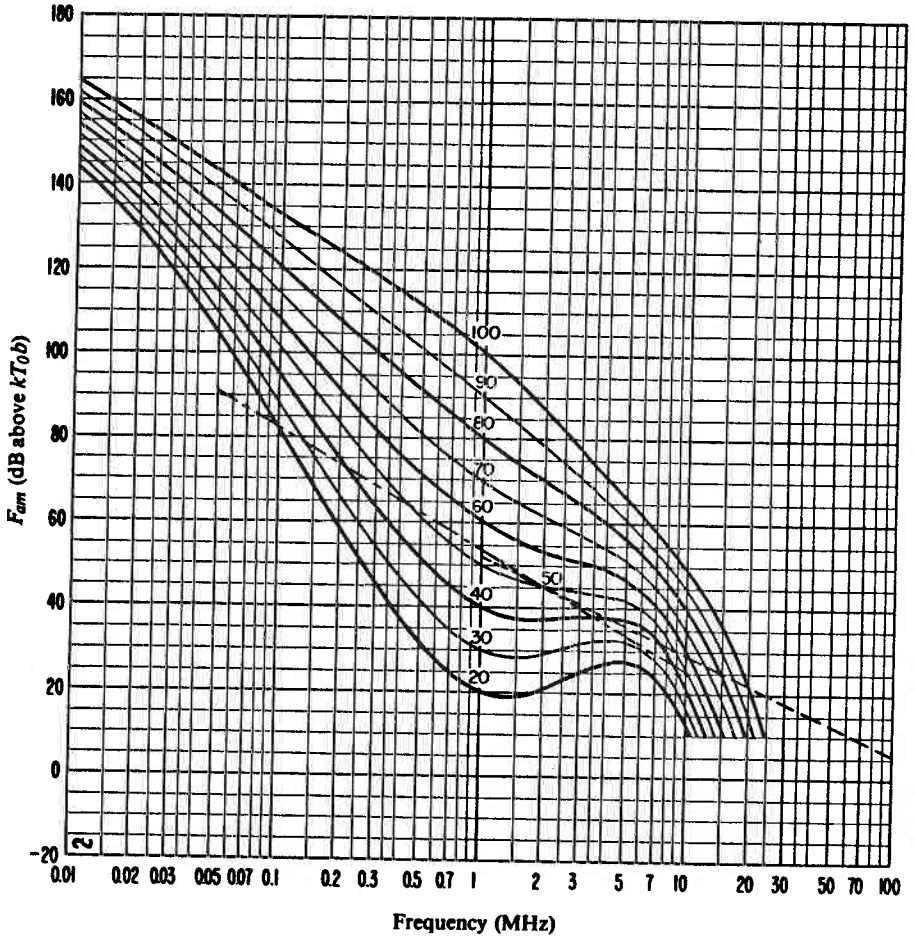

FIGURE 2b – *Variation of radio noise with frequency (Winter; 0000-0400 h)*

——— Expected values of atmospheric noise

— · — · — · — Expected values of man-made noise at a quiet receiving location

— — — — — Expected values of galactic noise

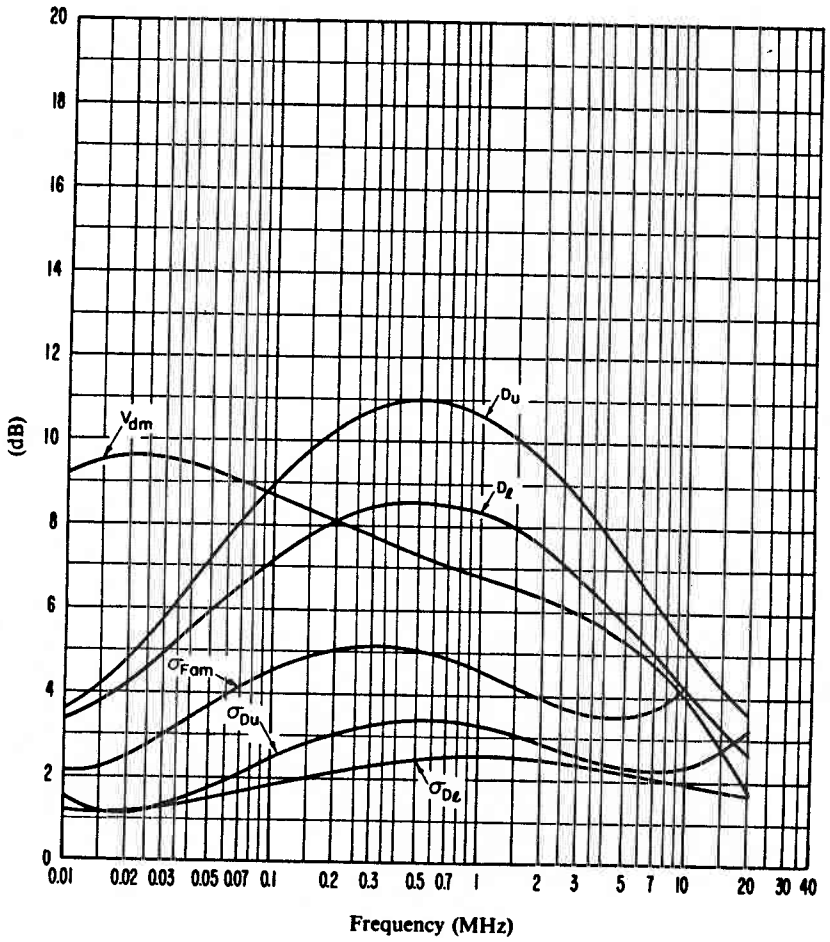

FIGURE 2c – *Data on noise variability and character (Winter; 0000-0400 h)*

σ_{Fam} : Standard deviation of values of F_{am}
D_u : Ratio of upper decile to median value, F_{am}
σ_{Du} : Standard deviation of values of D_u
D_l : Ratio of median value, F_{am}, to lower decile
σ_{Dl} : Standard deviation of value of D_l
V_{dm} : Expected value of median deviation of average voltage. The values shown are for a bandwidth of 200 Hz.

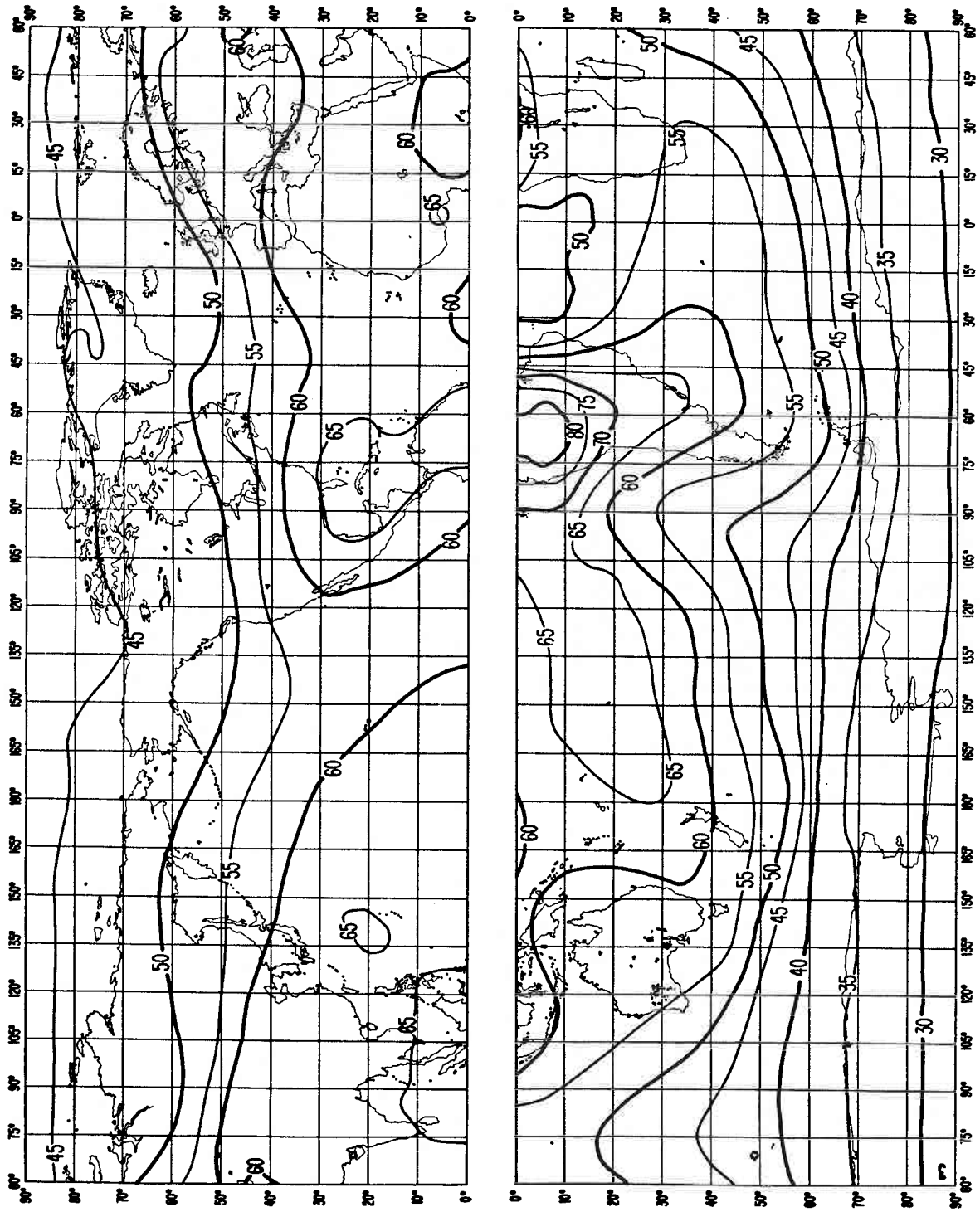

FIGURE 3a – *Expected values of atmospheric radio noise, F_{am} (dB above kT_0b at 1 MHz)*
(Winter; 0400-0800 h)

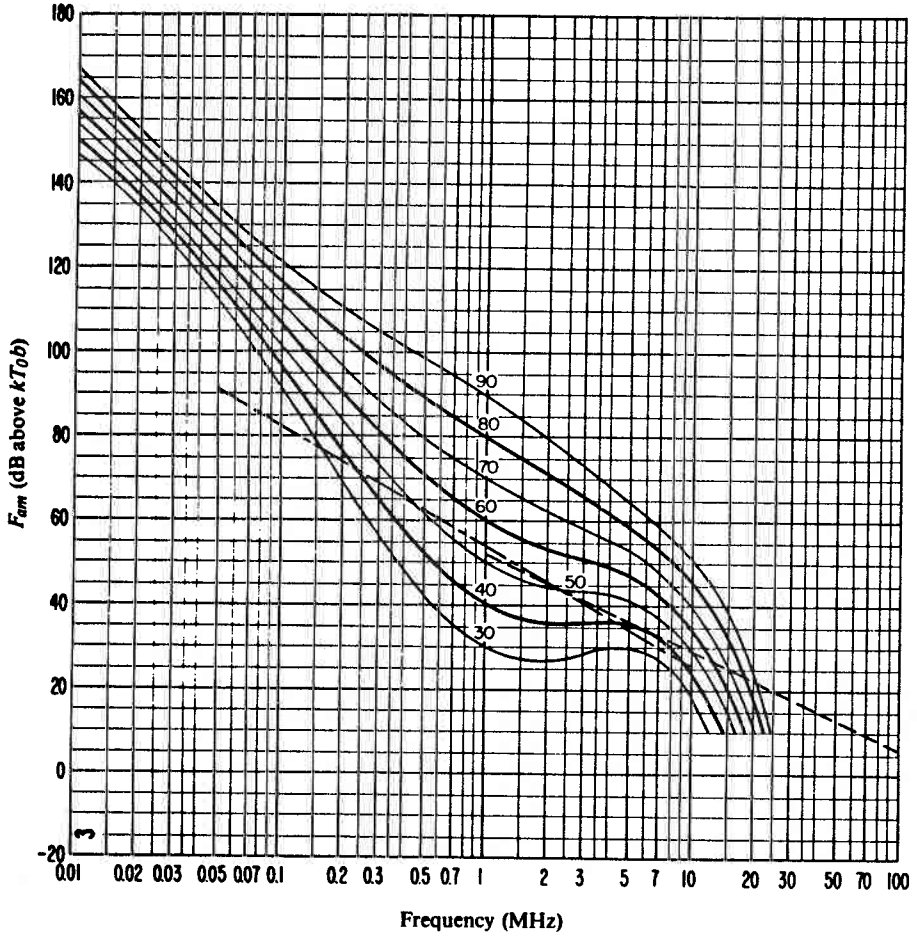

FIGURE 3b – *Variation of radio noise with frequency (Winter; 0400-0800 h)*

——— Expected values of atmospheric noise

— · — · — · — Expected values of man-made noise at a quiet receiving location

— — — — — Expected values of galactic noise

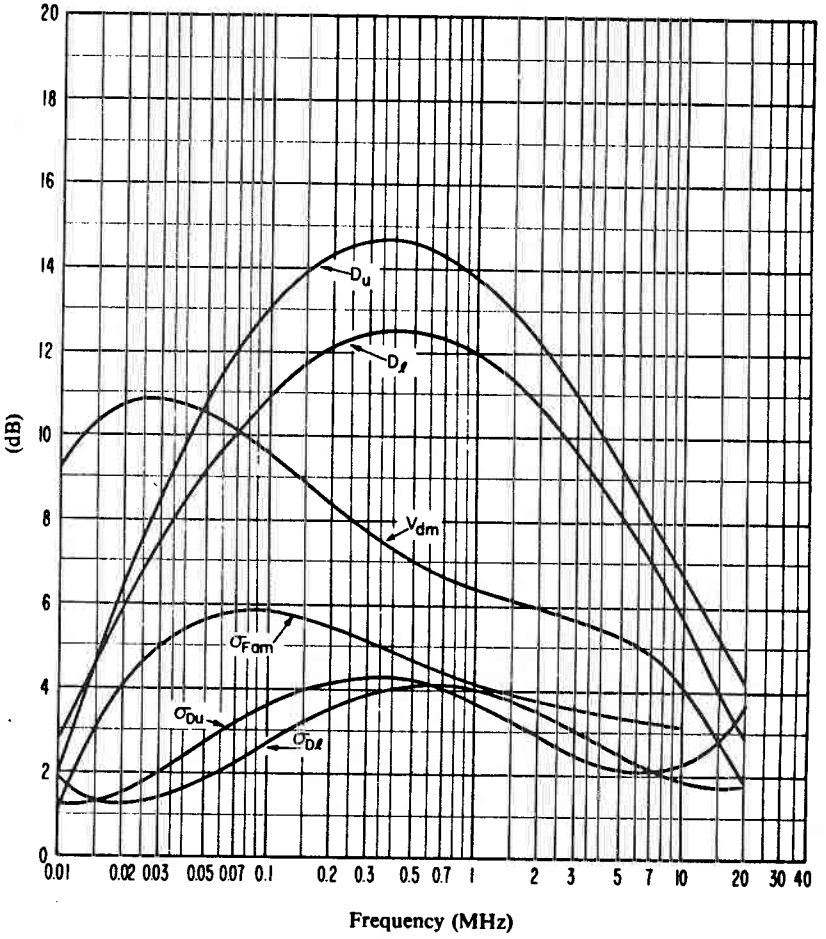

FIGURE 3c – *Data on noise variability and character (Winter; 0400-0800 h)*

σ_{Fam} : Standard deviation of values of F_{am}
D_u : Ratio of upper decile to median value, F_{am}
σ_{Du} : Standard deviation of values of D_u
D_l : Ratio of median value, F_{am}, to lower decile
σ_{Dl} : Standard deviation of value of D_l
V_{dm} : Expected value of median deviation of average voltage. The values shown are for a bandwidth of 200 Hz.

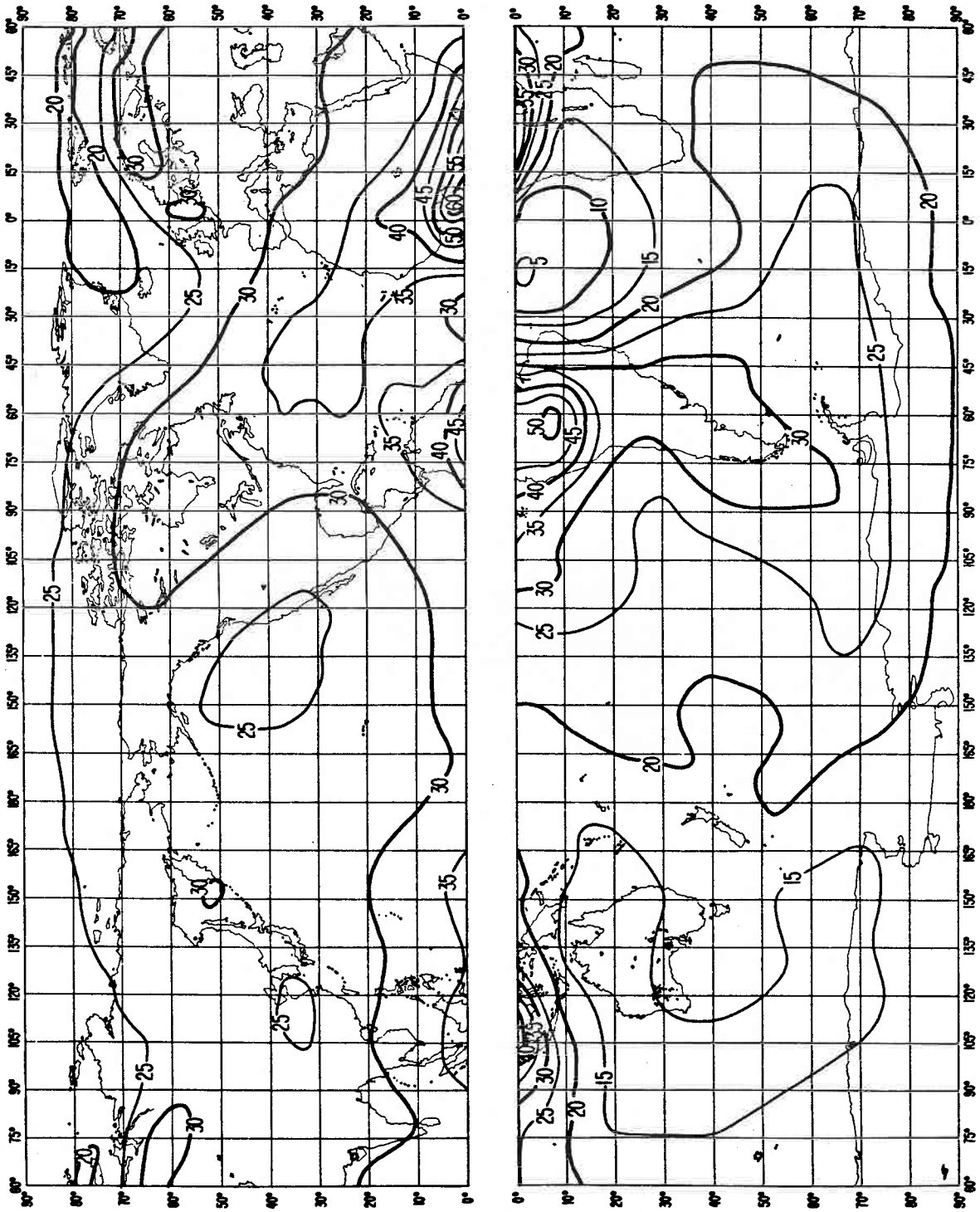

FIGURE 4a – *Expected values of atmospheric radio noise, F_{am} (dB above kT_0b at 1 MHz)*
(Winter; 0800-1200 h)

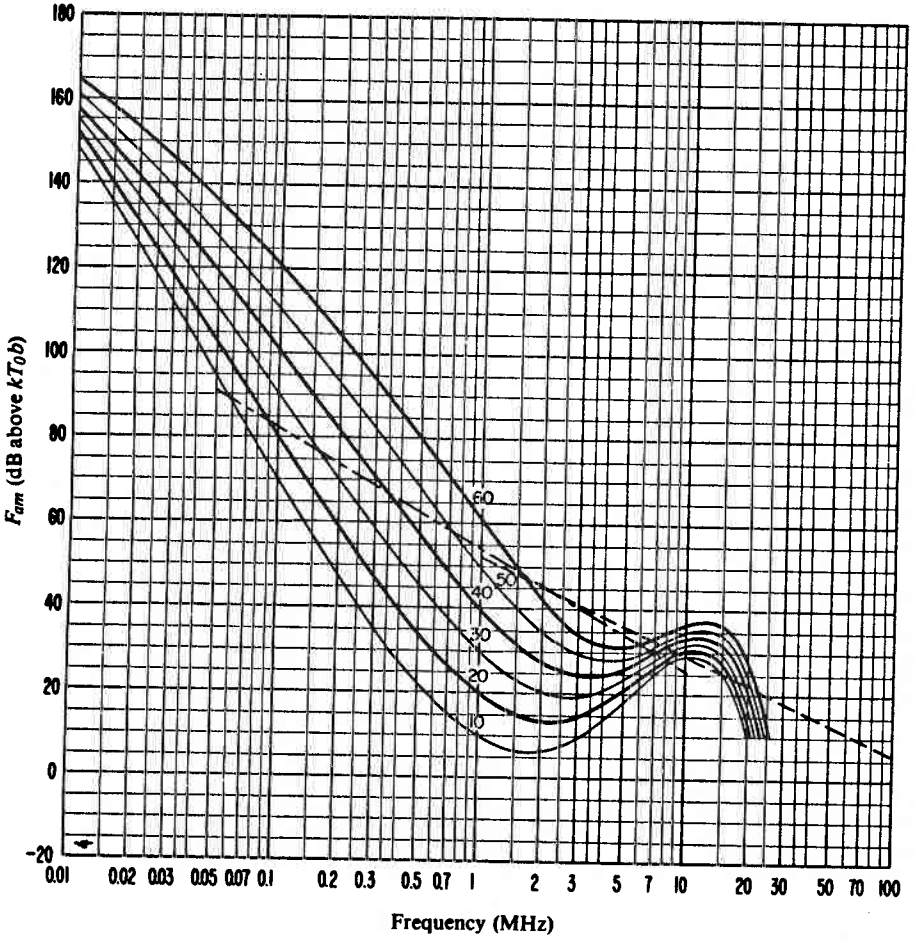

FIGURE 4b – *Variation of radio noise with frequency (Winter; 0800-1200 h)*

——— Expected values of atmospheric noise

— · — · — · — Expected values of man-made noise at a quiet receiving location

— — — — — Expected values of galactic noise

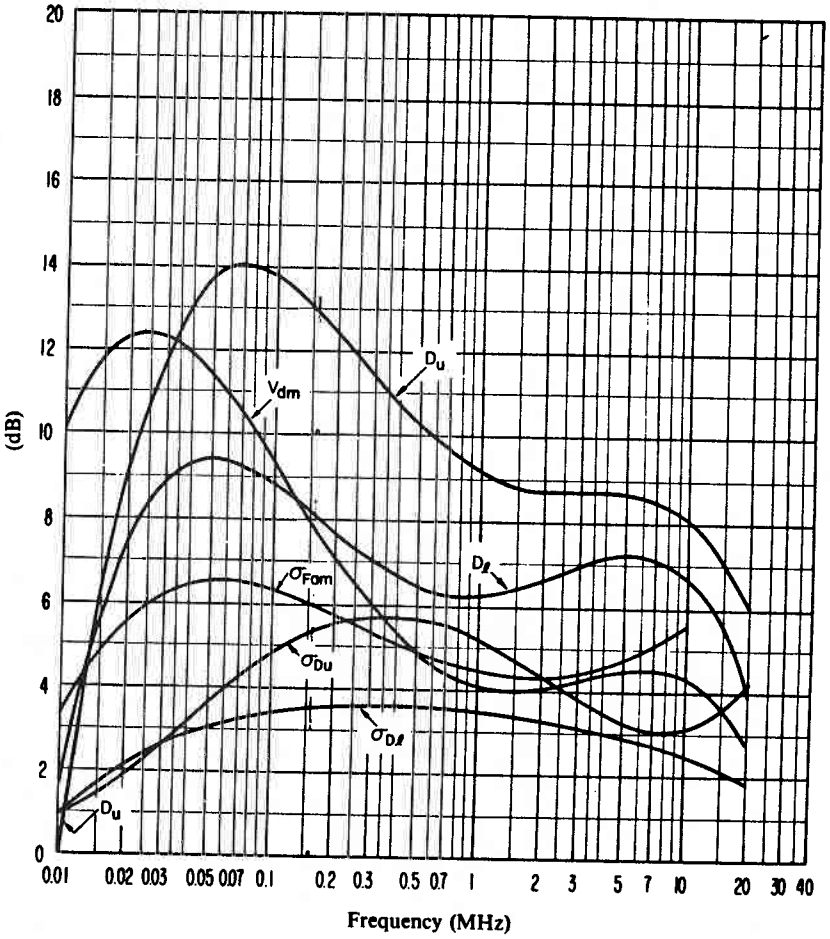

FIGURE 4c – *Data on noise variability and character (Winter; 0800-1200 h)*

σ_{Fam} : Standard deviation of values of F_{am}
D_u : Ratio of upper decile to median value, F_{am}
σ_{Du} : Standard deviation of values of D_u
D_l : Ratio of median value, F_{am}, to lower decile
σ_{Dl} : Standard deviation of value of D_l
V_{dm} : Expected value of median deviation of average voltage. The values shown are for a bandwidth of 200 Hz.

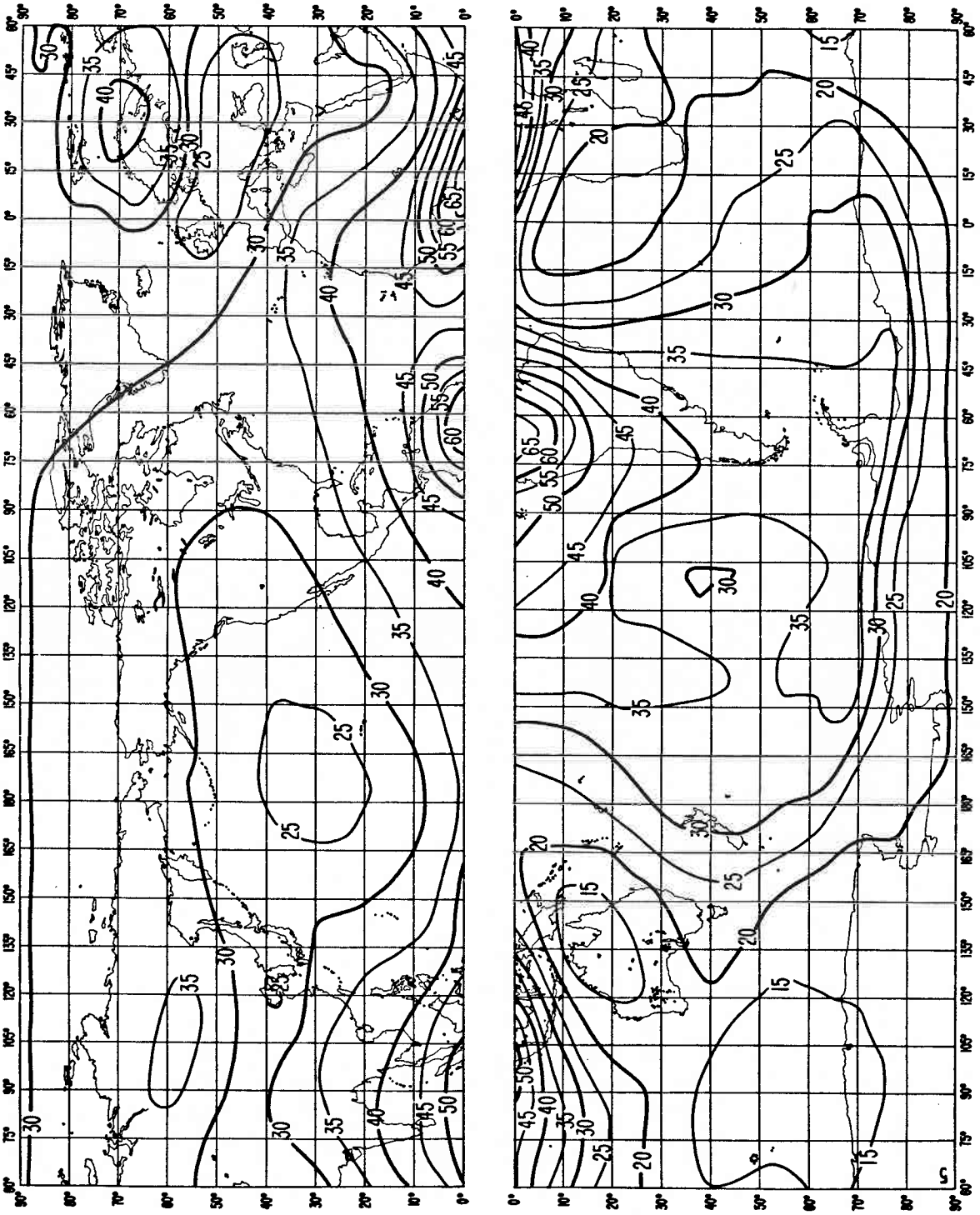

FIGURE 5a – *Expected values of atmospheric radio noise, F_{am} (dB above kT_0b at 1 MHz)*
(Winter; 1200-1600 h)

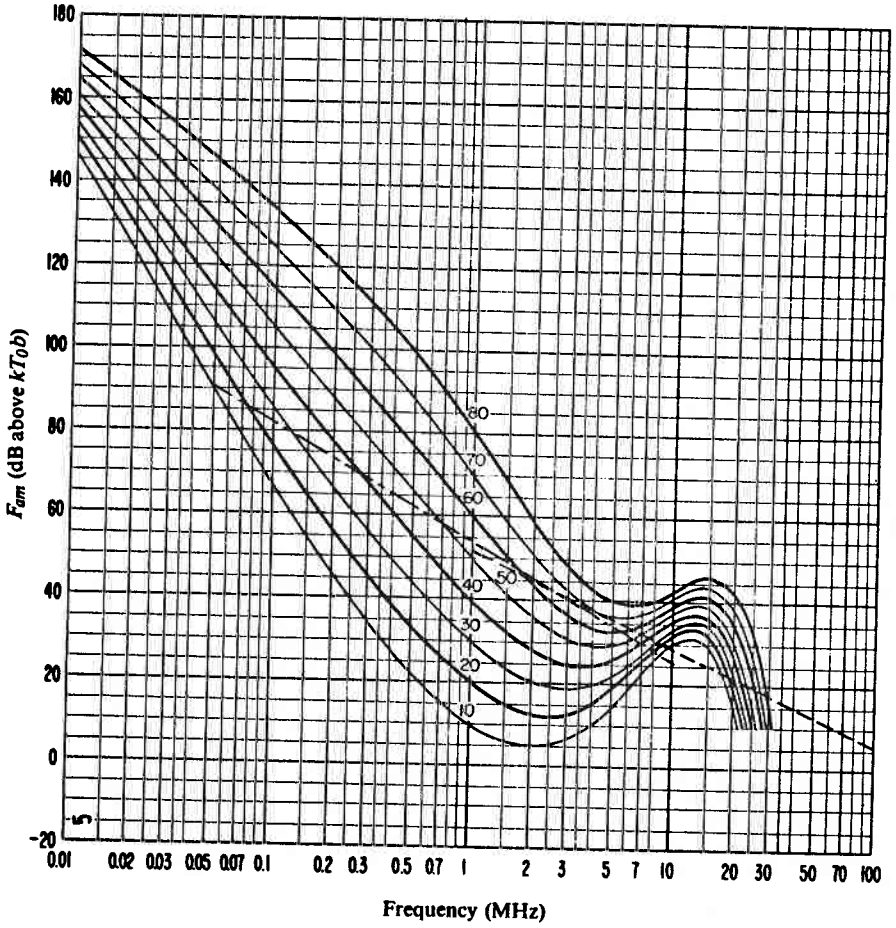

FIGURE 5b – *Variation of radio noise with frequency (Winter; 1200-1600 h)*

——————— Expected values of atmospheric noise

— · — · — · — Expected values of man-made noise at a quiet receiving location

— — — — — Expected values of galactic noise

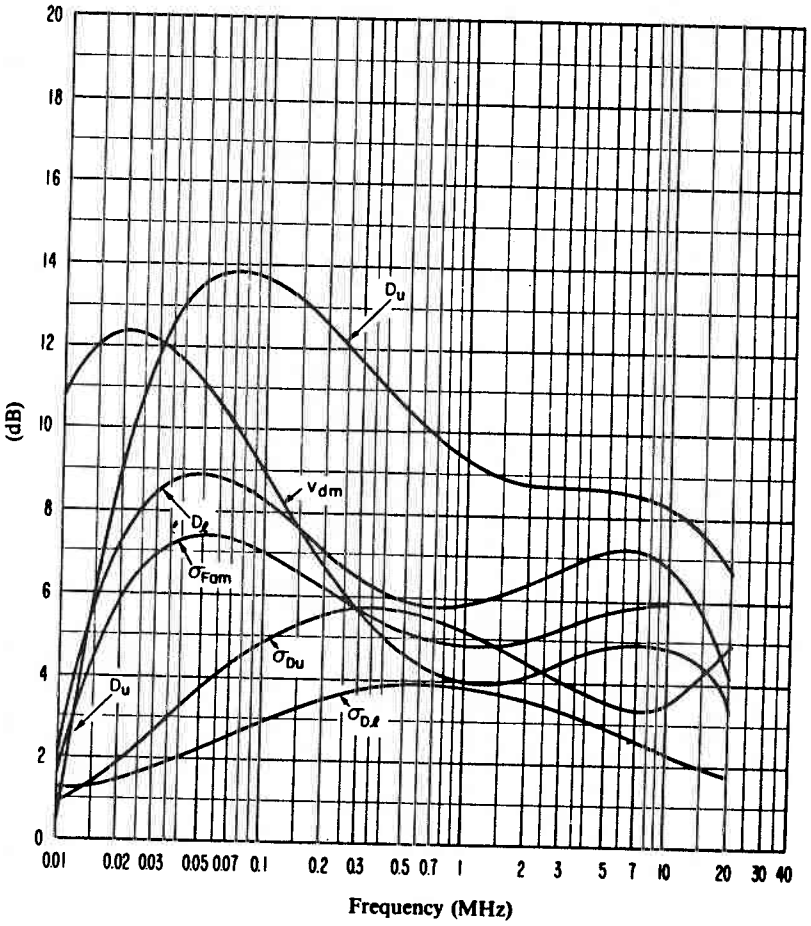

FIGURE 5c – *Data on noise variability and character (Winter; 1200-1600 h)*

σ_{Fam} : Standard deviation of values of F_{am}
D_u : Ratio of upper decile to median value, F_{am}
σ_{Du} : Standard deviation of values of D_u
D_l : Ratio of median value, F_{am}, to lower decile
σ_{Dl} : Standard deviation of value of D_l
V_{dm} : Expected value of median deviation of average voltage. The values shown are for a bandwidth of 200 Hz.

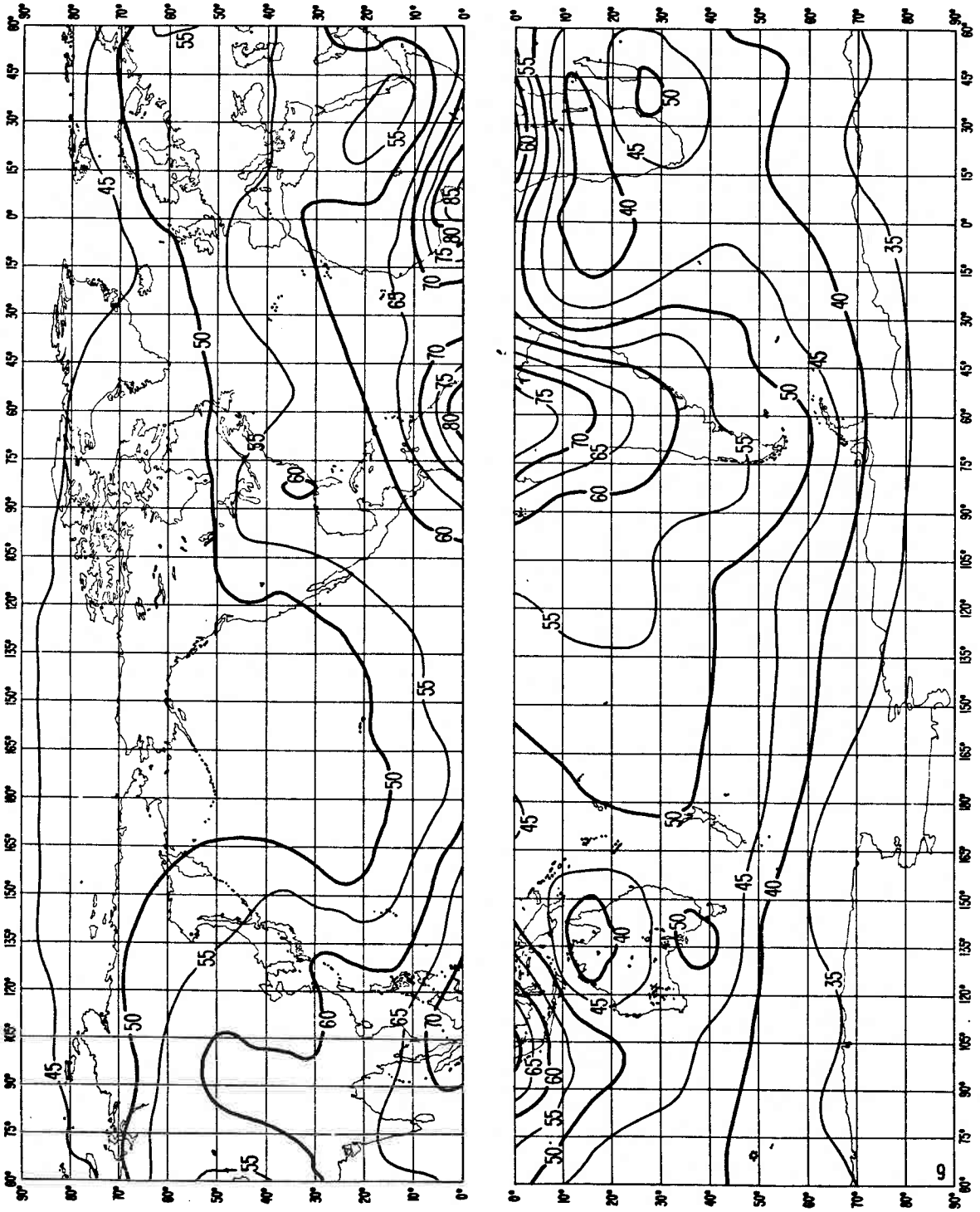

FIGURE 6a – *Expected values of atmospheric radio noise, F_{am} (dB above kT_0b at 1 MHz)*
(Winter; 1600-2000 h)

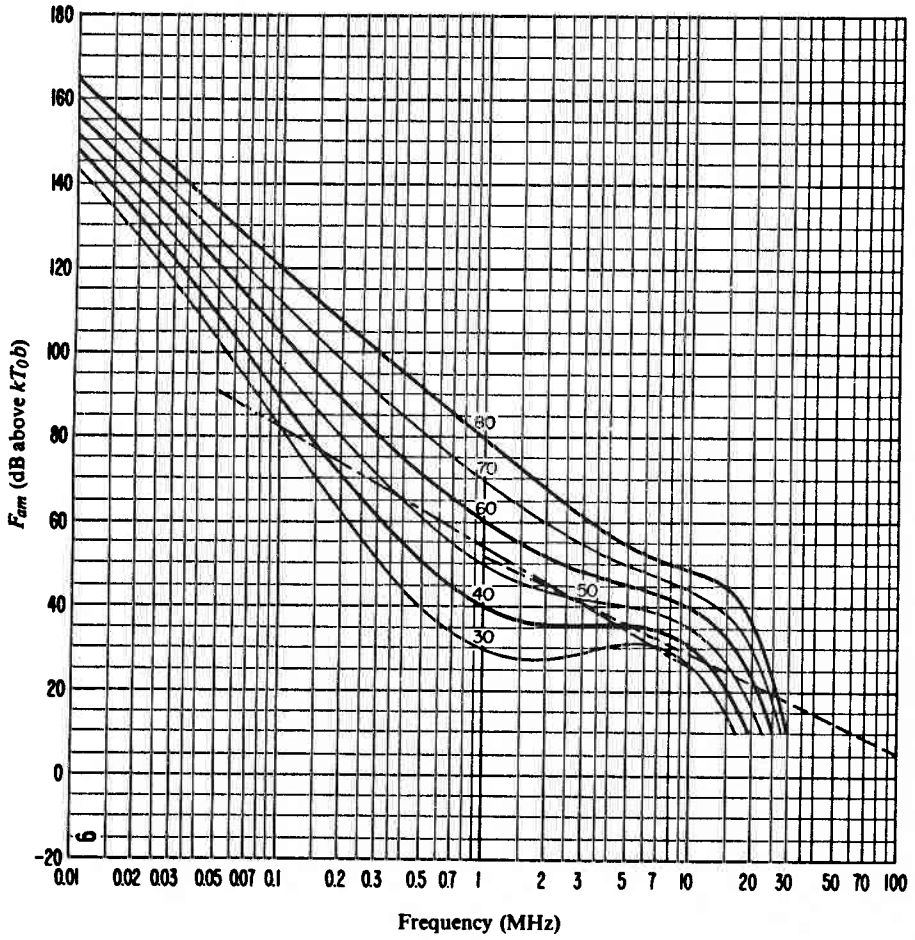

FIGURE 6b – *Variation of radio noise with frequency (Winter; 1600-2000 h)*

———— Expected values of atmospheric noise

— · — · — · — Expected values of man-made noise at a quiet receiving location

— — — — — Expected values of galactic noise

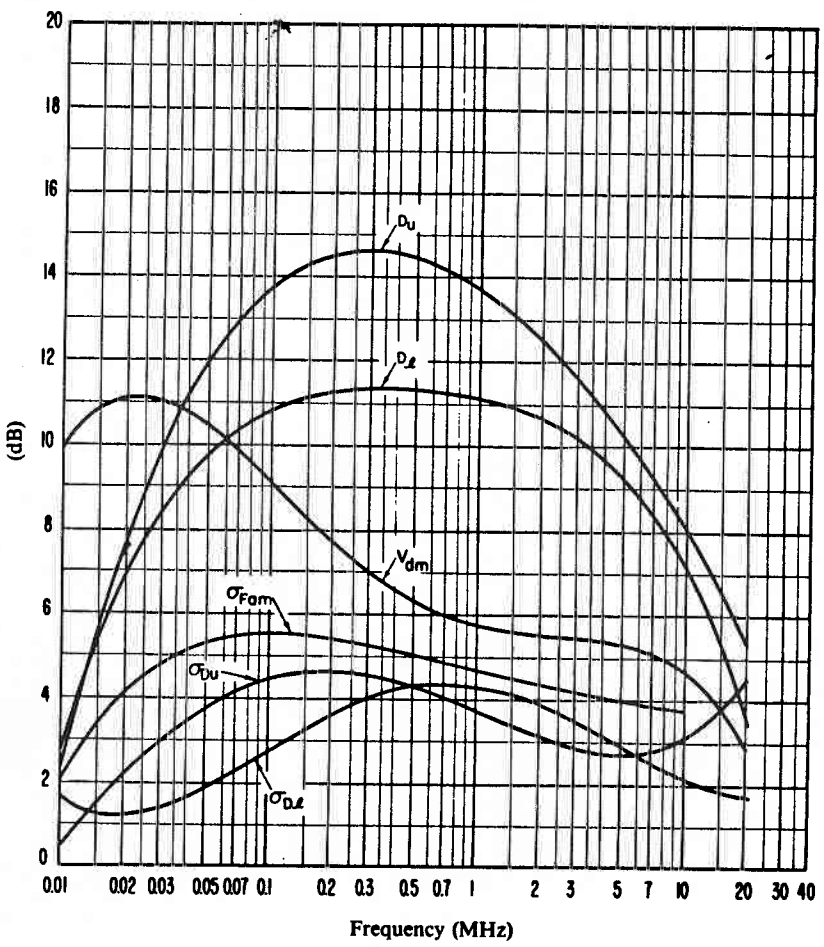

FIGURE 6c – *Data on noise variability and character (Winter; 1600-2000 h)*

σ_{Fam} : Standard deviation of values of F_{am}
D_u : Ratio of upper decile to median value, F_{am}
σ_{Du} : Standard deviation of values of D_u
D_l : Ratio of median value, F_{am}, to lower decile
σ_{Dl} : Standard deviation of value of D_l
V_{dm} : Expected value of median deviation of average voltage. The values shown are for a bandwidth of 200 Hz.

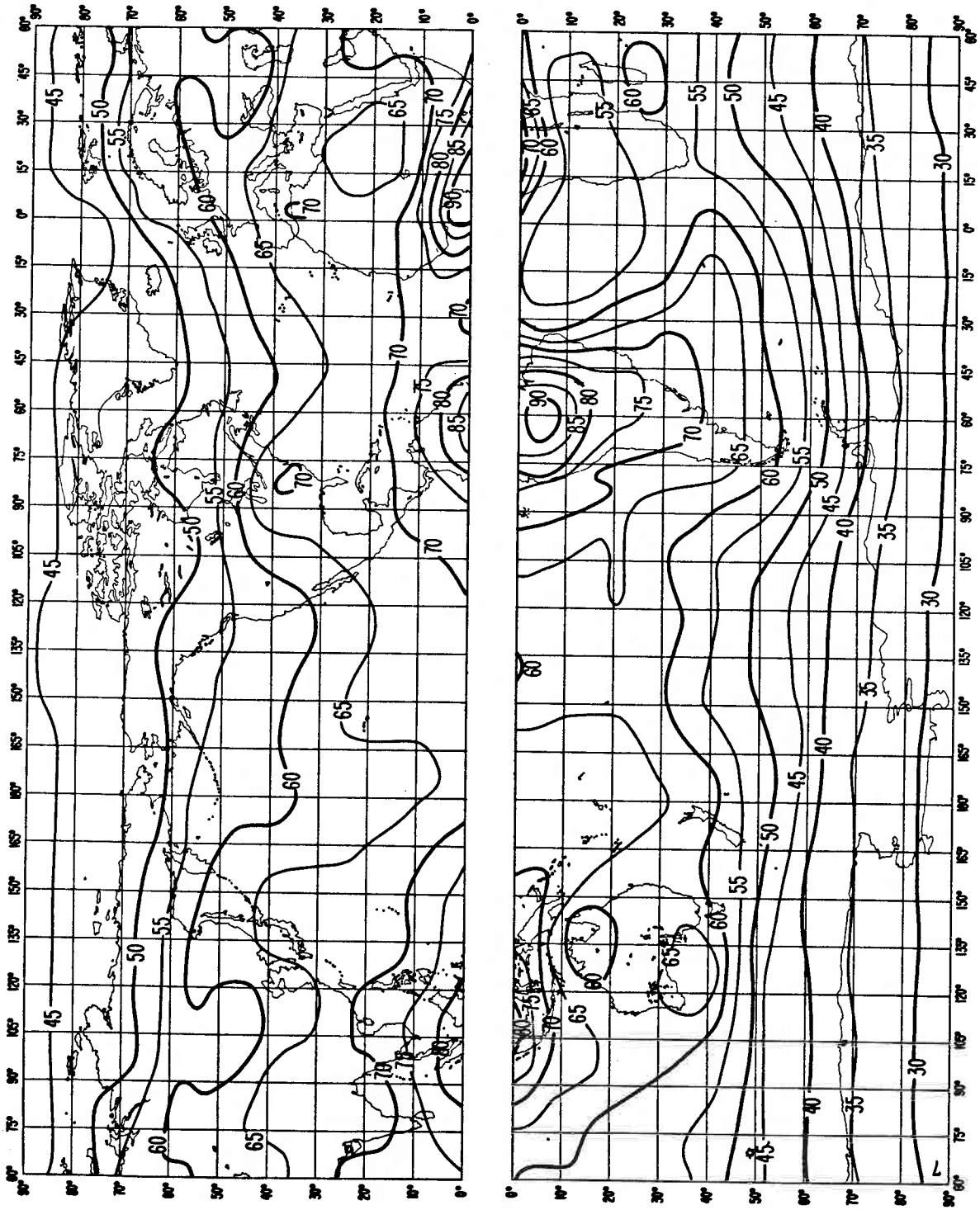

FIGURE 7a – *Expected values of atmospheric radio noise, F_{am} (dB above kT_0b at 1 MHz)*
(Winter; 2000-2400 h)

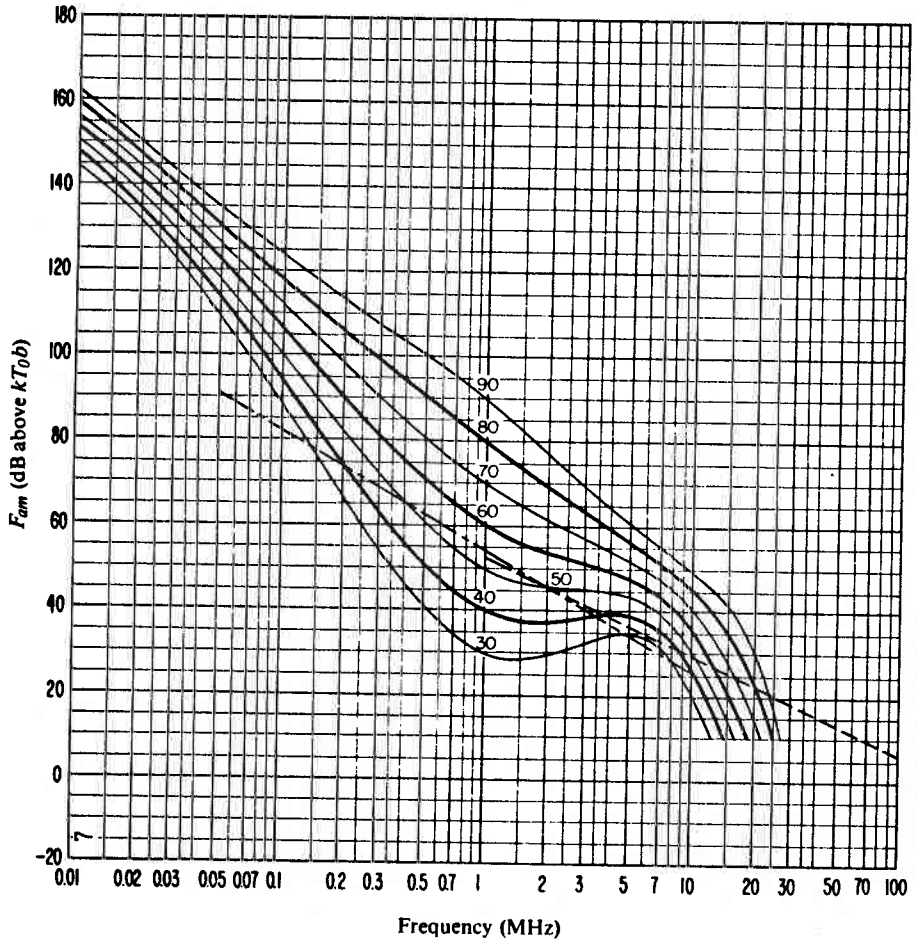

FIGURE 7b – *Variation of radio noise with frequency (Winter; 2000-2400 h)*

——— Expected values of atmospheric noise

— · — · — · — Expected values of man-made noise at a quiet receiving location

— — — — — Expected values of galactic noise

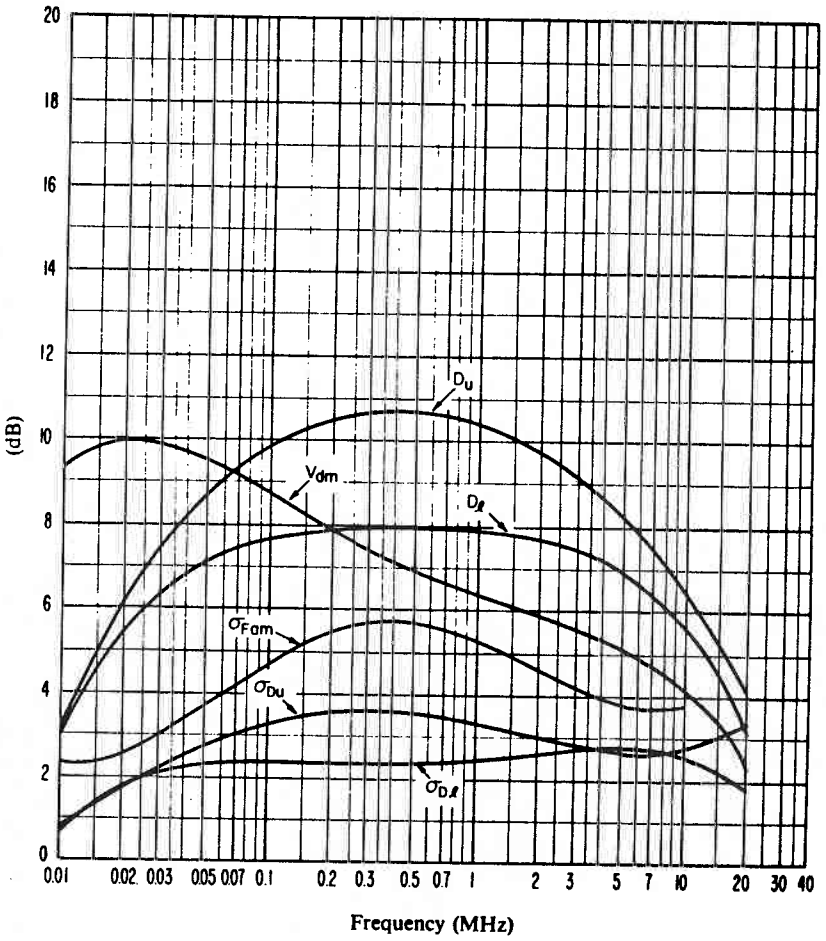

FIGURE 7c – *Data on noise variability and character (Winter; 2000-2400 h)*

σ_{Fam} : Standard deviation of values of F_{am}
D_u : Ratio of upper decile to median value, F_{am}
σ_{Du} : Standard deviation of values of D_u
D_l : Ratio of median value, F_{am}, to lower decile
σ_{Dl} : Standard deviation of value of D_l
V_{dm} : Expected value of median deviation of average voltage. The values shown are for a bandwidth of 200 Hz.

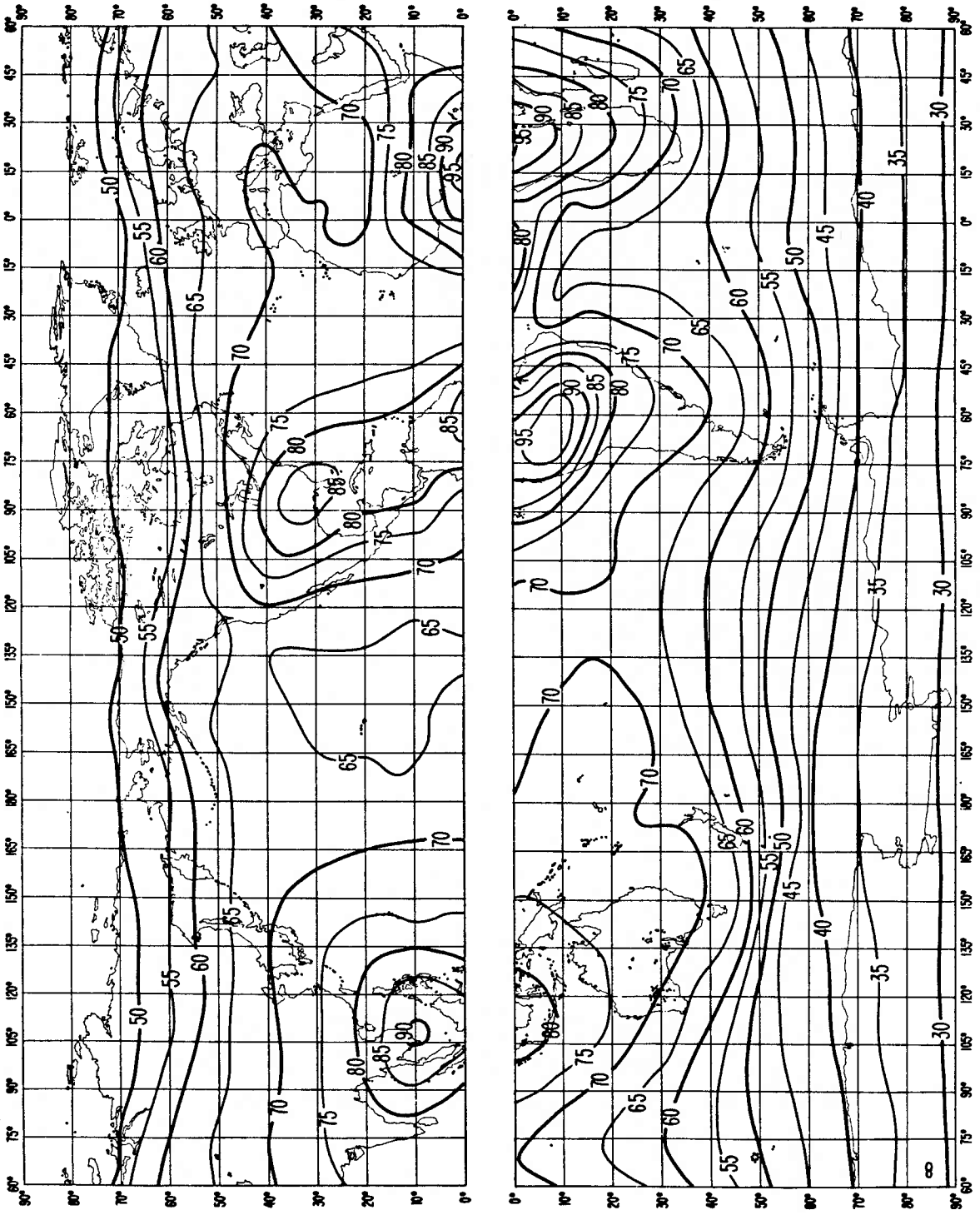

FIGURE 8a – *Expected values of atmospheric radio noise, F_{am} (dB above kT_0b at 1 MHz)*
(Spring; 0000-0400 h)

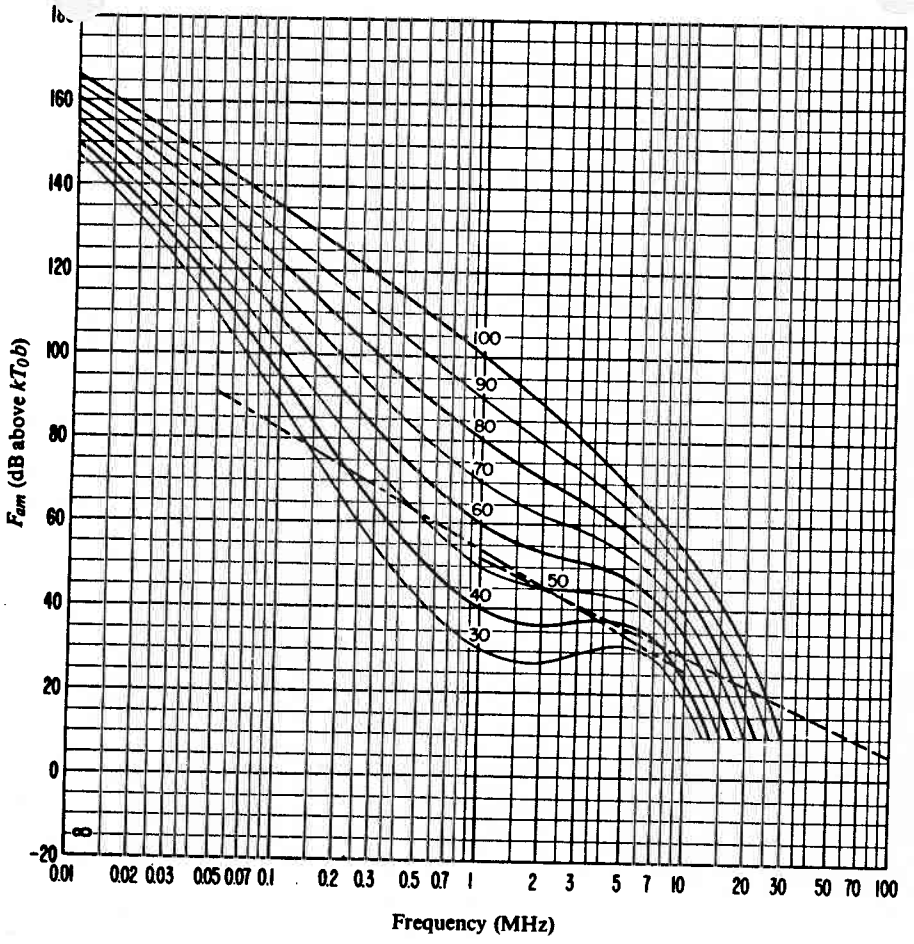

FIGURE 8b – *Variation of radio noise with frequency (Spring; 0000-0400 h)*

——— Expected values of atmospheric noise

— · — · — · — Expected values of man-made noise at a quiet receiving location

— — — — — Expected values of galactic noise

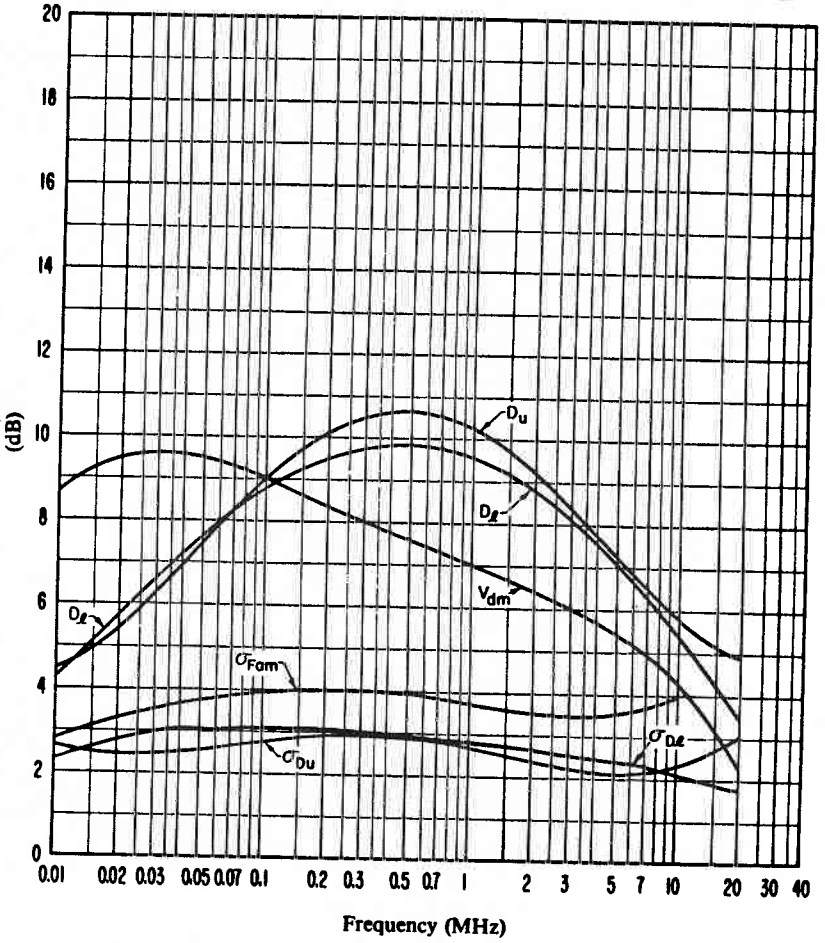

FIGURE 8c – *Data on noise variability and character (Spring; 0000-0400 h)*

σ_{Fam} : Standard deviation of values of F_{am}
D_u : Ratio of upper decile to median value, F_{am}
σ_{Du} : Standard deviation of values of D_u
D_l : Ratio of median value, F_{am}, to lower decile
σ_{Dl} : Standard deviation of value of D_l
V_{dm} : Expected value of median deviation of average voltage. The values shown are for a bandwidth of 200 Hz.

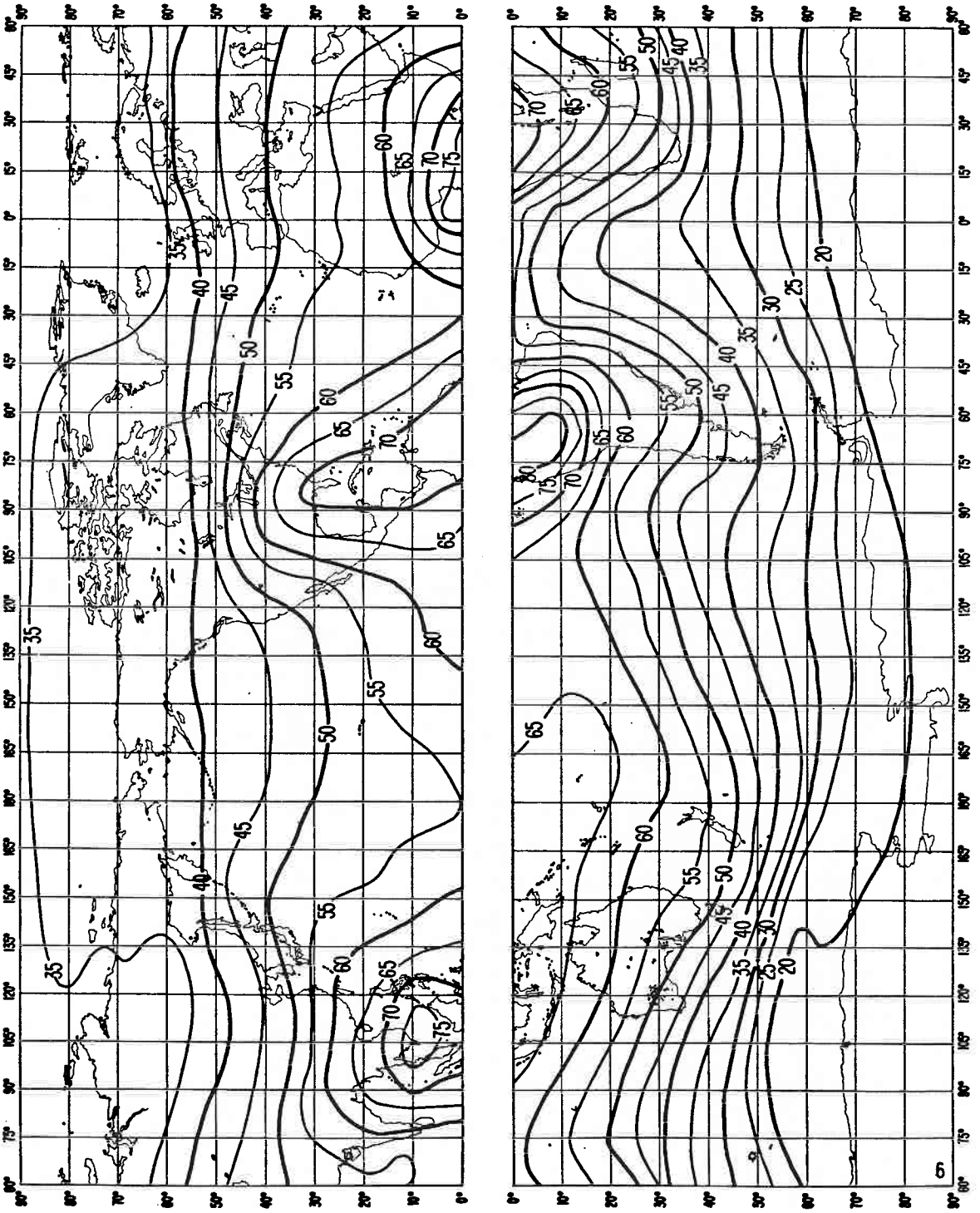

FIGURE 9a – *Expected values of atmospheric radio noise, F_{am} (dB above kT_0b at 1 MHz)*
(Spring; 0400-0800 h)

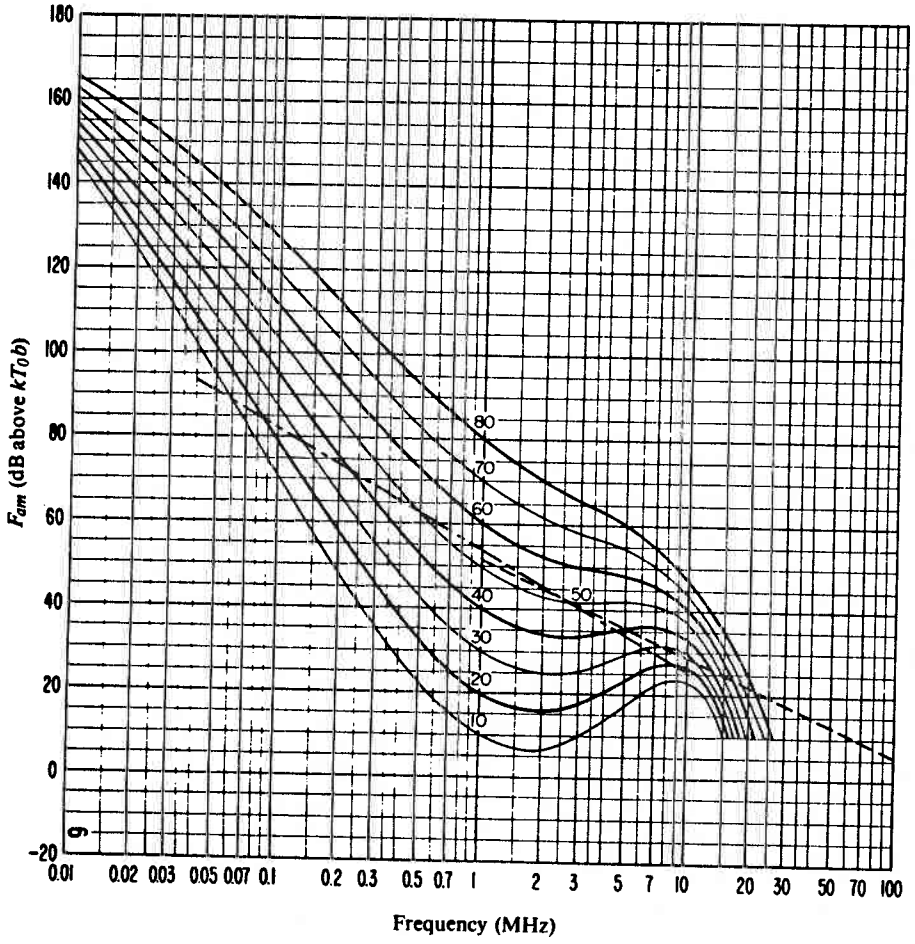

FIGURE 9b – *Variation of radio noise with frequency*
(Spring; 0400-0800 h)

———— Expected values of atmospheric noise

— · — · — · — Expected values of man-made noise at a quiet receiving location

— — — — — Expected values of galactic noise

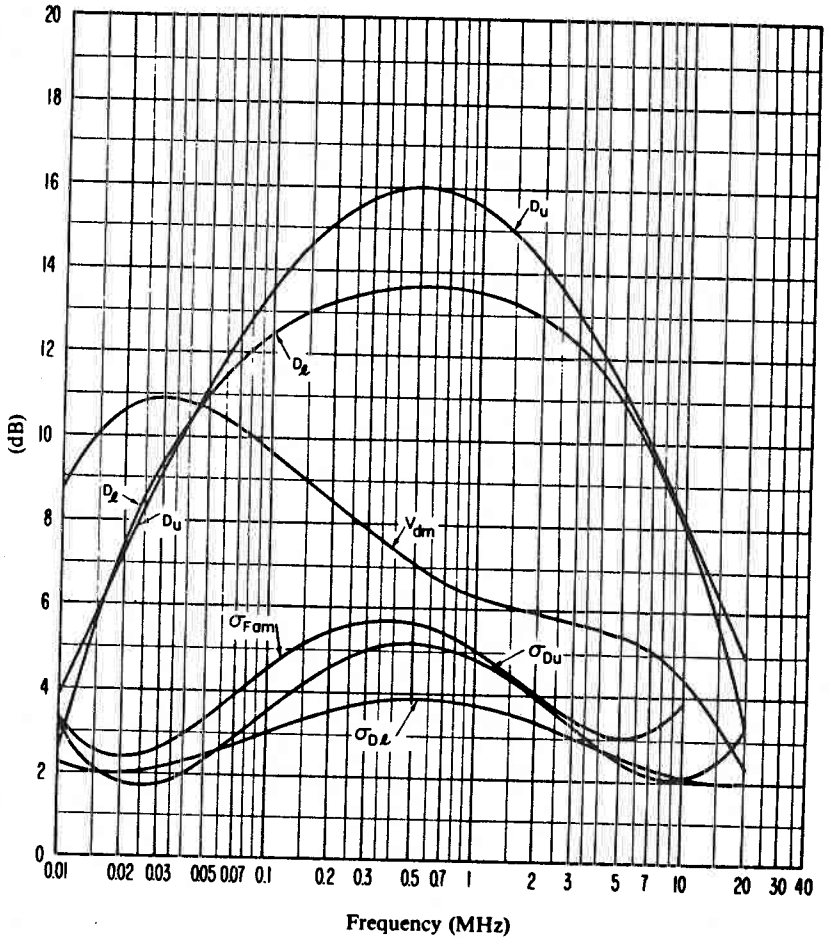

FIGURE 9c – *Data on noise variability and character*
(Spring; 0400-0800 h)

σ_{Fam} : Standard deviation of values of F_{am}
D_u : Ratio of upper decile to median value, F_{am}
σ_{Du} : Standard deviation of values of D_u
D_l : Ratio of median value, F_{am}, to lower decile
σ_{Dl} : Standard deviation of value of D_l
V_{dm} : Expected value of median deviation of average voltage. The values shown are for a bandwidth of 200 Hz.

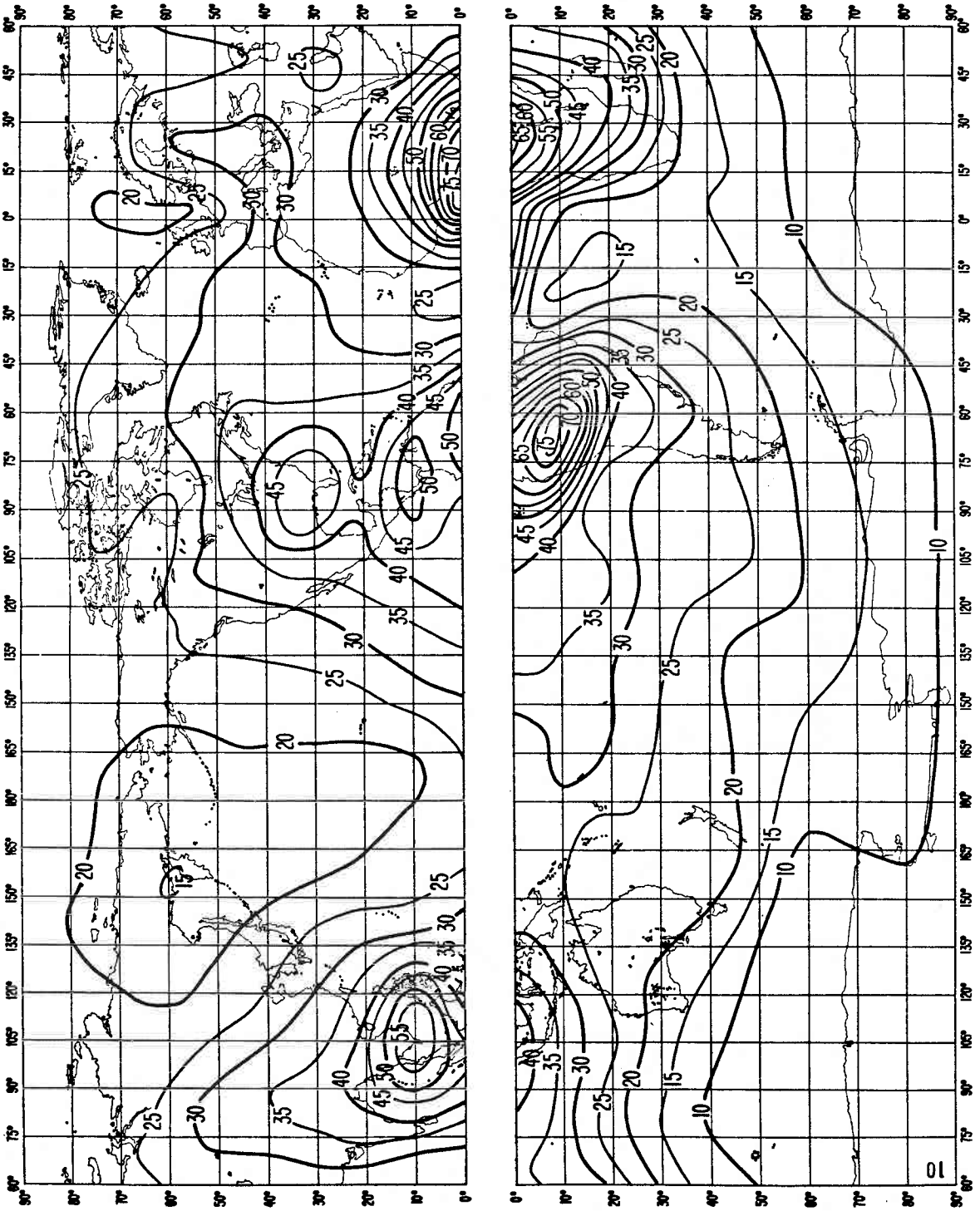

FIGURE 10a – *Expected values of atmospheric radio noise, F_{am} (dB above kT_0b at 1 MHz)*
(Spring; 0800-1200 h)

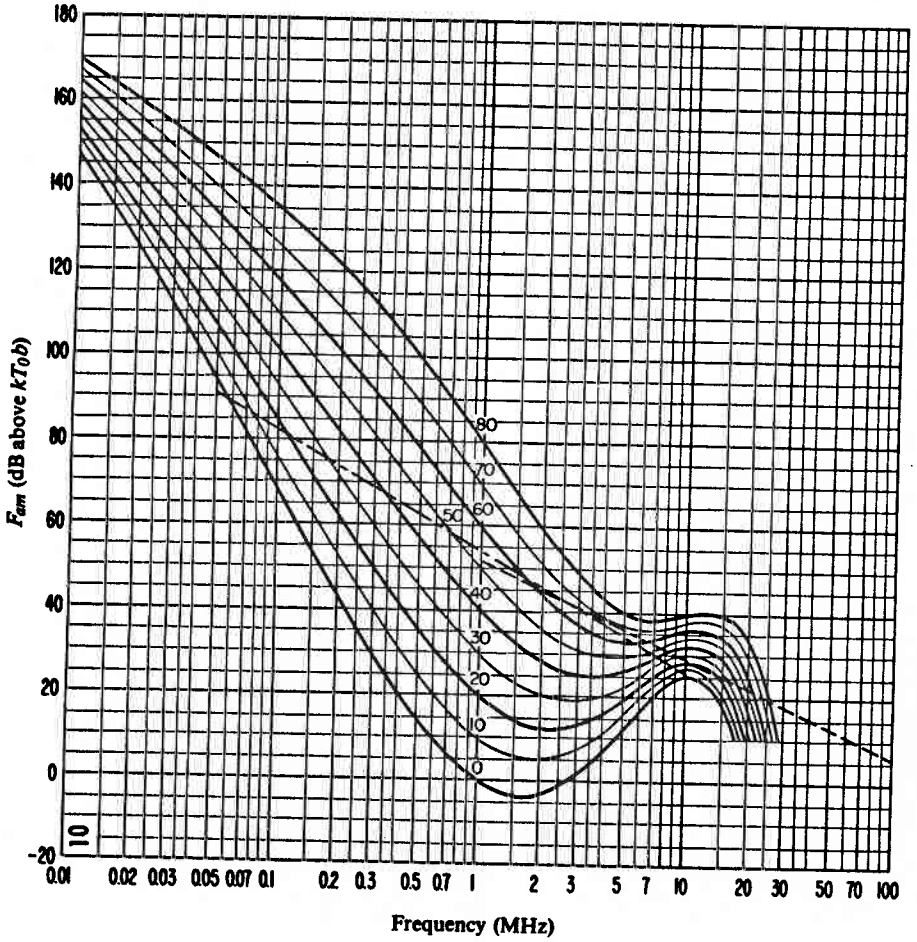

FIGURE 10b – *Variation of radio noise with frequency (Spring; 0800-1200 h)*

——— Expected values of atmospheric noise

– · – · – · – Expected values of man-made noise at a quiet receiving location

– – – – – Expected values of galactic noise

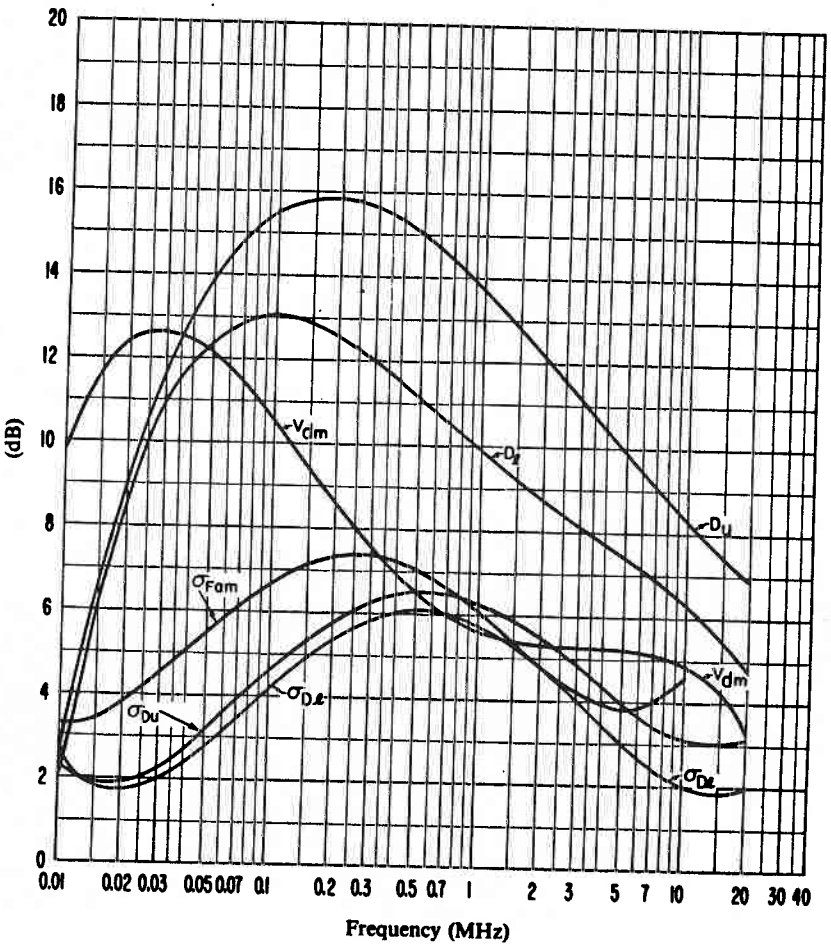

FIGURE 10c – *Data on noise variability and character (Spring; 0800-1200 h)*

σ_{Fam} : Standard deviation of values of F_{am}
D_u : Ratio of upper decile to median value, F_{am}
σ_{Du} : Standard deviation of values of D_u
D_l : Ratio of median value, F_{am}, to lower decile
σ_{Dl} : Standard deviation of value of D_l
V_{dm} : Expected value of median deviation of average voltage. The values shown are for a bandwidth of 200 Hz.

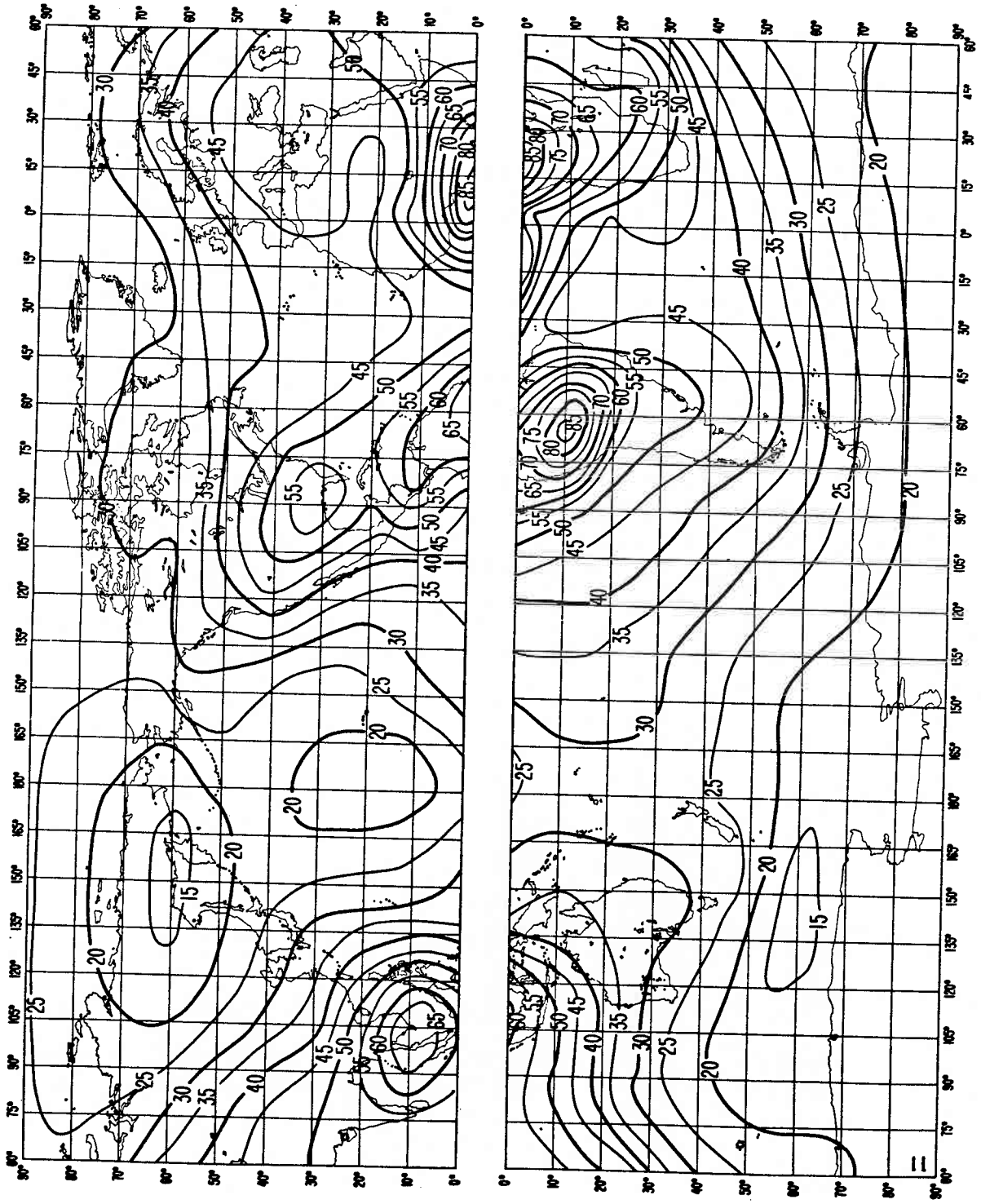

FIGURE 11a – *Expected values of atmospheric radio noise, F_{am} (dB above kT_0b at 1 MHz)*
(Spring; 1200-1600 h)

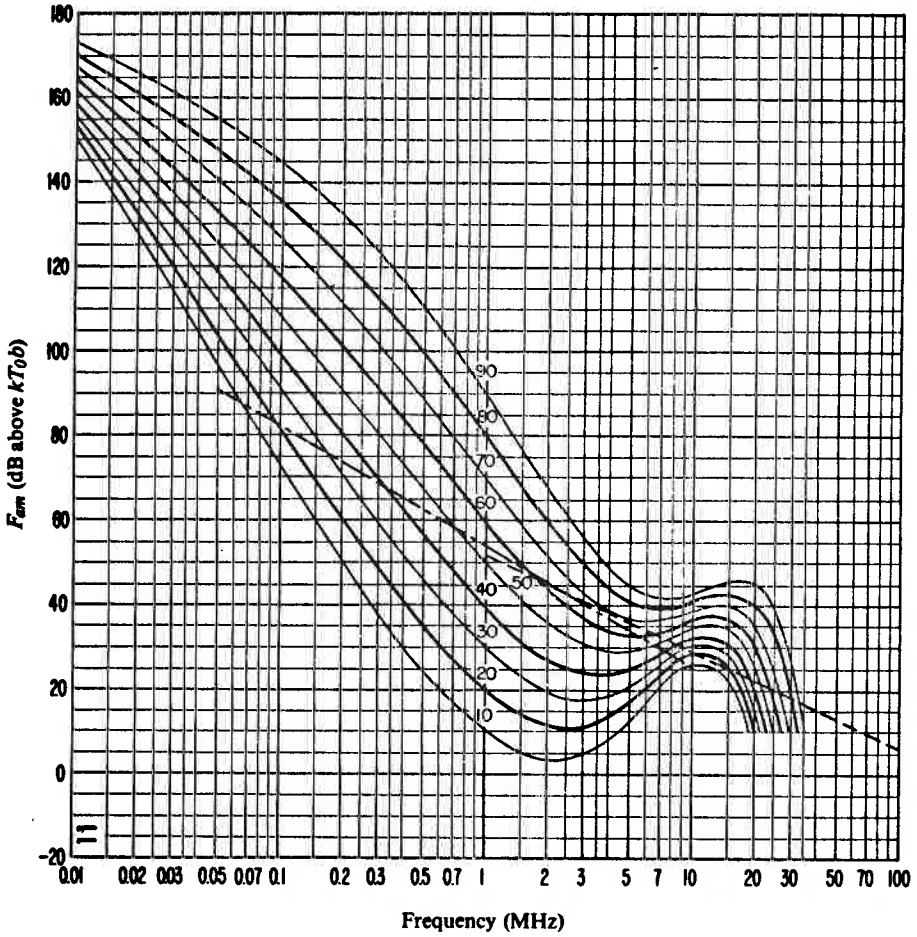

FIGURE 11b – *Variation of radio noise with frequency (Spring; 1200-1600 h)*

——————— Expected values of atmospheric noise

— · — · — · — Expected values of man-made noise at a quiet receiving location

— — — — — Expected values of galactic noise

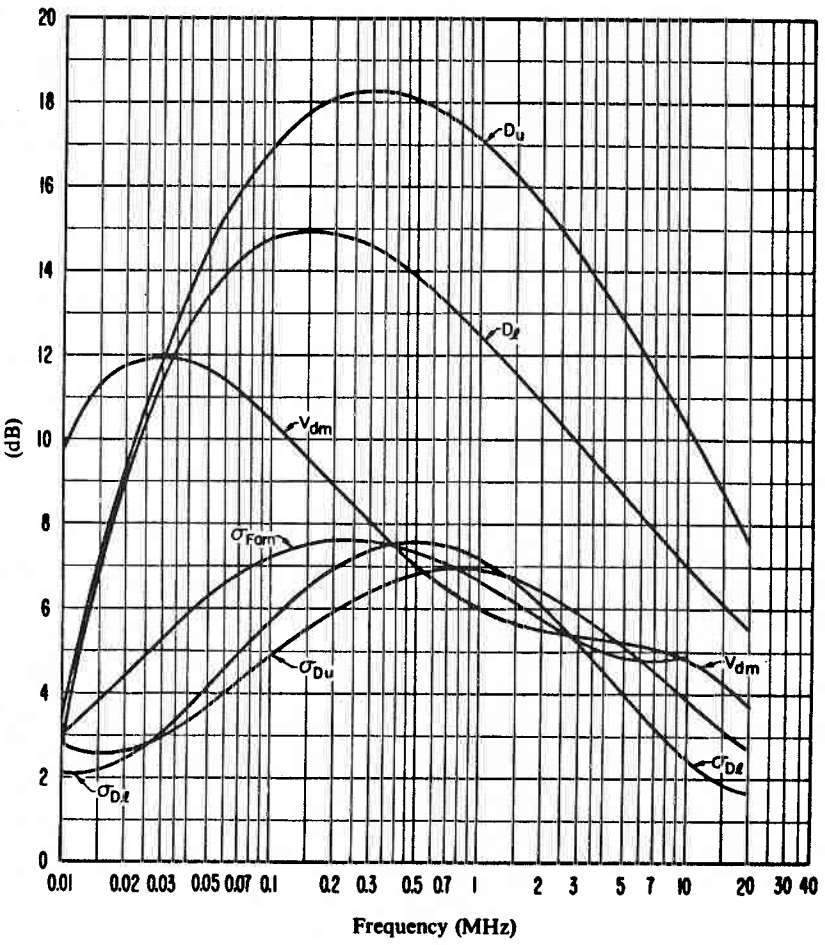

FIGURE 11c – *Data on noise variability and character (Spring; 1200-1600 h)*

σ_{Fam} : Standard deviation of values of F_{am}
D_u : Ratio of upper decile to median value, F_{am}
σ_{Du} : Standard deviation of values of D_u
D_l : Ratio of median value, F_{am}, to lower decile
σ_{Dl} : Standard deviation of value of D_l
V_{dm} : Expected value of median deviation of average voltage. The values shown are for a bandwidth of 200 Hz.

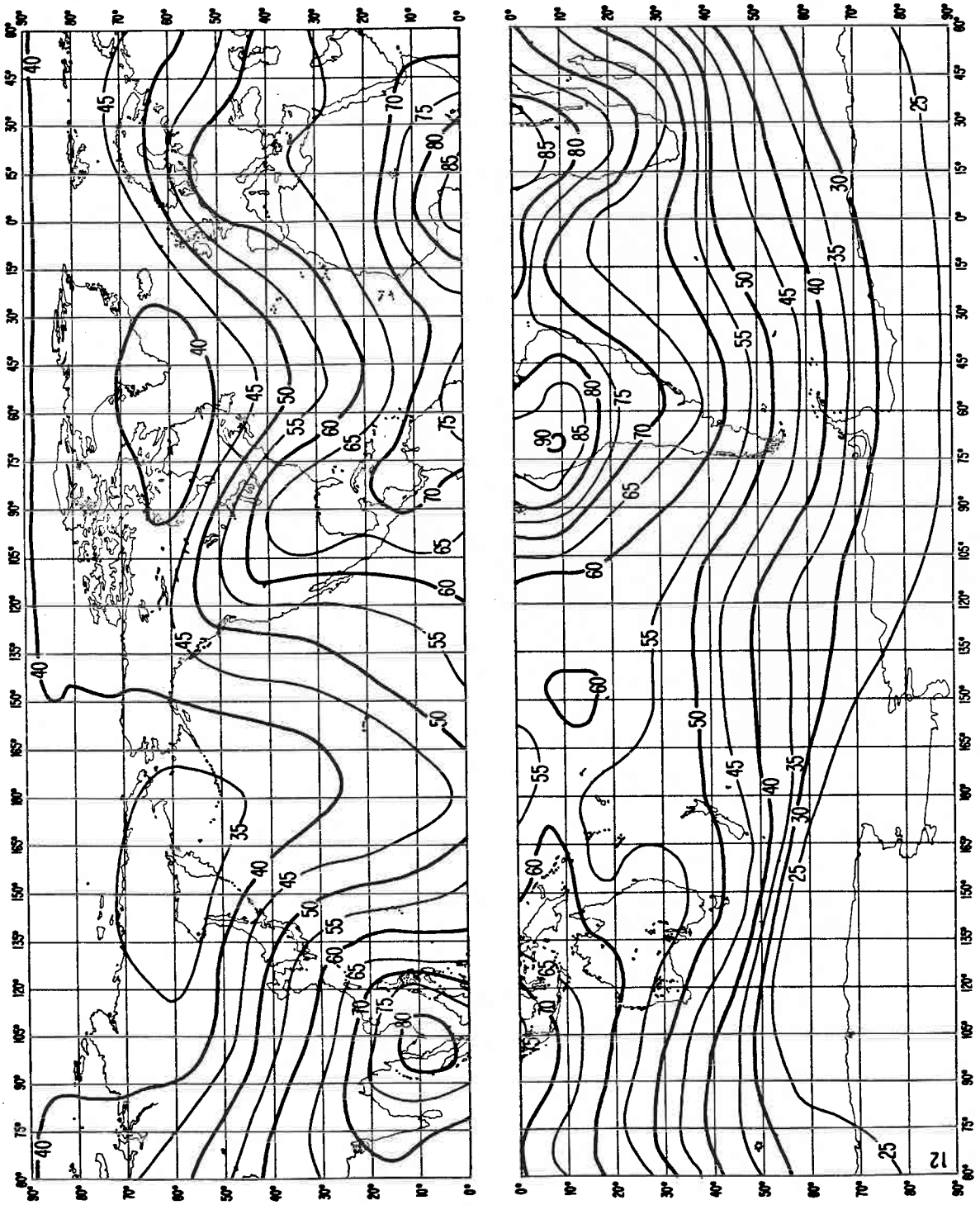

FIGURE 12a – *Expected values of atmospheric radio noise, F_{am} (dB above kT_0b at 1 MHz)*
(Spring; 1600-2000 h)

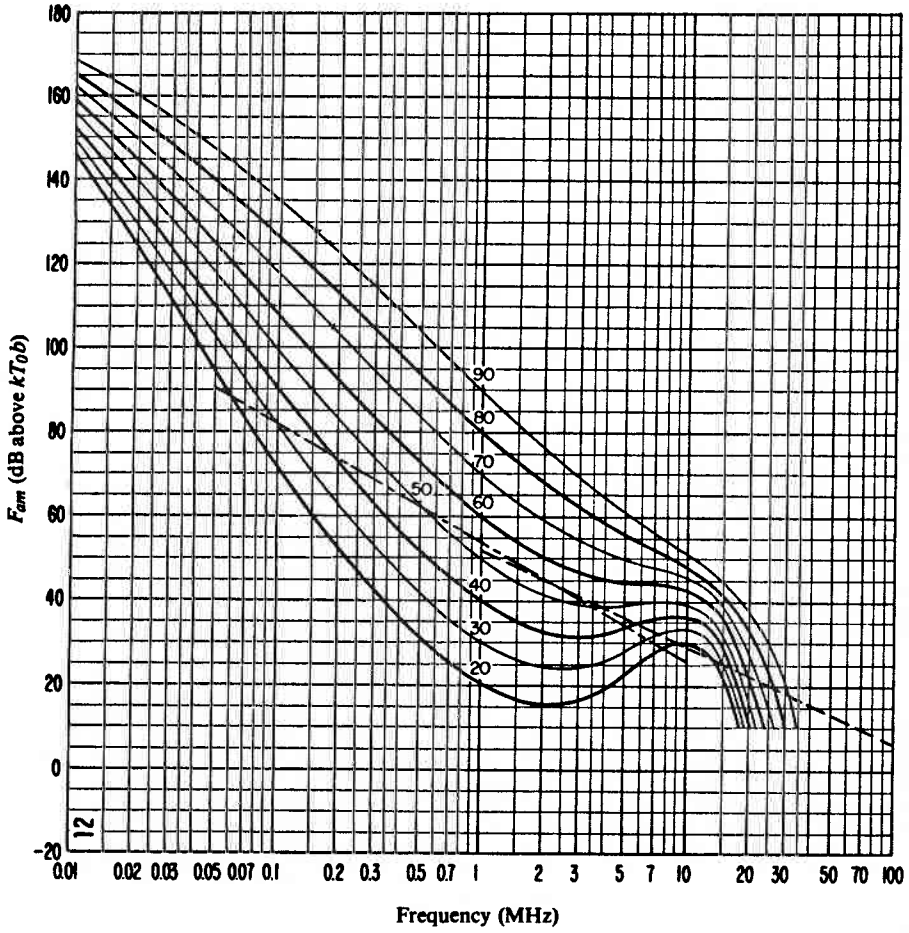

FIGURE 12b – *Variation of radio noise with frequency (Spring; 1600-2000 h)*

——————— Expected values of atmospheric noise

— · — · — · — Expected values of man-made noise at a quiet receiving location

— — — — — Expected values of galactic noise

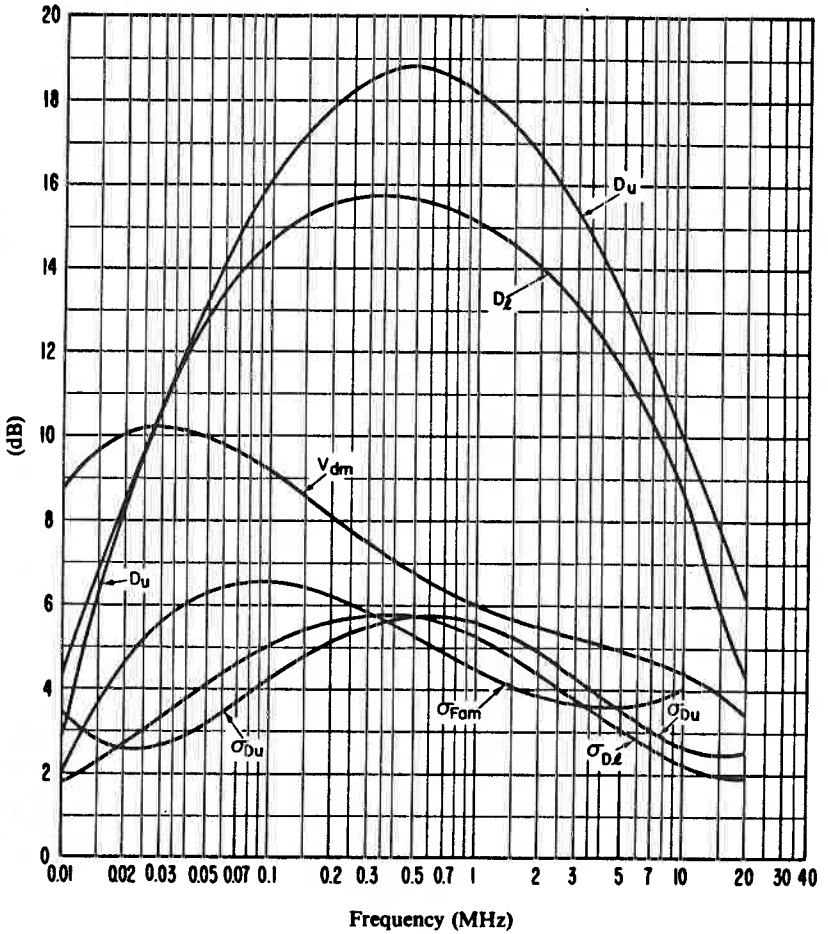

FIGURE 12c – *Data on noise variability and character (Spring; 1600-2000 h)*

σ_{Fam} : Standard deviation of values of F_{am}
D_u : Ratio of upper decile to median value, F_{am}
σ_{Du} : Standard deviation of values of D_u
D_l : Ratio of median value, F_{am}, to lower decile
σ_{Dl} : Standard deviation of value of D_l
V_{dm} : Expected value of median deviation of average voltage. The values shown are for a bandwidth of 200 Hz.

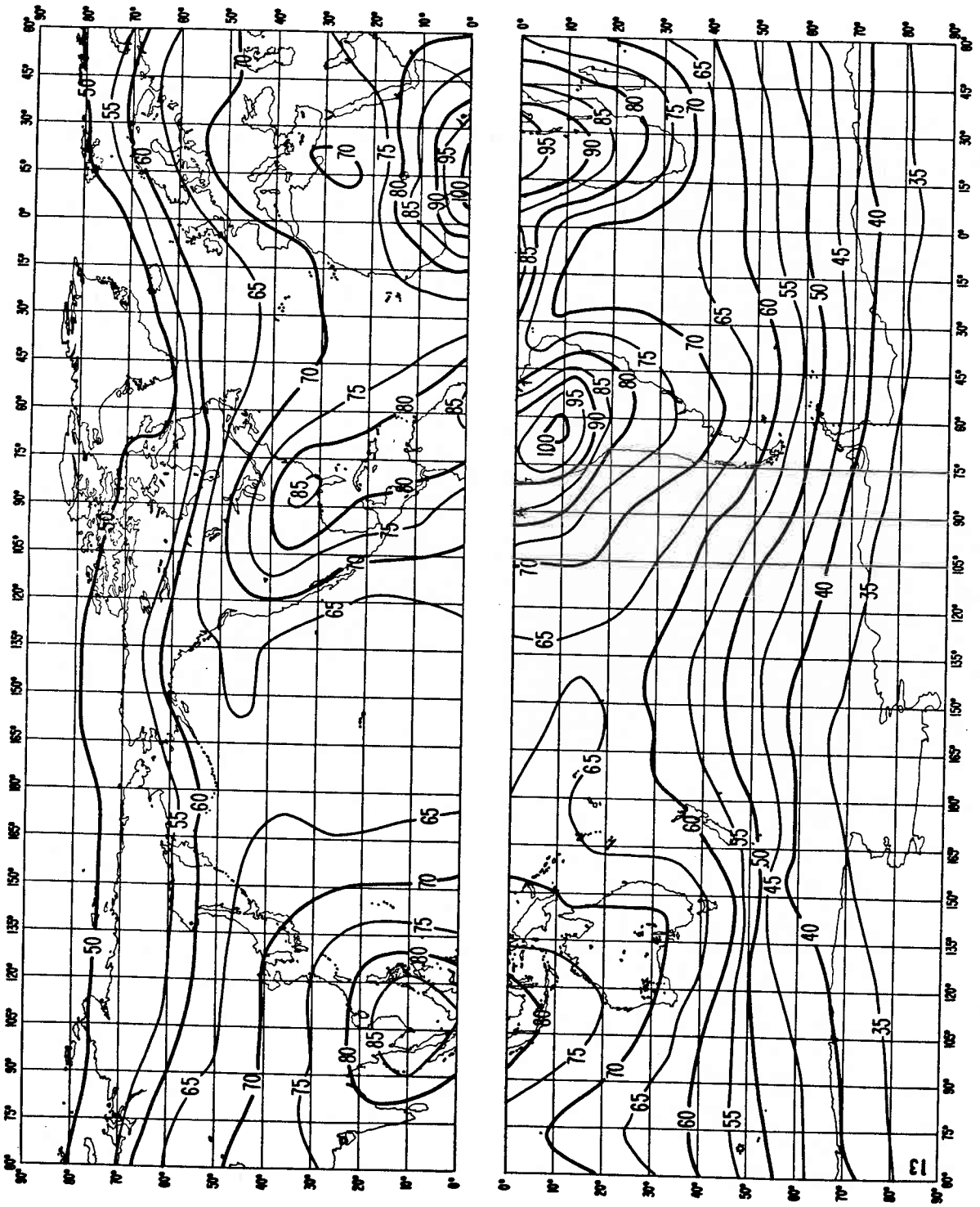

FIGURE 13a – *Expected values of atmospheric radio noise, F_{am} (dB above kT_0b at 1 MHz)*
(Spring; 2000-2400 h)

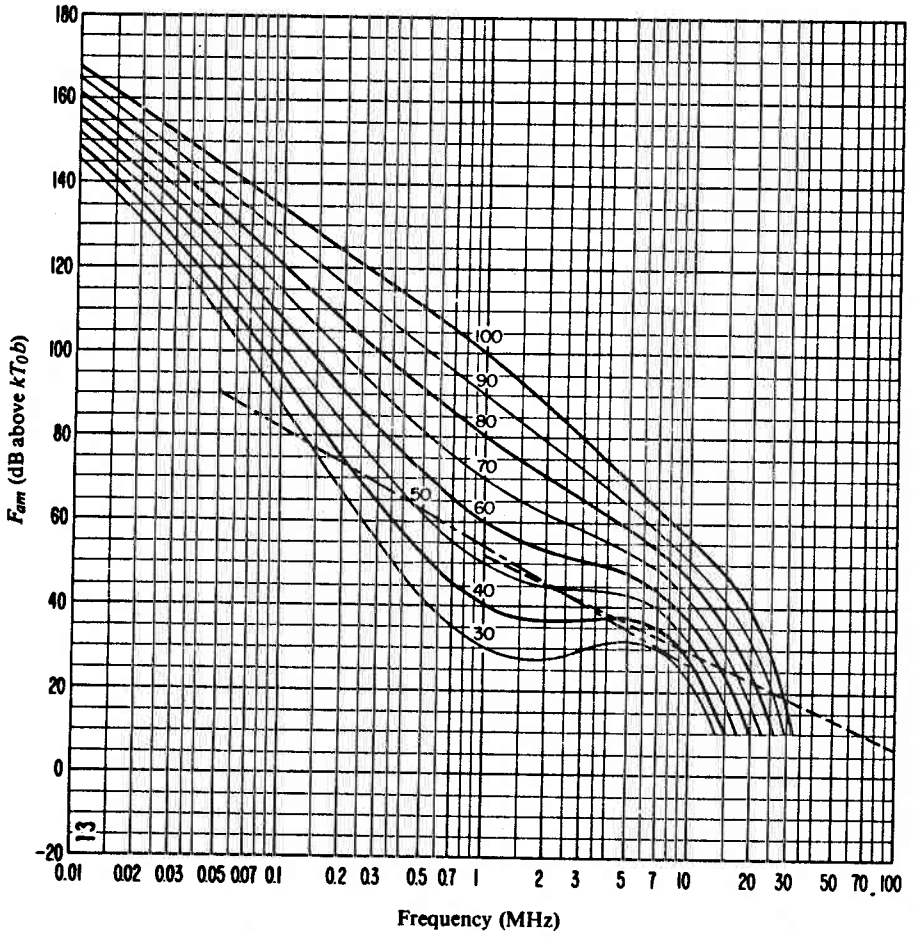

FIGURE 13b – *Variation of radio noise with frequency (Spring; 2000-2400 h)*

——— Expected values of atmospheric noise

— · — · — · — Expected values of man-made noise at a quiet receiving location

— — — — — Expected values of galactic noise

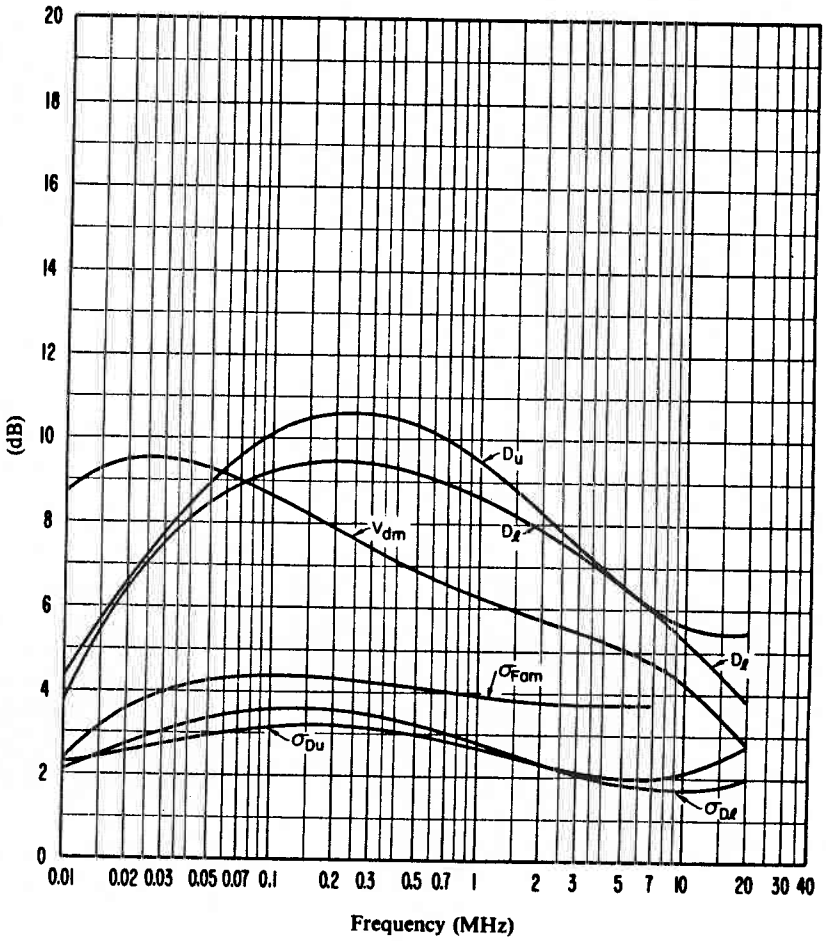

FIGURE 13c – *Data on noise variability and character (Spring; 2000-2400 h)*

σ_{Fam} : Standard deviation of values of F_{am}
D_u : Ratio of upper decile to median value, F_{am}
σ_{Du} : Standard deviation of values of D_u
D_l : Ratio of median value, F_{am}, to lower decile
σ_{Dl} : Standard deviation of value of D_l
V_{dm} : Expected value of median deviation of average voltage. The values shown are for a bandwidth of 200 Hz.

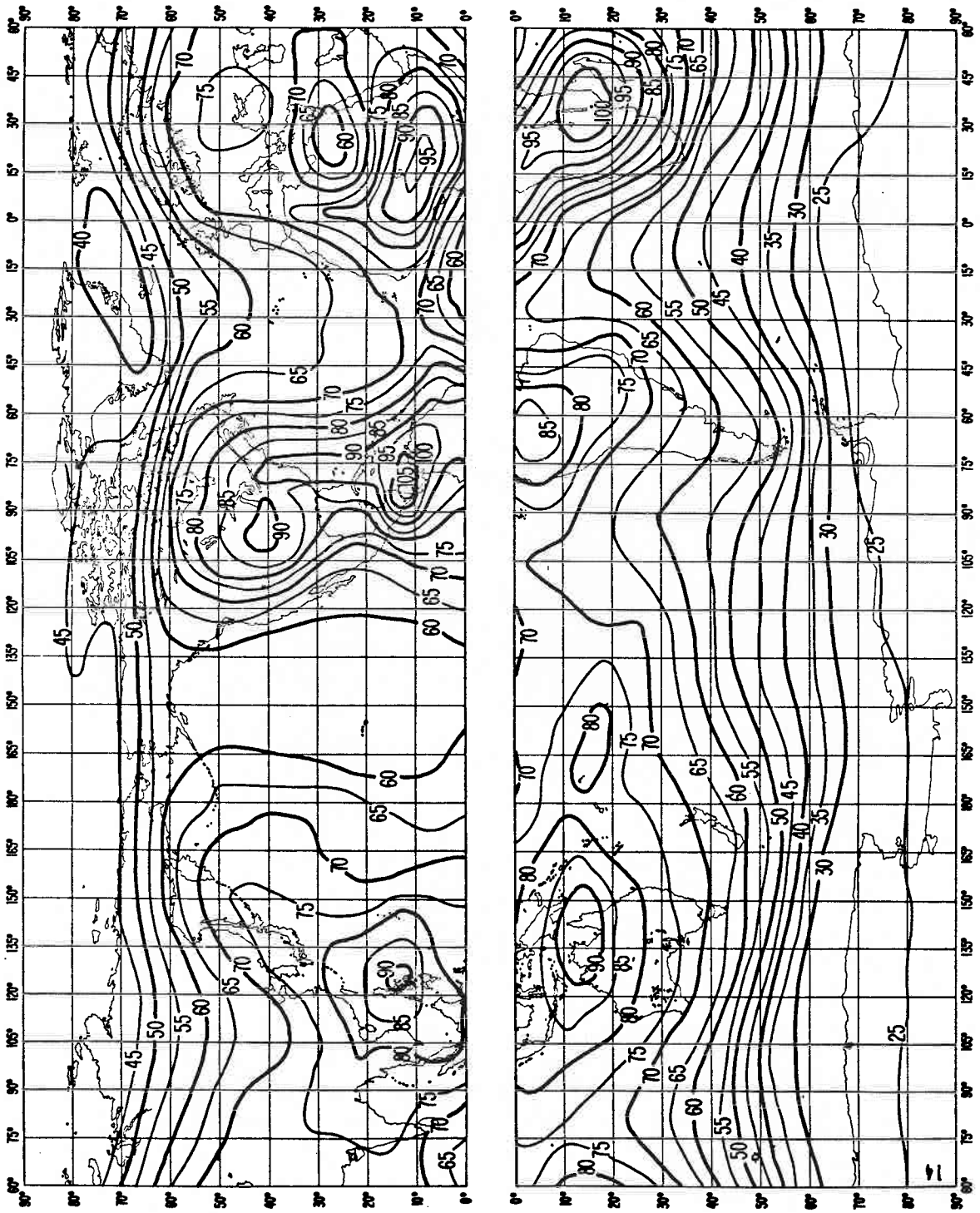

FIGURE 14a – *Expected values of atmospheric radio noise, F_{am} (dB above kT_0b at 1 MHz)*
(Summer; 0000-0400 h)

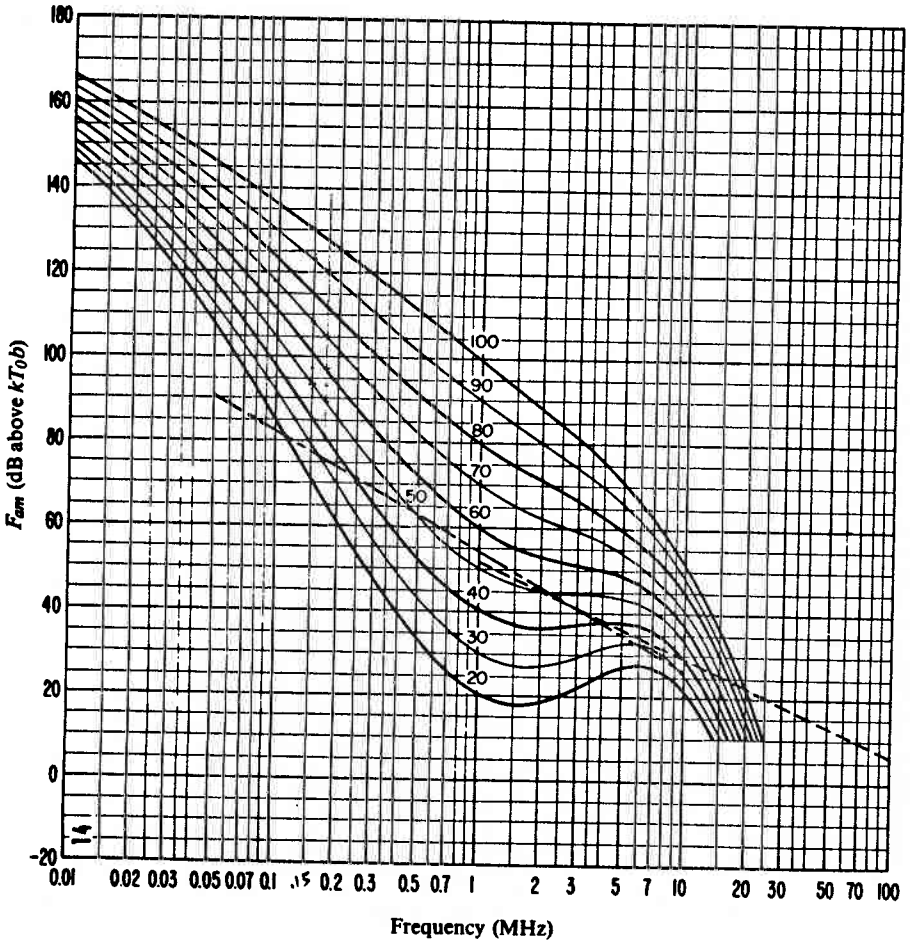

FIGURE 14b – *Variation of radio noise with frequency*
(Summer; 0000-0400 h)

———— Expected values of atmospheric noise

— · — · — · — Expected values of man-made noise at a quiet receiving location

— — — — — Expected values of galactic noise

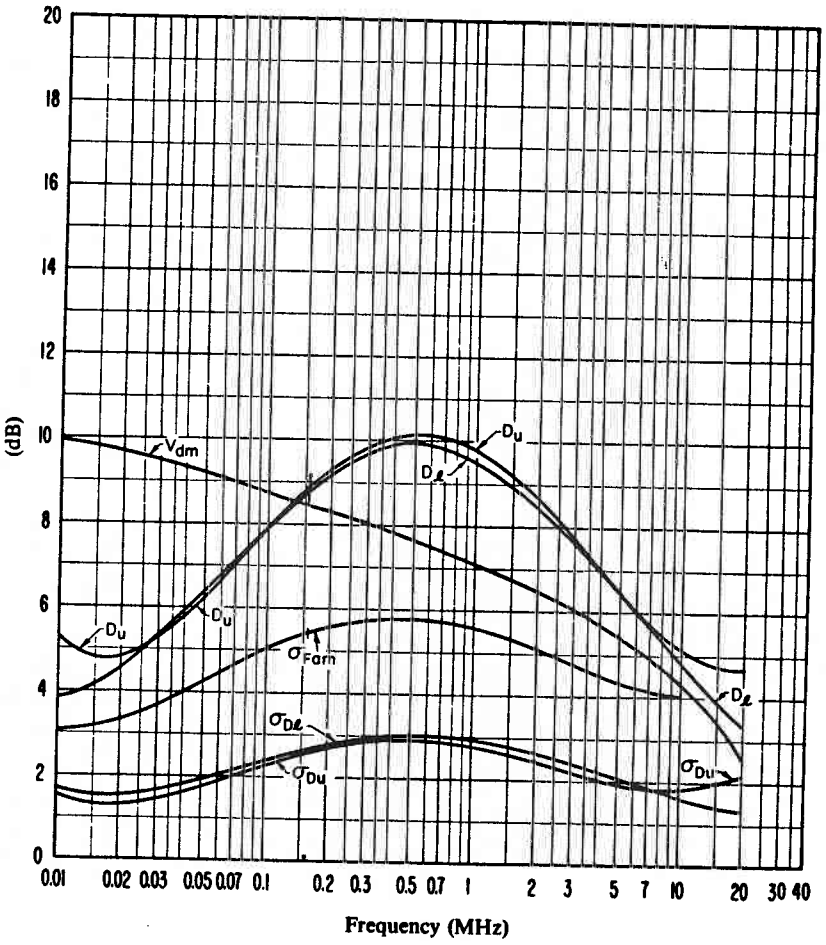

FIGURE 14c – *Data on noise variability and character*
(Summer; 0000-0400 h)

σ_{Fam} : Standard deviation of values of F_{am}
D_u : Ratio of upper decile to median value, F_{am}
σ_{Du} : Standard deviation of values of D_u
D_l : Ratio of median value, F_{am}, to lower decile
σ_{Dl} : Standard deviation of value of D_l
V_{dm} : Expected value of median deviation of average voltage. The values shown are for a bandwidth of 200 Hz.

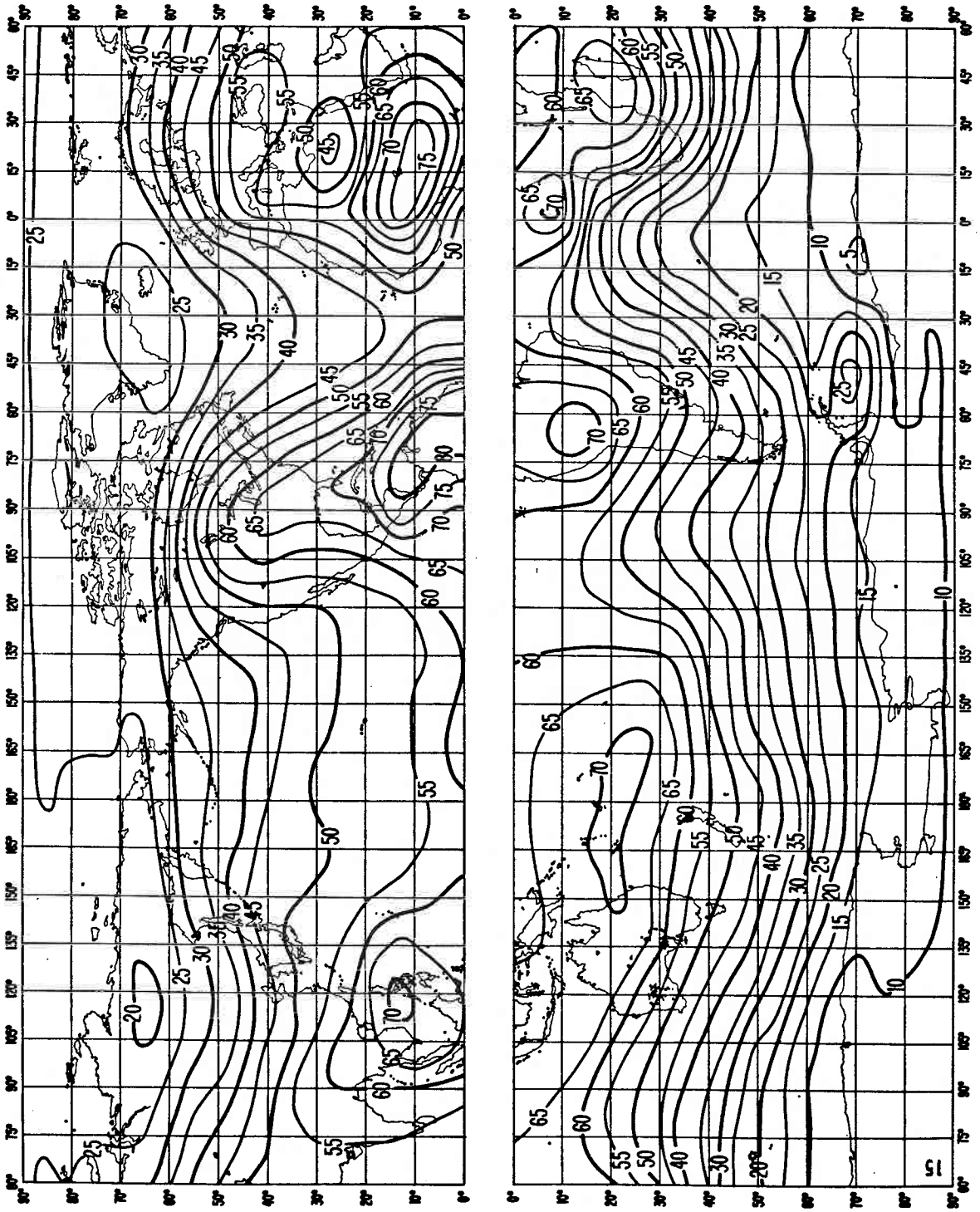

FIGURE 15a – *Expected values of atmospheric radio noise, F_{am} (dB above kT_0b at 1 MHz)*
(Summer; 0400-0800 h)

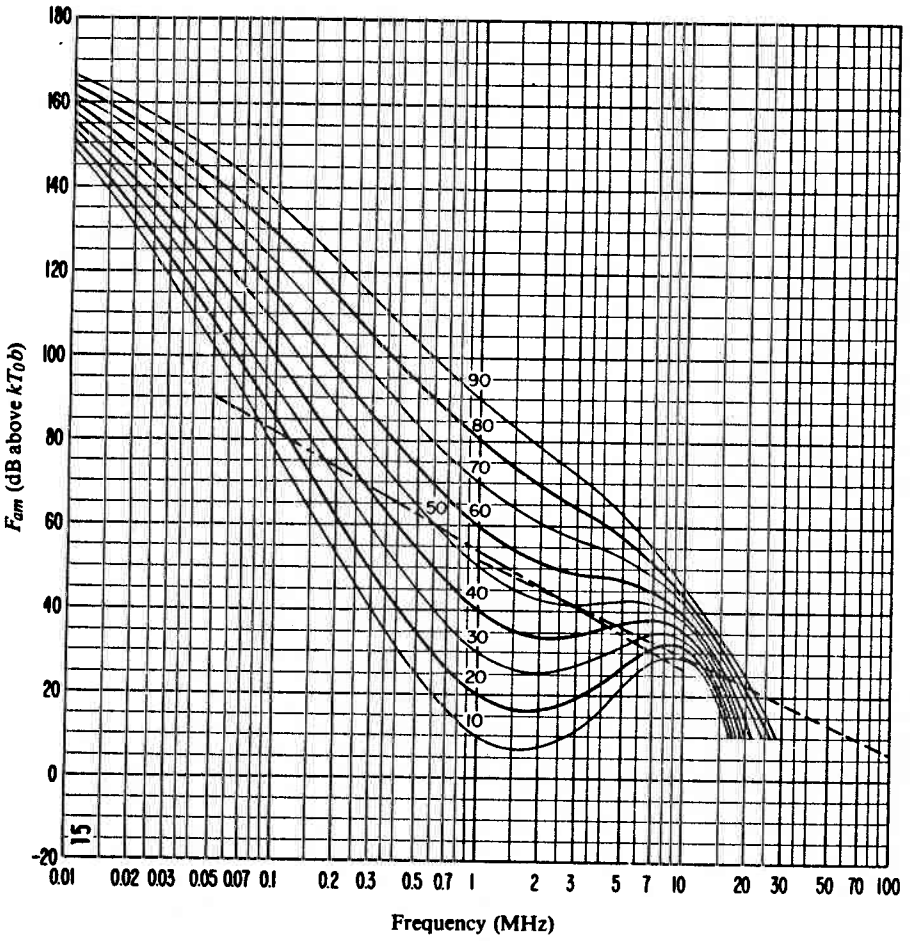

FIGURE 15b – *Variation of radio noise with frequency*
(Summer; 0400-0800 h)

———— Expected values of atmospheric noise

— · — · — · — Expected values of man-made noise at a quiet receiving location

— — — — — Expected values of galactic noise

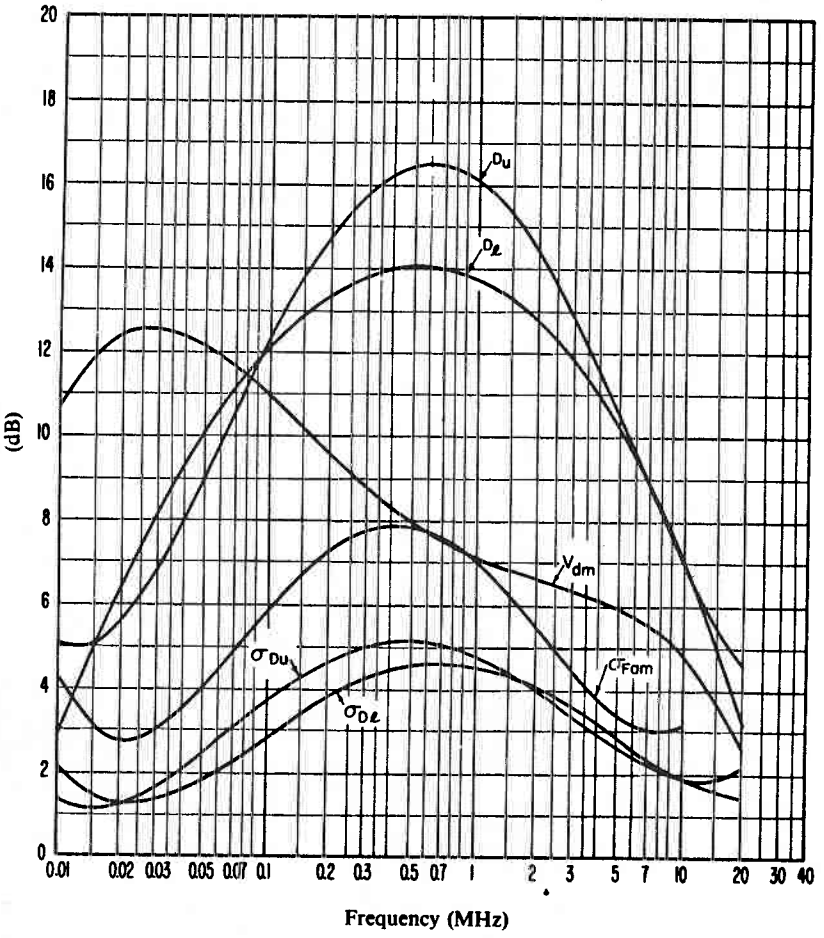

FIGURE 15c – *Data on noise variability and character*
(Summer; 0400-0800 h)

σ_{Fam} : Standard deviation of values of F_{am}
D_u : Ratio of upper decile to median value, F_{am}
σ_{Du} : Standard deviation of values of D_u
D_l : Ratio of median value, F_{am}, to lower decile
σ_{Dl} : Standard deviation of value of D_l
V_{dm} : Expected value of median deviation of average voltage. The values shown are for a bandwidth of 200 Hz.

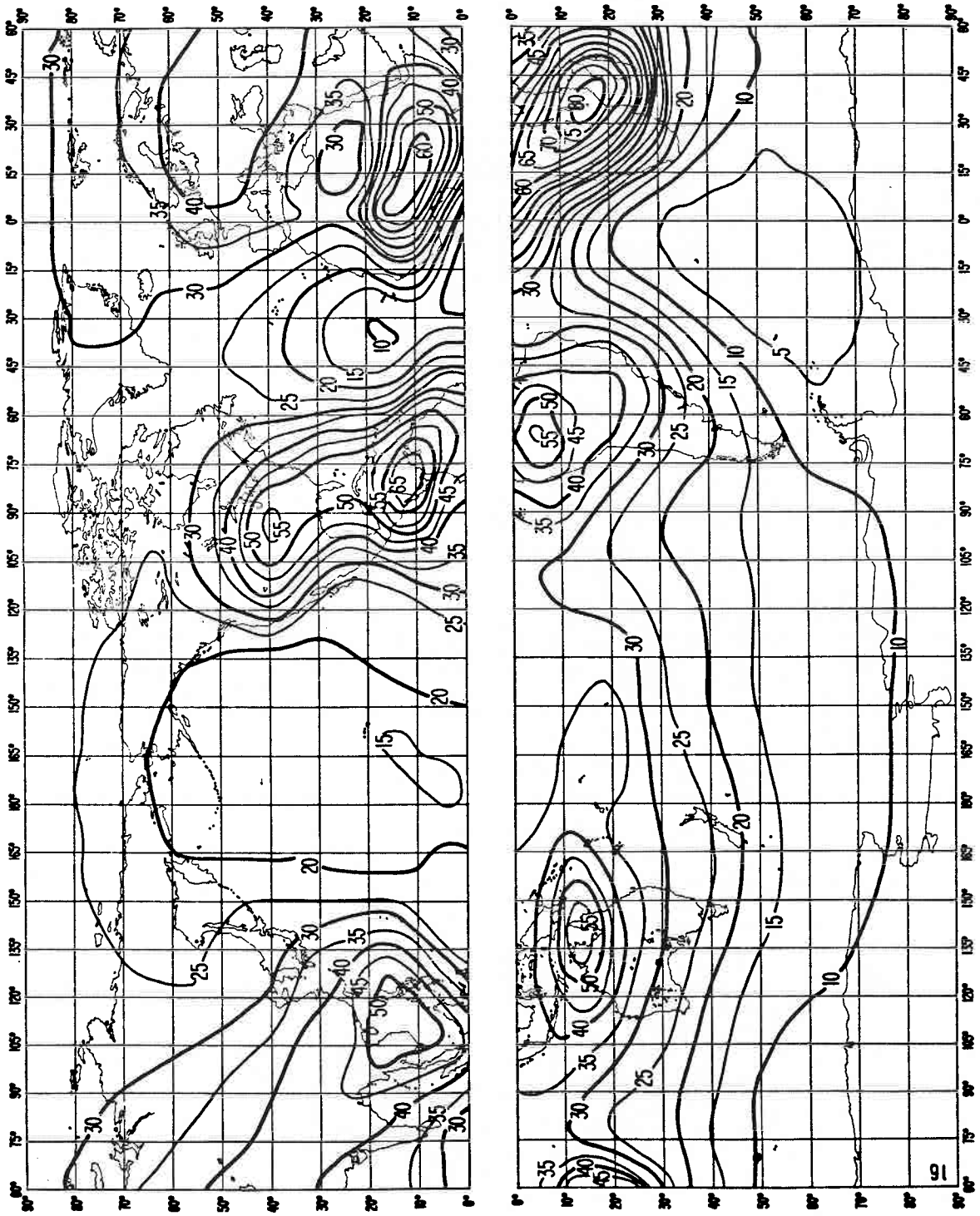

FIGURE 16a – *Expected values of atmospheric radio noise, F_{am} (dB above kT_0b at 1 MHz)*
(Summer; 0800-1200 h)

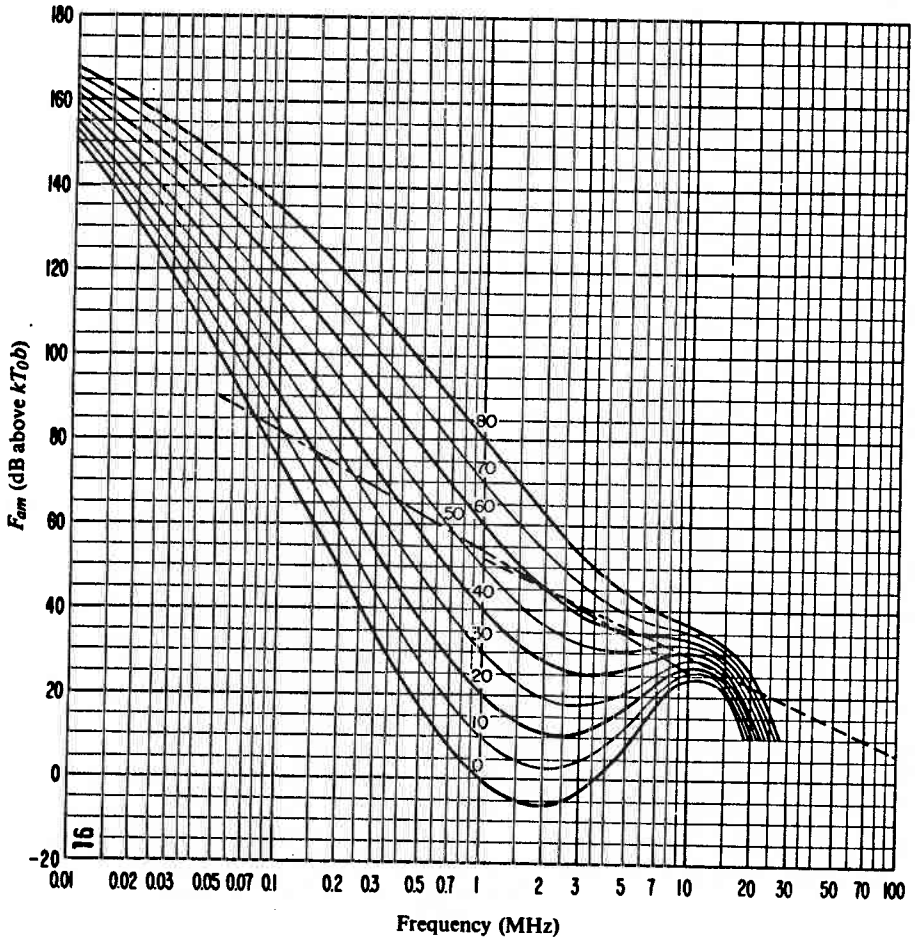

FIGURE 16b – *Variation of radio noise with frequency*
(Summer; 0800-1200 h)

——————— Expected values of atmospheric noise

— · — · — · — Expected values of man-made noise at a quiet receiving location

— — — — — Expected values of galactic noise

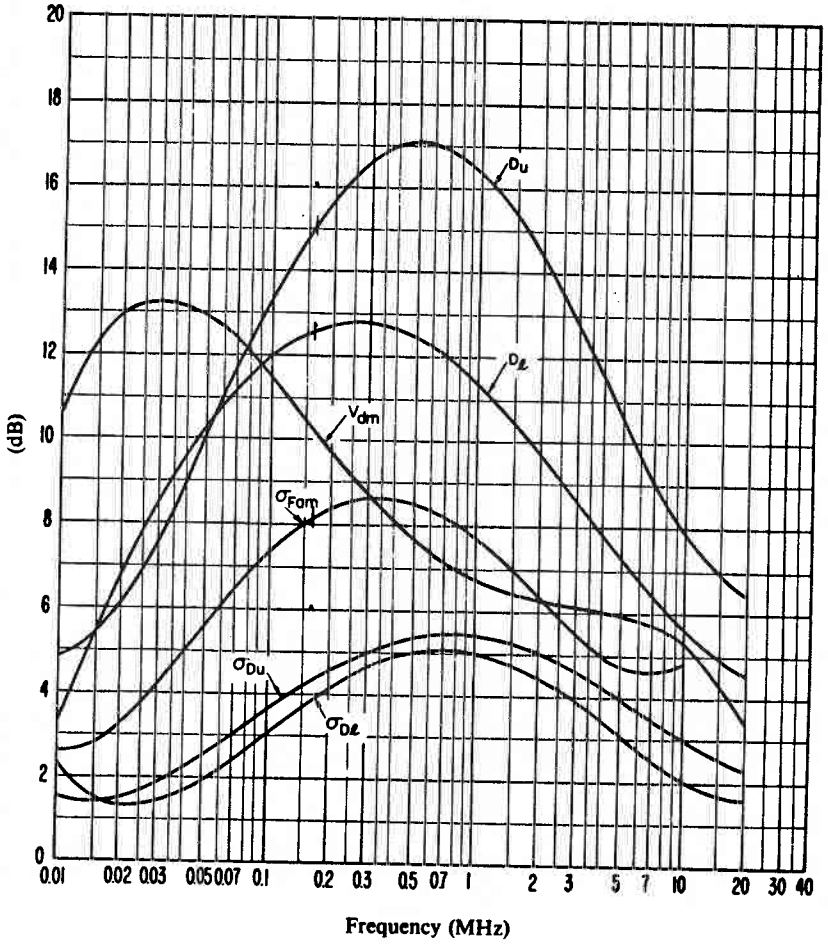

FIGURE 16c – *Data on noise variability and character*
(Summer; 0800-1200 h)

σ_{Fam} : Standard deviation of values of F_{am}
D_u : Ratio of upper decile to median value, F_{am}
σ_{Du} : Standard deviation of values of D_u
D_l : Ratio of median value, F_{am}, to lower decile
σ_{Dl} : Standard deviation of value of D_l
V_{dm} : Expected value of median deviation of average voltage. The values shown are for a bandwidth of 200 Hz.

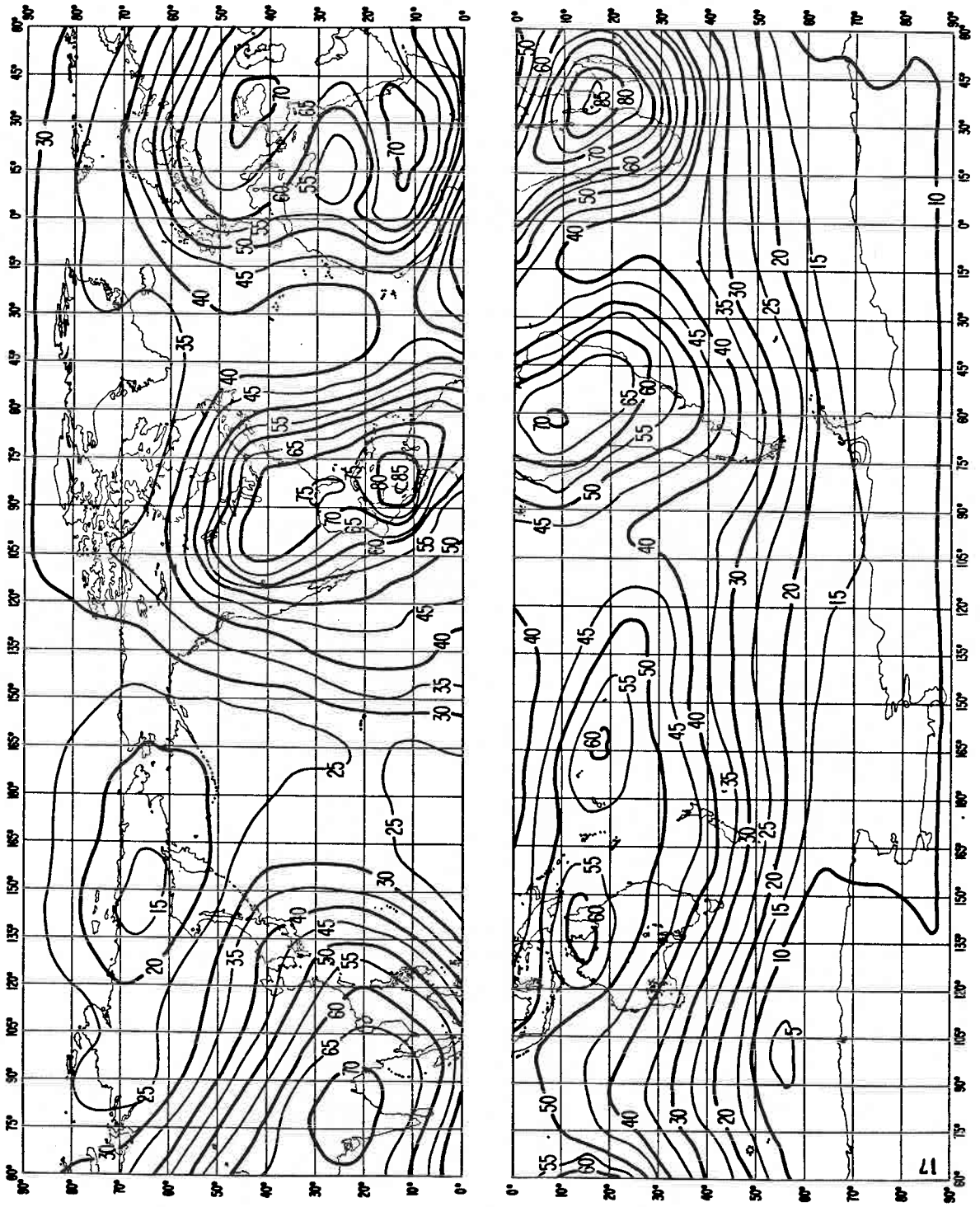

FIGURE 17a – *Expected values of atmospheric radio noise, F_{am} (dB above kT_0b at 1 MHz)*
(Summer; 1200-1600 h)

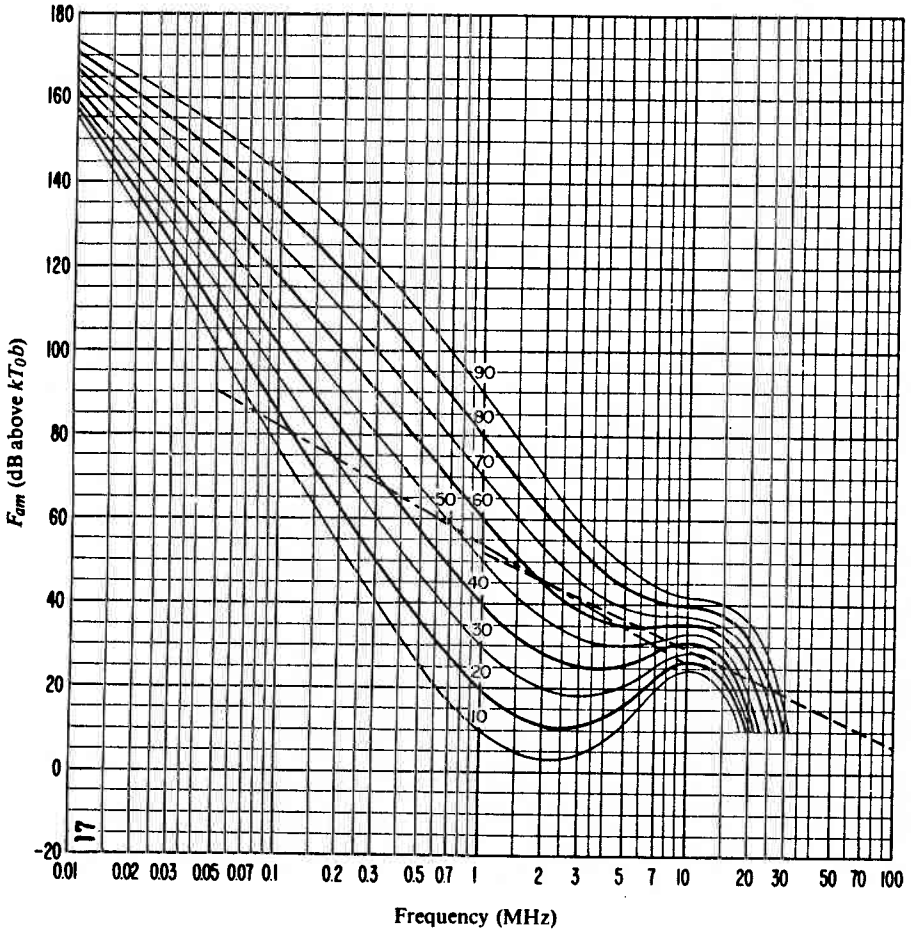

FIGURE 17b – *Variation of radio noise with frequency*
(Summer; 1200-1600 h)

——— Expected values of atmospheric noise

— · — · — · — Expected values of man-made noise at a quiet receiving location

— — — — — Expected values of galactic noise

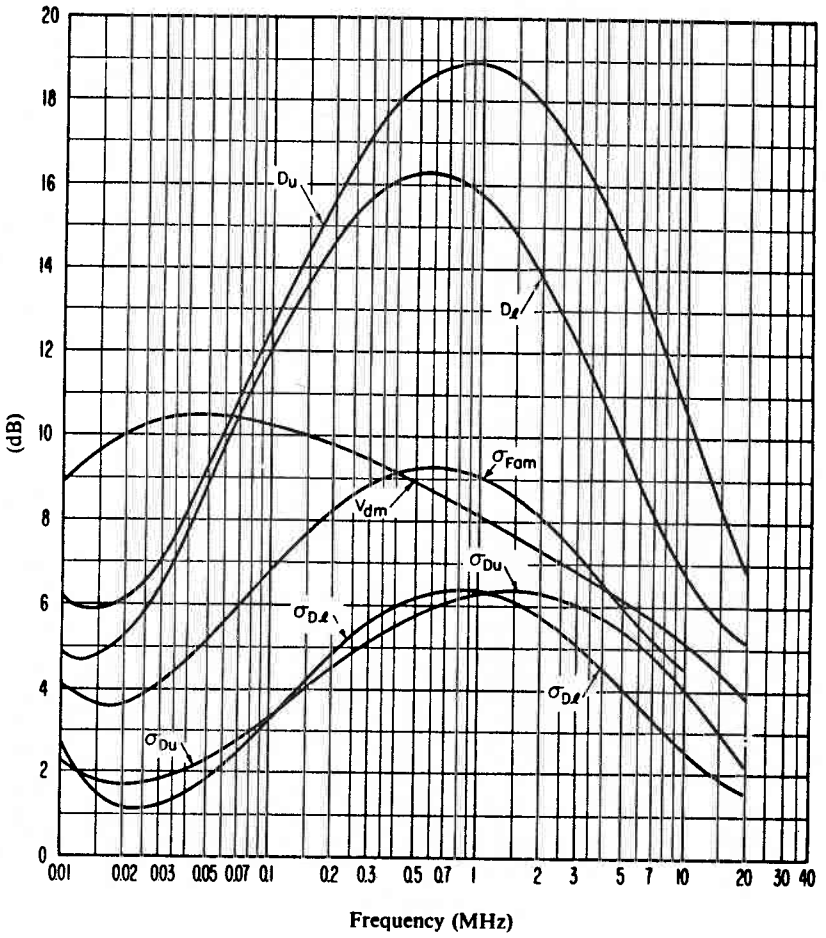

FIGURE 17c – *Data on noise variability and character*
(Summer; 1200-1600 h)

σ_{Fam} : Standard deviation of values of F_{am}
D_u : Ratio of upper decile to median value, F_{am}
σ_{Du} : Standard deviation of values of D_u
D_l : Ratio of median value, F_{am}, to lower decile
σ_{Dl} : Standard deviation of value of D_l
V_{dm} : Expected value of median deviation of average voltage. The values shown are for a bandwidth of 200 Hz.

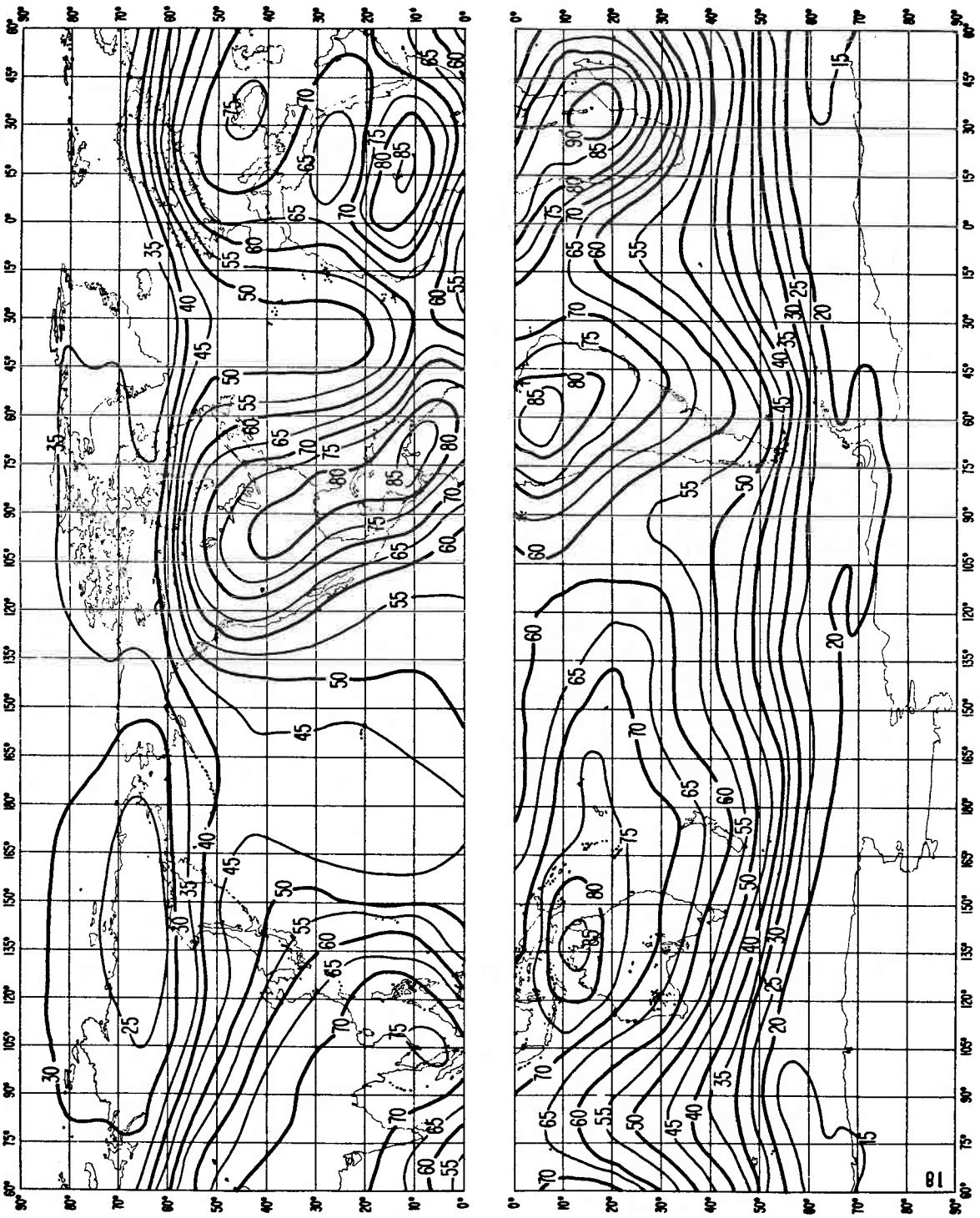

FIGURE 18a – *Expected values of atmospheric radio noise, F_{am} (dB above kT_0b at 1 MHz)*
(Summer; 1600-2000 h)

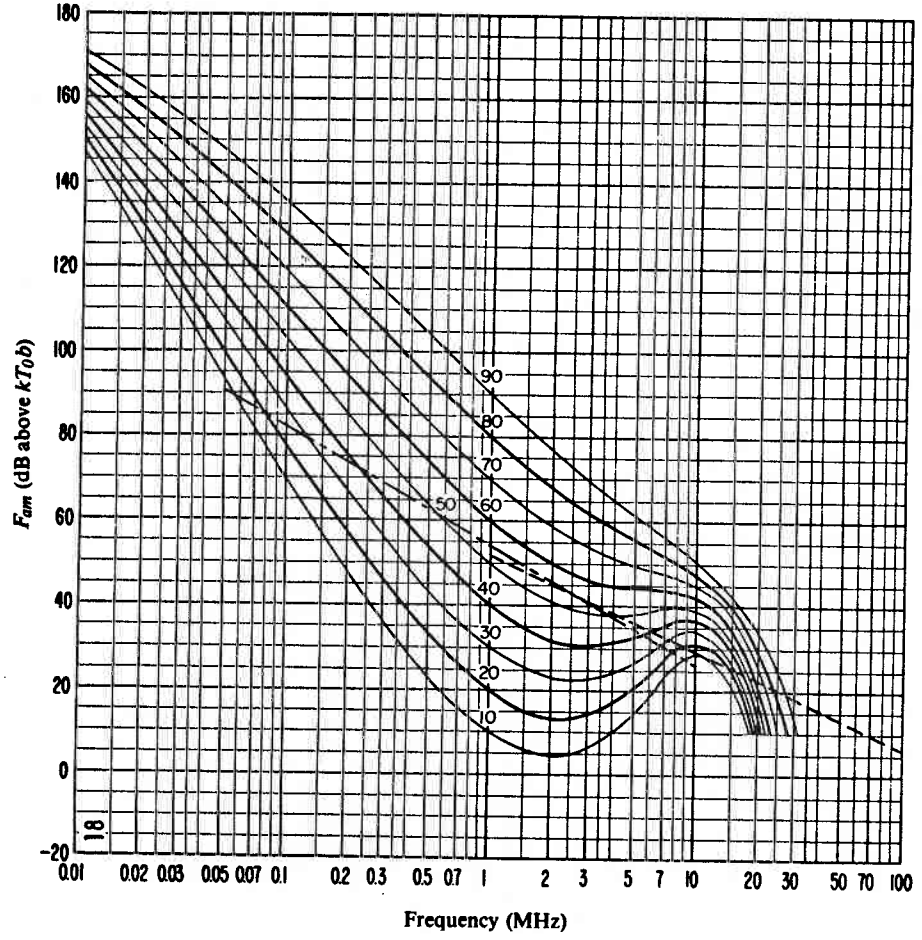

FIGURE 18b – *Variation of radio noise with frequency (Summer; 1600-2000 h)*

——— Expected values of atmospheric noise

— · — · — · — Expected values of man-made noise at a quiet receiving location

— — — — — Expected values of galactic noise

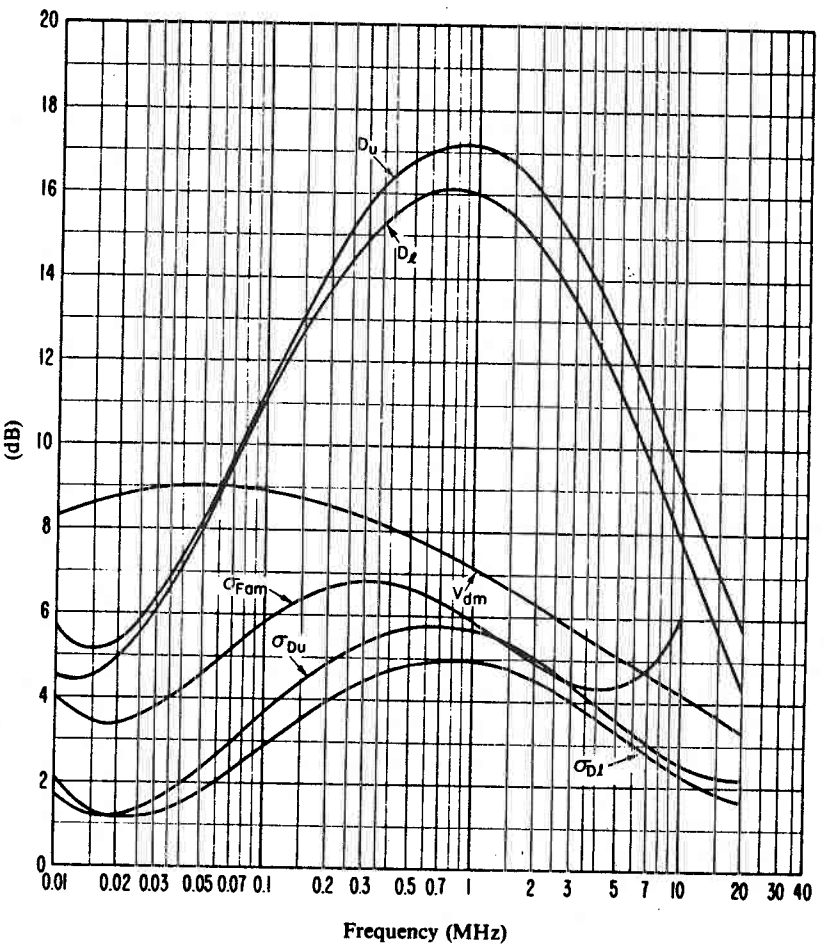

FIGURE 18c – *Data on noise variability and character (Summer; 1600-2000 h)*

σ_{Fam} : Standard deviation of values of F_{am}
D_u : Ratio of upper decile to median value, F_{am}
σ_{Du} : Standard deviation of values of D_u
D_l : Ratio of median value, F_{am}, to lower decile
σ_{Dl} : Standard deviation of value of D_l
V_{dm} : Expected value of median deviation of average voltage. The values shown are for a bandwidth of 200 Hz.

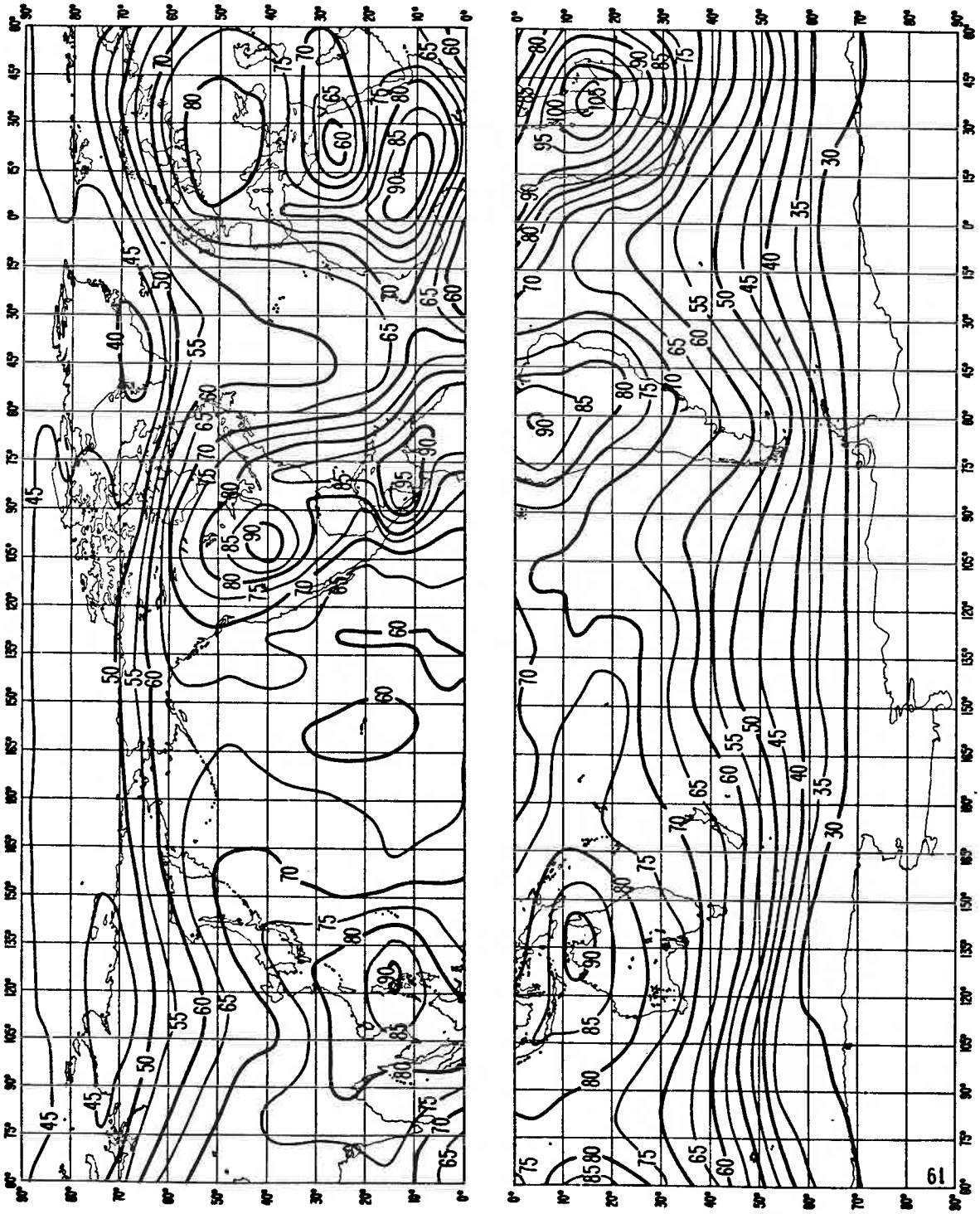

FIGURE 19a – *Expected values of atmospheric radio noise, F_{am} (dB above kT_0b at 1 MHz)*
(Summer; 2000-2400 h)

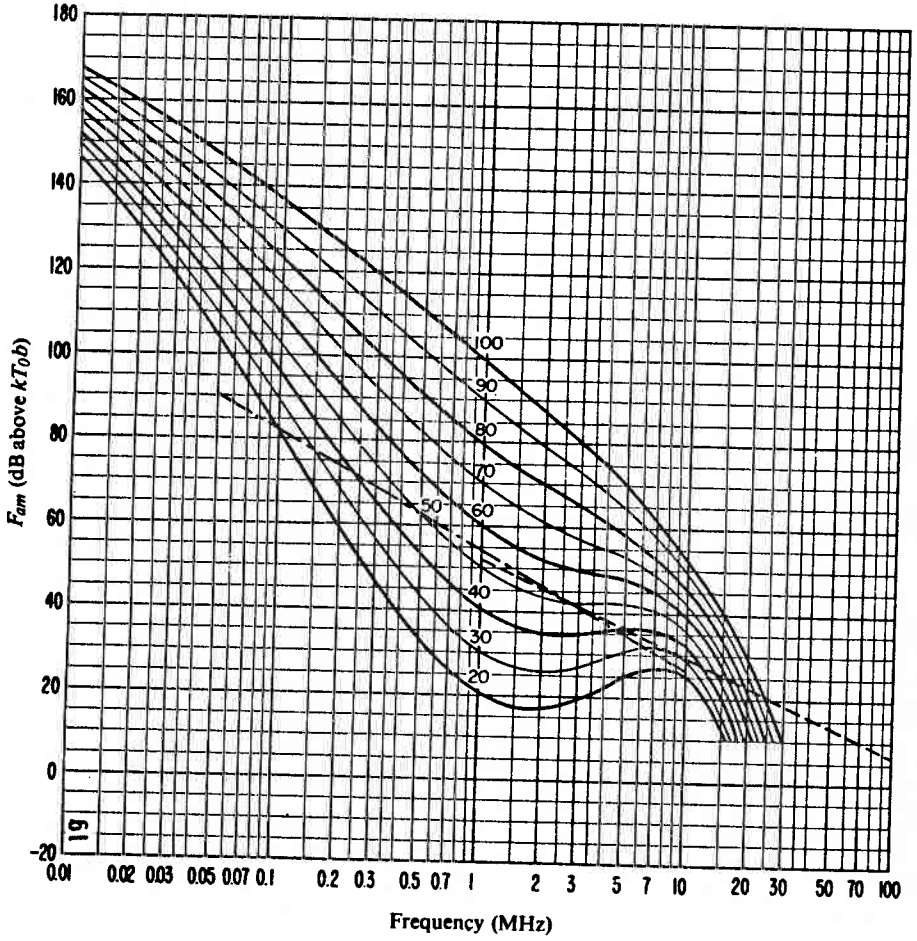

FIGURE 19b – *Variation of radio noise with frequency*
(Summer; 2000-2400 h)

———— Expected values of atmospheric noise

— · — · — · — Expected values of man-made noise at a quiet receiving location

— — — — — Expected values of galactic noise

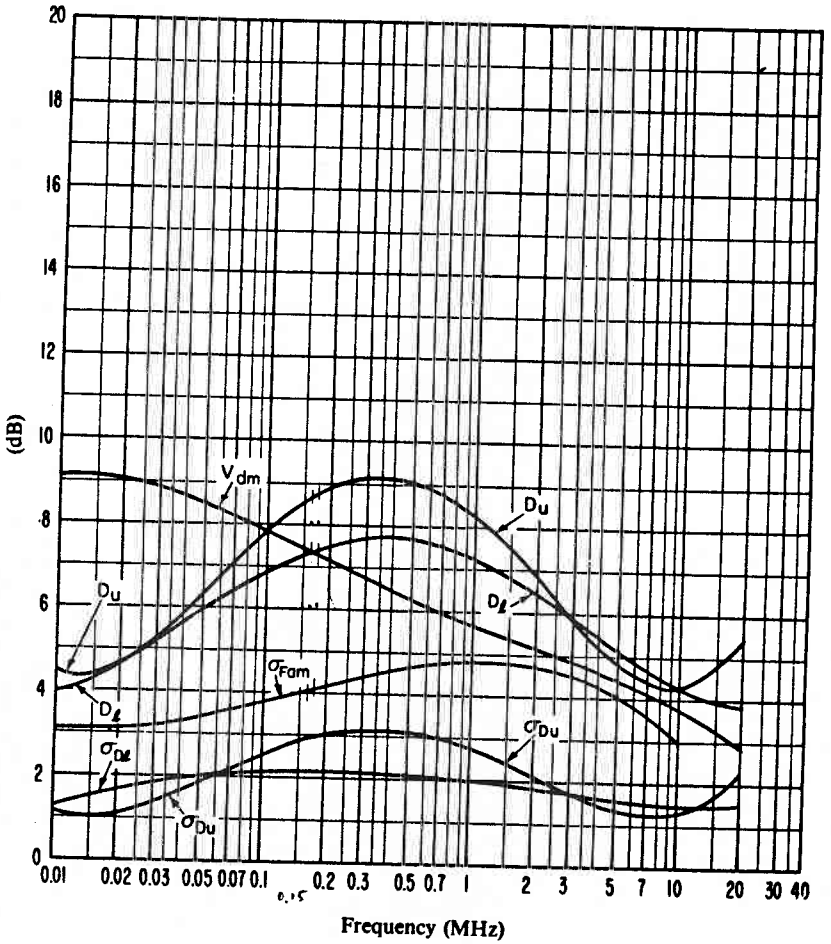

FIGURE 19c – *Data on noise variability and character*
(Summer; 2000-2400 h)

σ_{Fam} : Standard deviation of values of F_{am}
D_u : Ratio of upper decile to median value, F_{am}
σ_{Du} : Standard deviation of values of D_u
D_l : Ratio of median value, F_{am}, to lower decile
σ_{Dl} : Standard deviation of value of D_l
V_{dm} : Expected value of median deviation of average voltage. The values shown are for a bandwidth of 200 Hz.

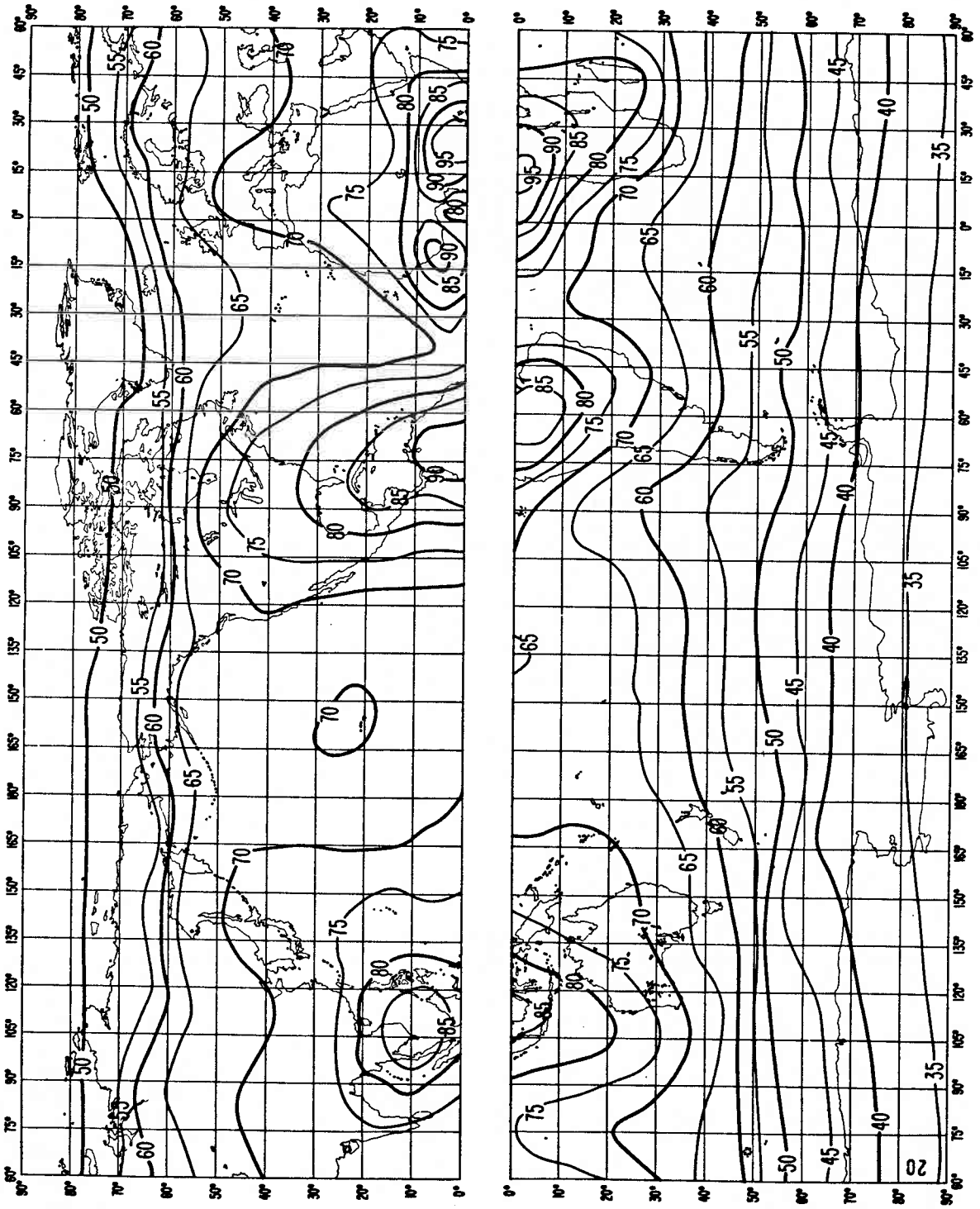

FIGURE 20a – *Expected values of atmospheric radio noise, F_{am} (dB above kT_0b at 1 MHz)*
(Autumn; 0000-0400 h)

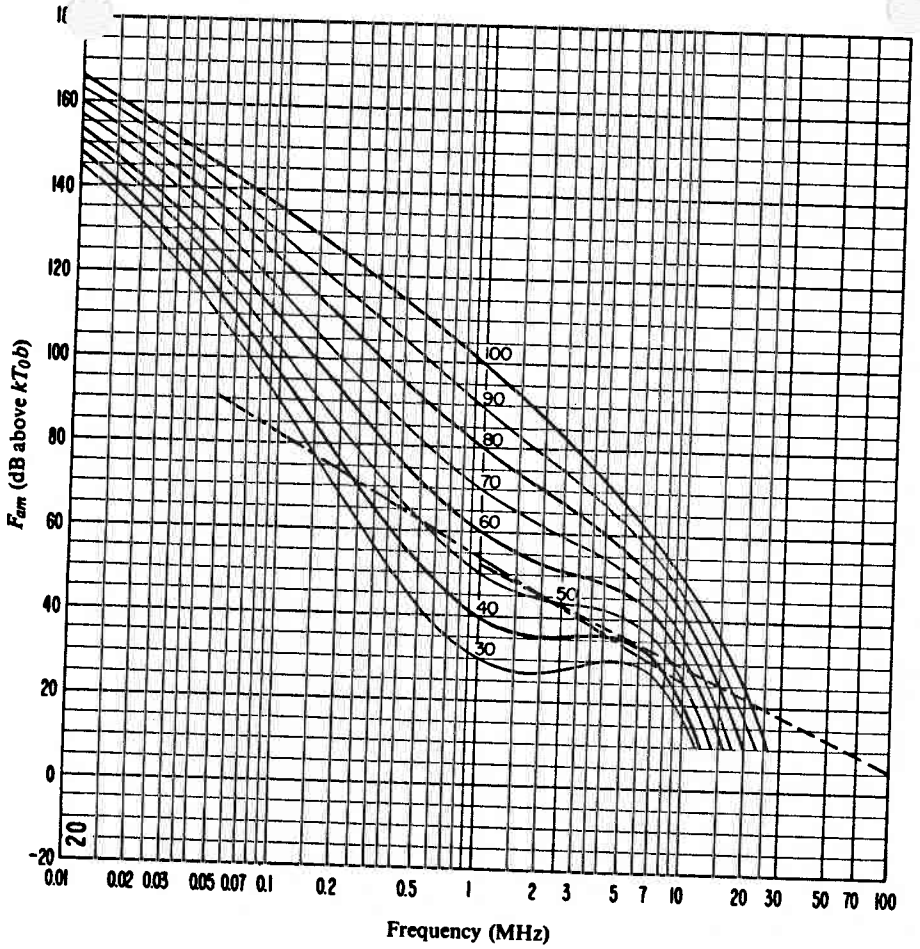

FIGURE 20b – *Variation of radio noise with frequency*
(Autumn; 0000-0400 h)

———— Expected values of atmospheric noise

— · — · — · — Expected values of man-made noise at a quiet receiving location

— — — — — Expected values of galactic noise

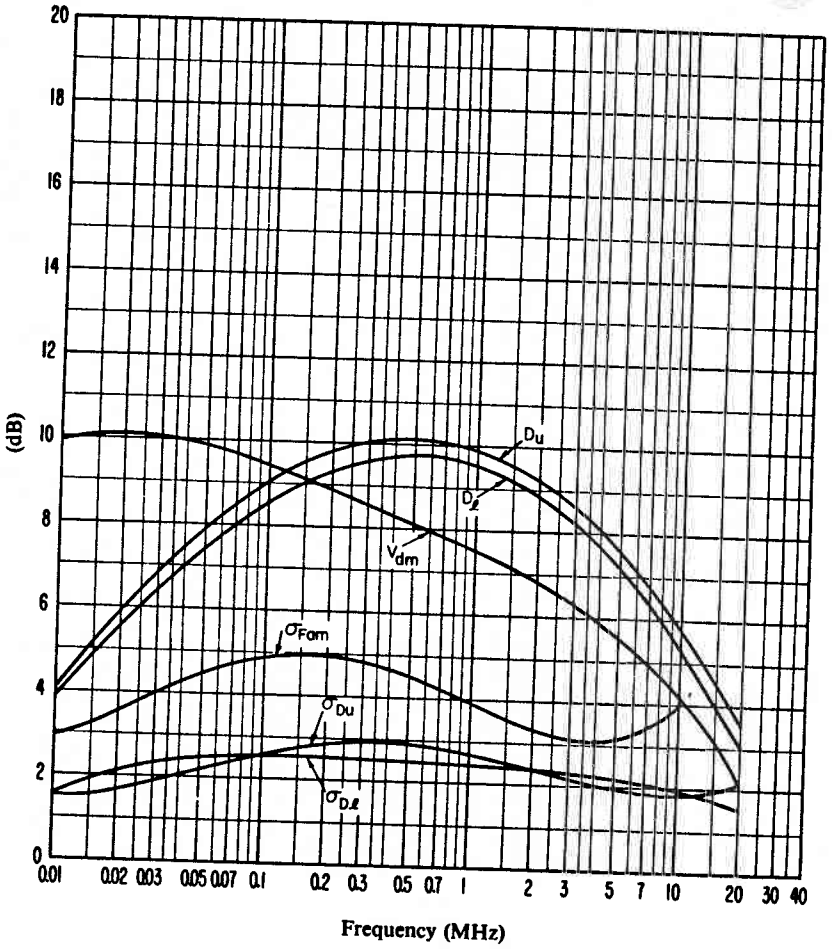

FIGURE 20c – *Data on noise variability and character*
(Autumn; 0000-0400 h)

σ_{Fam} : Standard deviation of values of F_{am}
D_u : Ratio of upper decile to median value, F_{am}
σ_{Du} : Standard deviation of values of D_u
D_l : Ratio of median value, F_{am}, to lower decile
σ_{Dl} : Standard deviation of value of D_l
V_{dm} : Expected value of median deviation of average voltage. The values shown are for a bandwidth of 200 Hz.

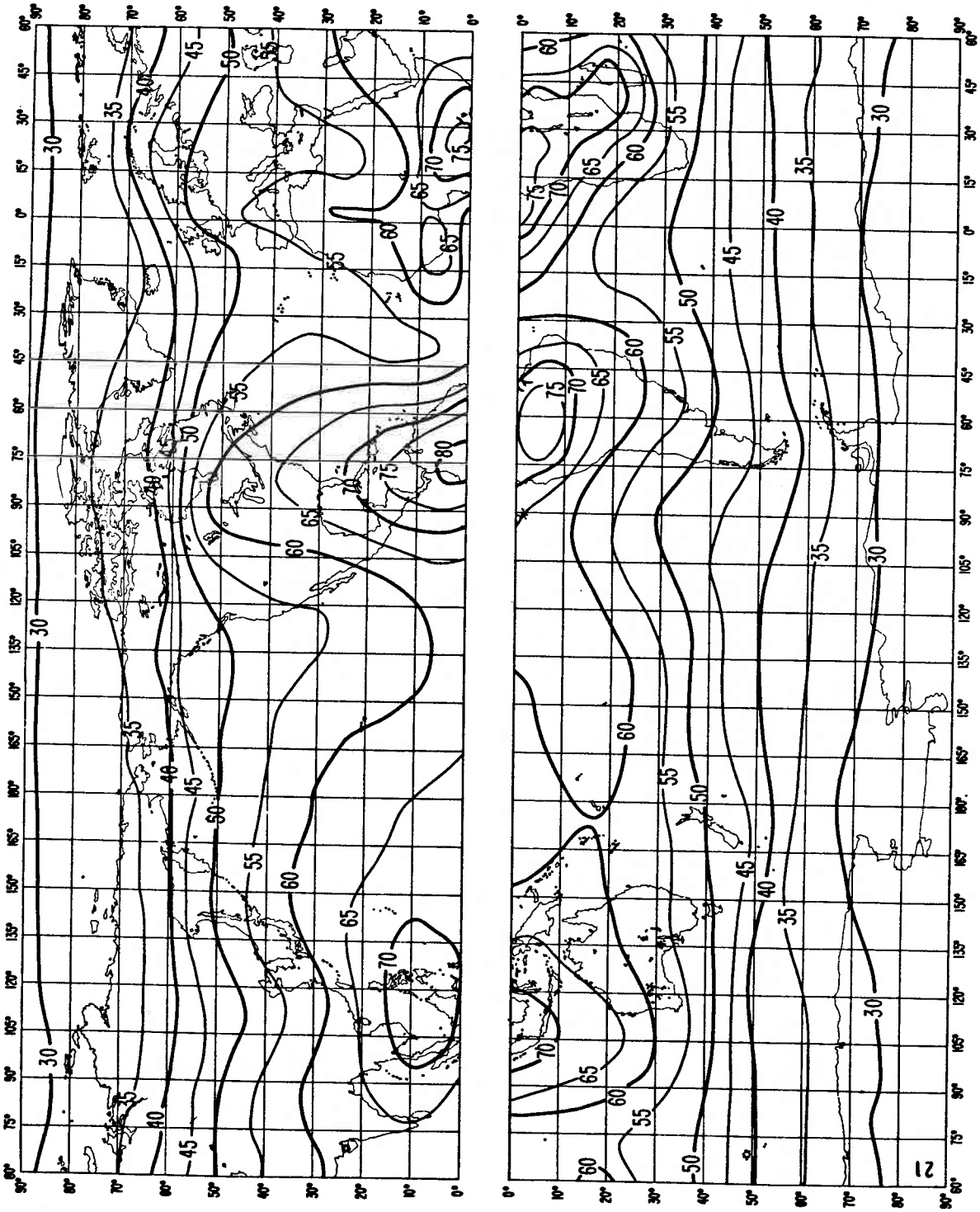

FIGURE 21a – *Expected values of atmospheric radio noise, F_{am} (dB above kT_0b at 1 MHz)*
(Autumn; 0400-0800 h)

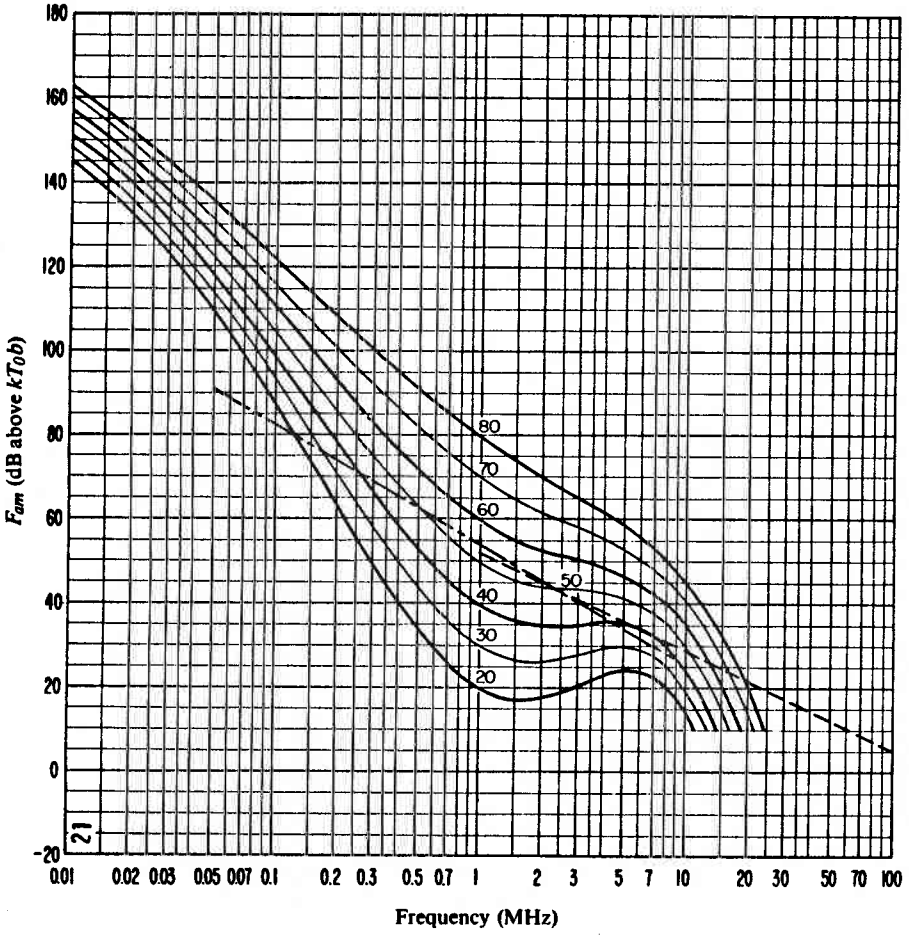

FIGURE 21b – *Variation of radio noise with frequency*
(Autumn; 0400-0800 h)

———— Expected values of atmospheric noise

— · — · — · — Expected values of man-made noise at a quiet receiving location

— — — — — Expected values of galactic noise

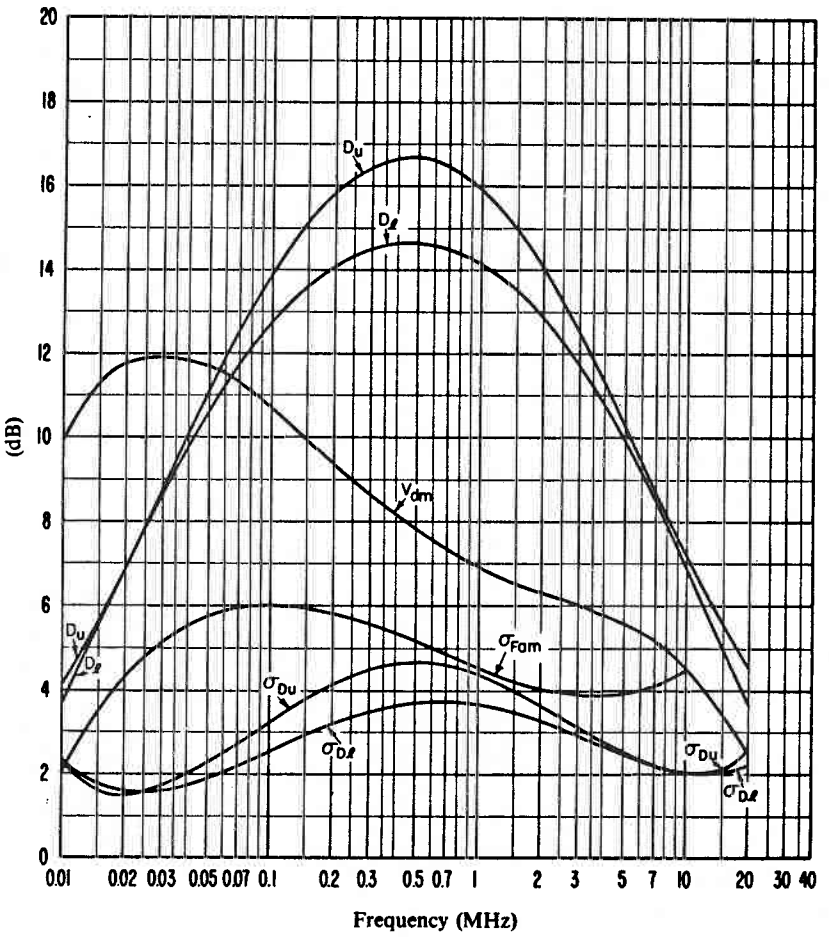

FIGURE 21c – *Data on noise variability and character*
(Autumn; 0400-0800 h)

σ_{Fam} : Standard deviation of values of F_{am}
D_u : Ratio of upper decile to median value, F_{am}
σ_{Du} : Standard deviation of values of D_u
D_l : Ratio of median value, F_{am}, to lower decile
σ_{Dl} : Standard deviation of value of D_l
V_{dm} : Expected value of median deviation of average voltage. The values shown are for a bandwidth of 200 Hz.

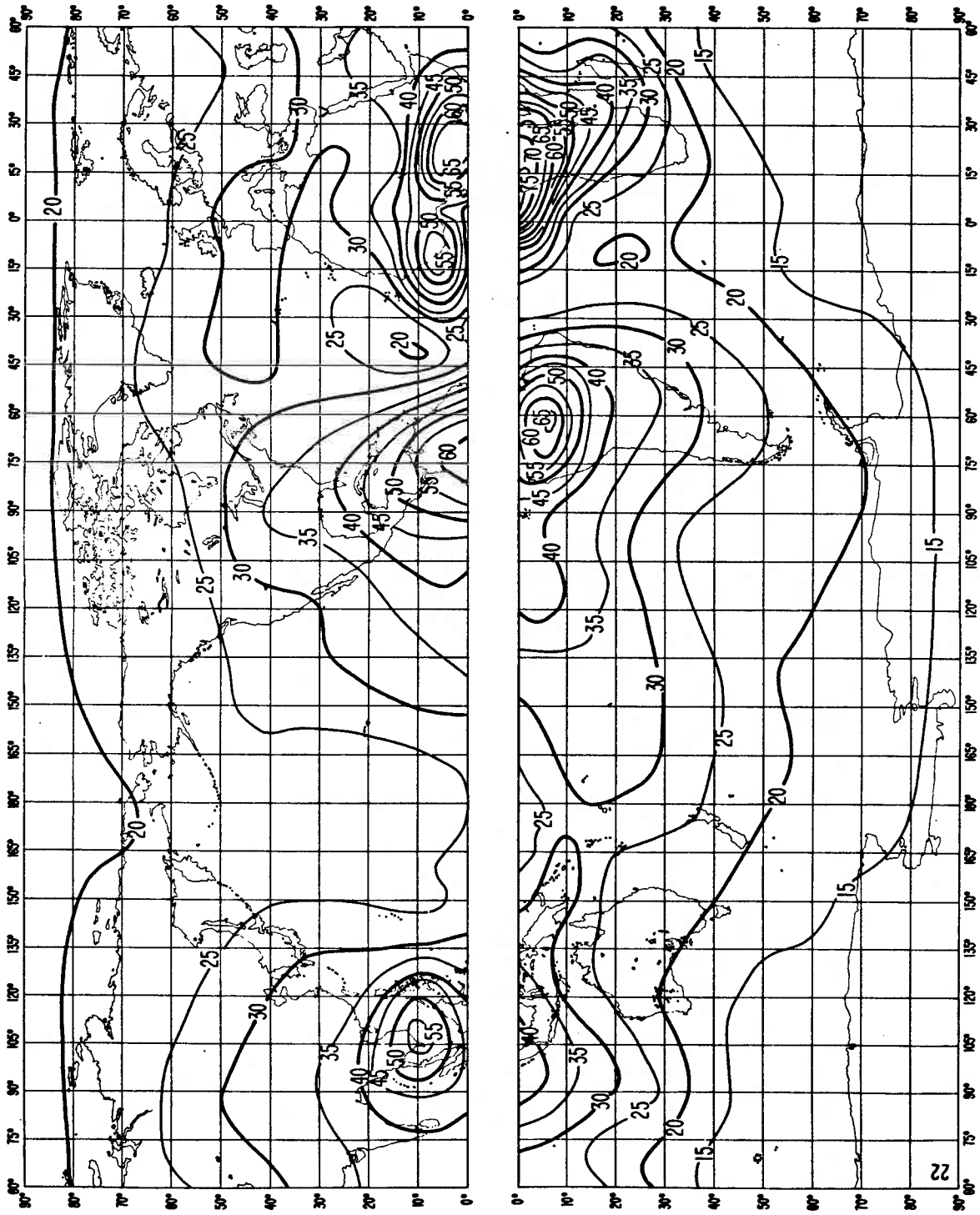

FIGURE 22a – *Expected values of atmospheric radio noise, F_{am} (dB above kT_0b at 1 MHz)*
(Autumn; 0800-1200 h)

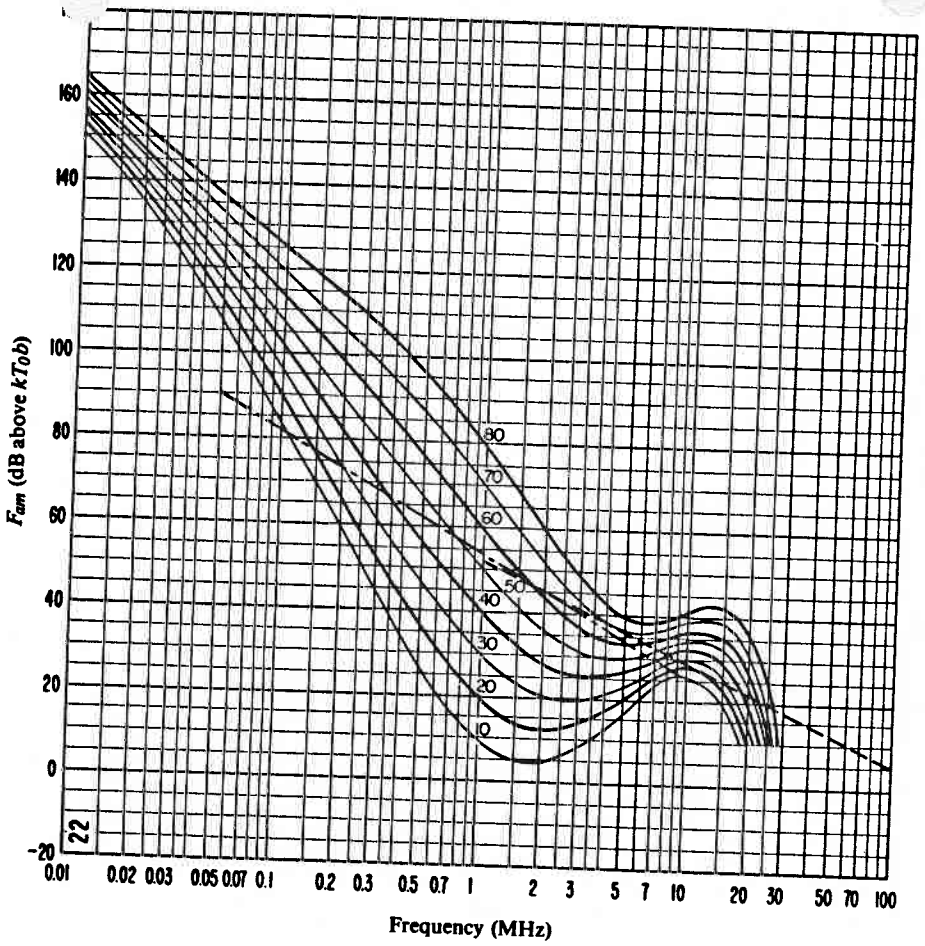

FIGURE 22b – *Variation of radio noise with frequency (Autumn; 0800-1200 h)*

——— Expected values of atmospheric noise

— · — · — — Expected values of man-made noise at a quiet receiving location

— — — — — Expected values of galactic noise

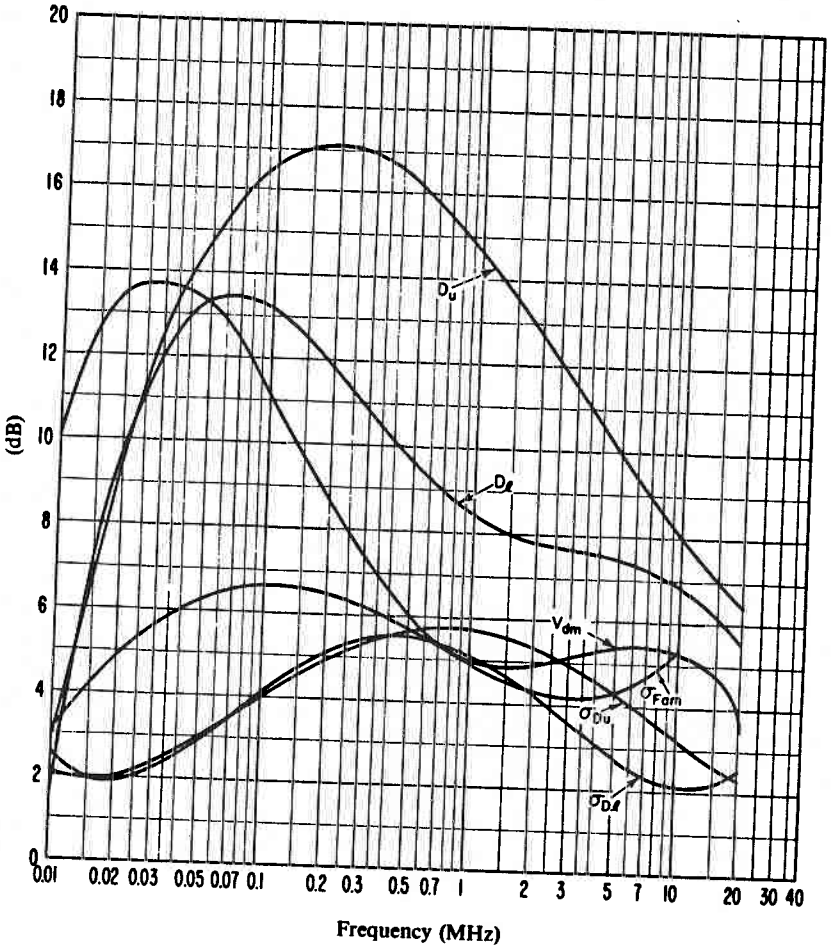

FIGURE 22c – *Data on noise variability and character (Autumn; 0800-1200 h)*

σ_{Fam} : Standard deviation of values of F_{am}
D_u : Ratio of upper decile to median value, F_{am}
σ_{Du} : Standard deviation of values of D_u
D_l : Ratio of median value, F_{am}, to lower decile
σ_{Dl} : Standard deviation of value of D_l
V_{dm} : Expected value of median deviation of average voltage. The values shown are for a bandwidth of 200 Hz.

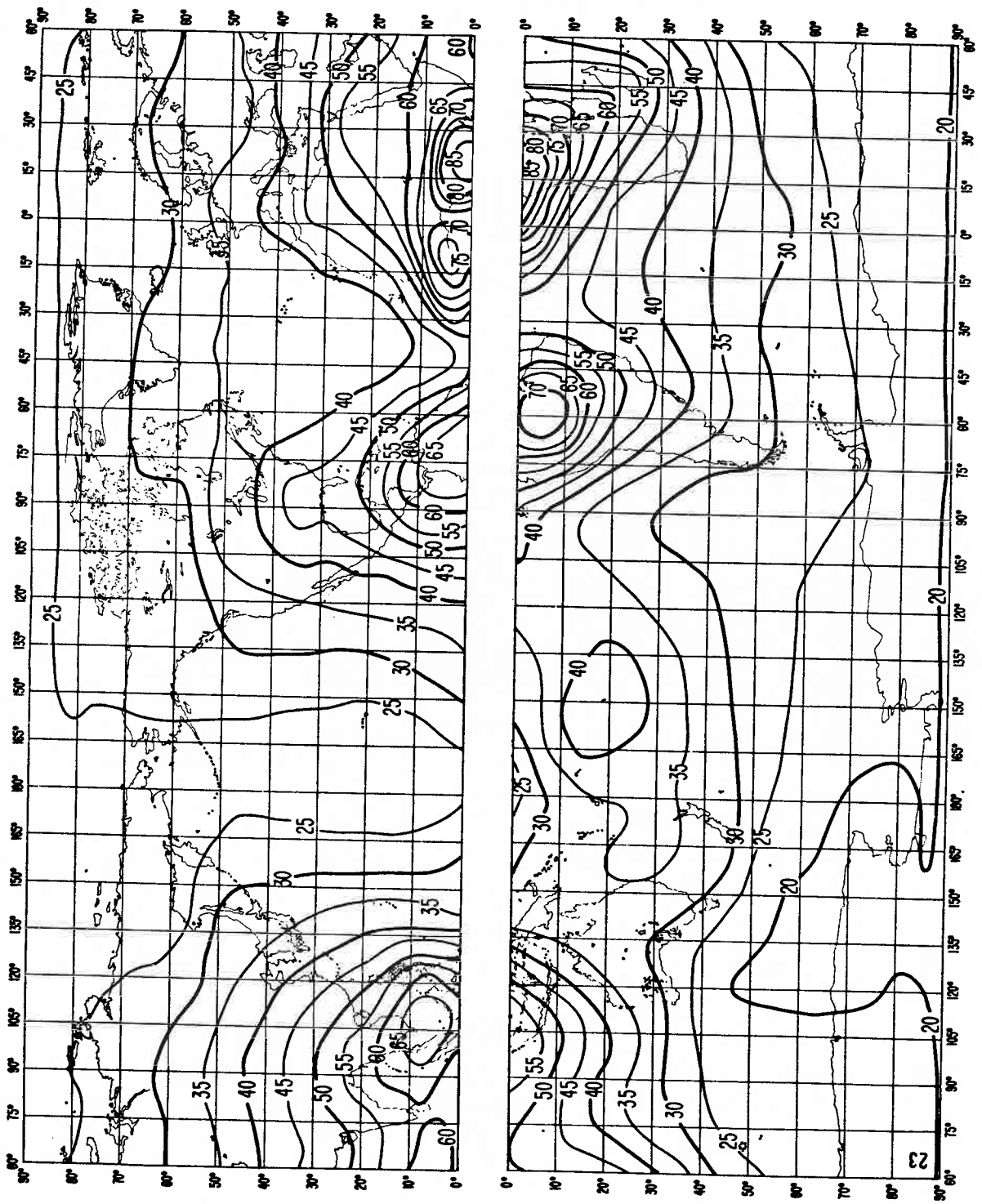

FIGURE 23a – *Expected values of atmospheric radio noise, F_{am} (dB above kT_0b at 1 MHz)*
(Autumn; 1200-1600 h)

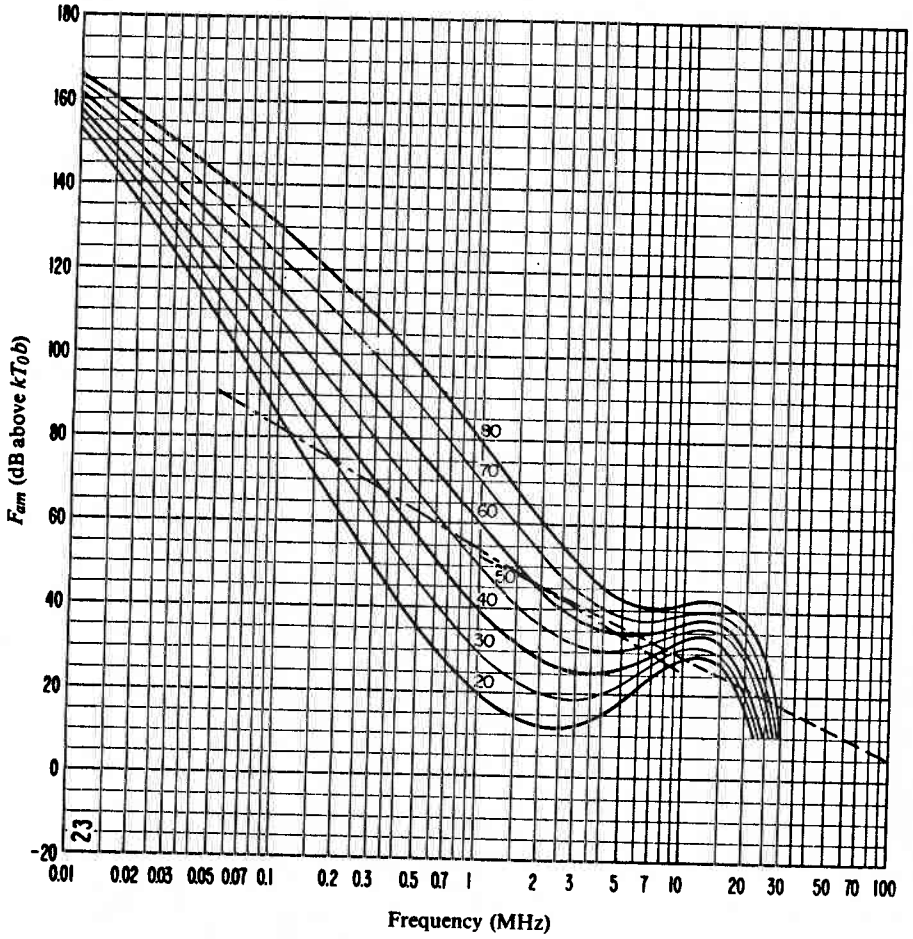

FIGURE 23b – *Variation of radio noise with frequency*
(Autumn; 1200-1600 h)

———— Expected values of atmospheric noise

— · — · — · — Expected values of man-made noise at a quiet receiving location

— — — — — Expected values of galactic noise

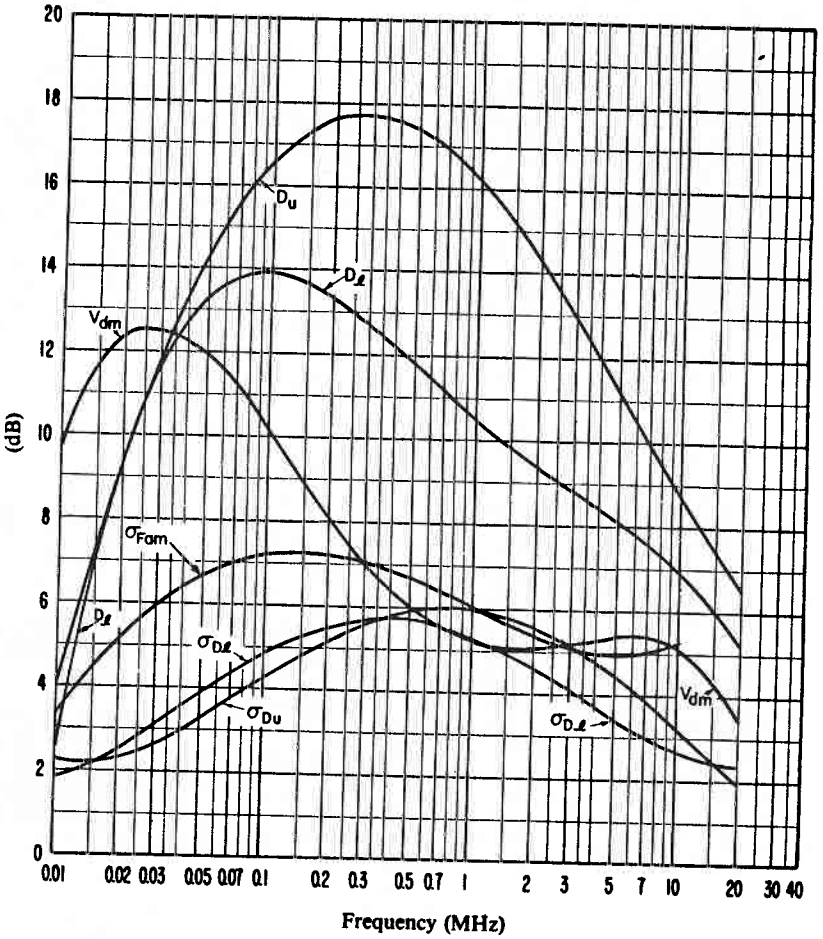

FIGURE 23c – *Data on noise variability and character*
(Autumn; 1200-1600 h)

σ_{Fam} : Standard deviation of values of F_{am}
D_u : Ratio of upper decile to median value, F_{am}
σ_{Du} : Standard deviation of values of D_u
D_l : Ratio of median value, F_{am}, to lower decile
σ_{Dl} : Standard deviation of value of D_l
V_{dm} : Expected value of median deviation of average voltage. The values shown are for a bandwidth of 200 Hz.

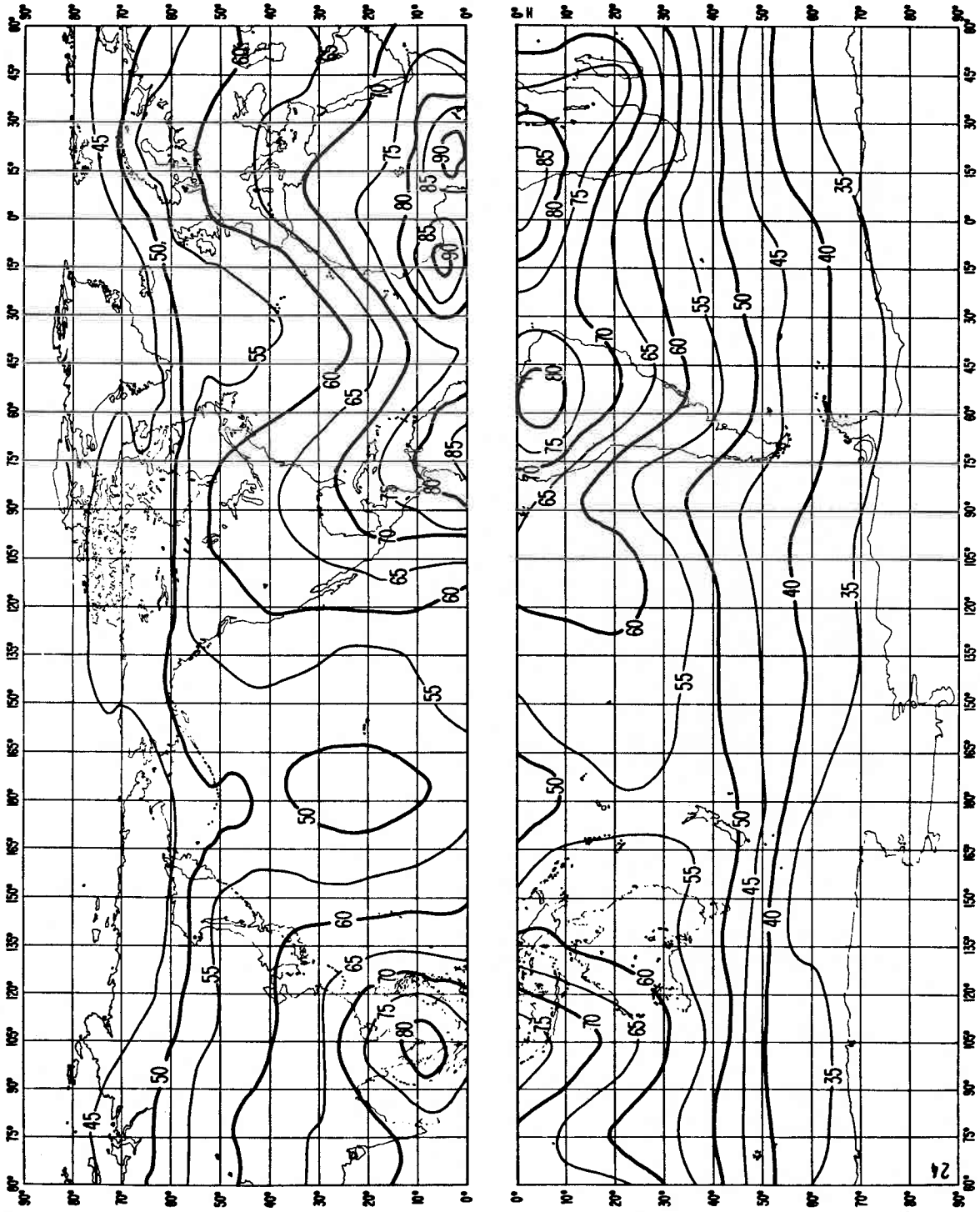

FIGURE 24a – *Expected values of atmospheric radio noise, F_{am} (dB above kT_0b at 1 MHz)*
(Autumn; 1600-2000 h)

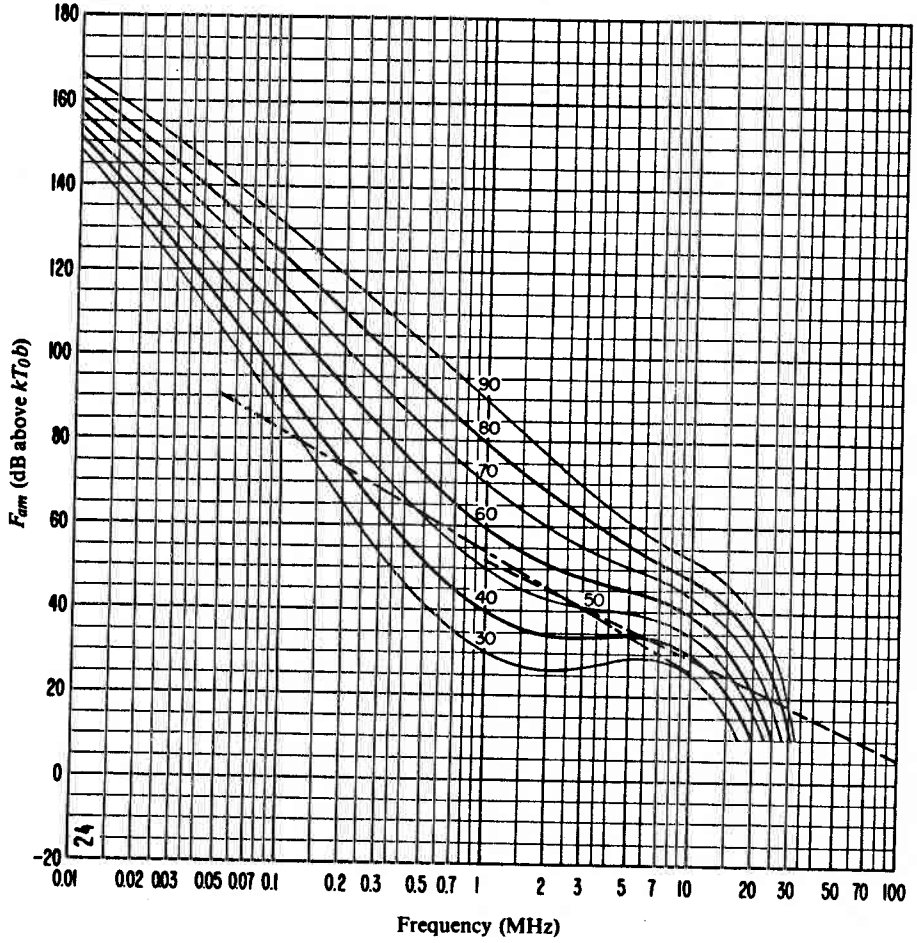

FIGURE 24b – *Variation of radio noise with frequency (Autumn; 1600-2000 h)*

——— Expected values of atmospheric noise

— · — · — · — Expected values of man-made noise at a quiet receiving location

— — — — — Expected values of galactic noise

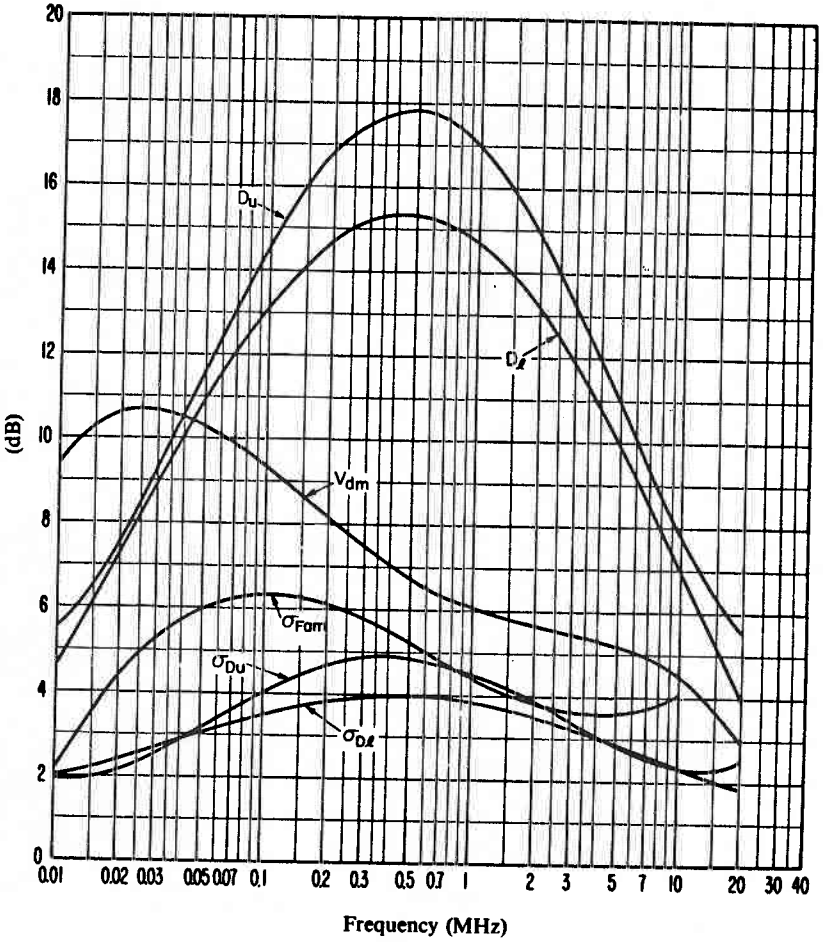

FIGURE 24c – *Data on noise variability and character (Autumn; 1600-2000 h)*

σ_{Fam} : Standard deviation of values of F_{am}
D_u : Ratio of upper decile to median value, F_{am}
σ_{Du} : Standard deviation of values of D_u
D_l : Ratio of median value, F_{am}, to lower decile
σ_{Dl} : Standard deviation of value of D_l
V_{dm} : Expected value of median deviation of average voltage. The values shown are for a bandwidth of 200 Hz.

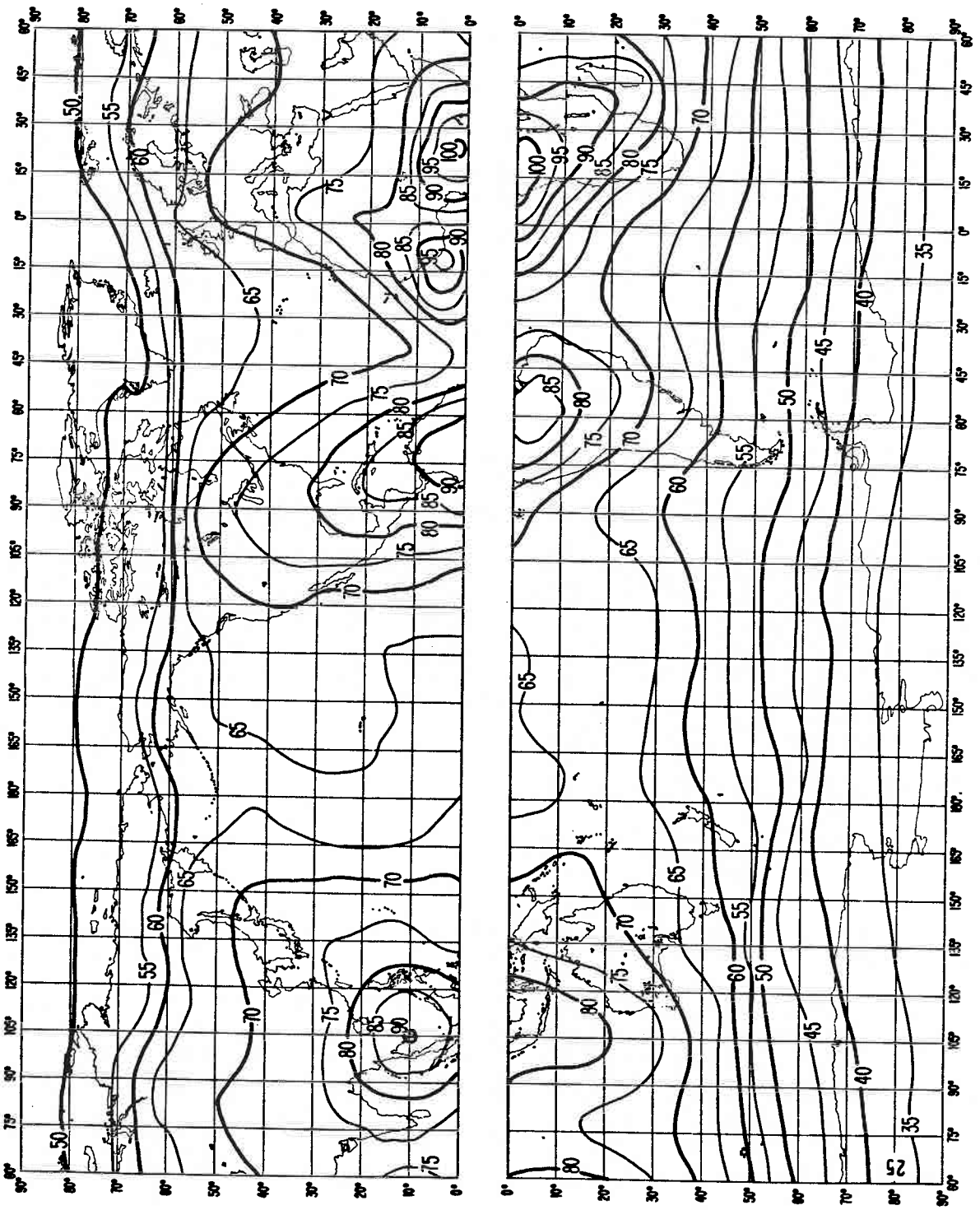

FIGURE 25a – *Expected values of atmospheric radio noise, F_{am} (dB above kT_0b at 1 MHz)*
(Autumn; 2000-2400 h)

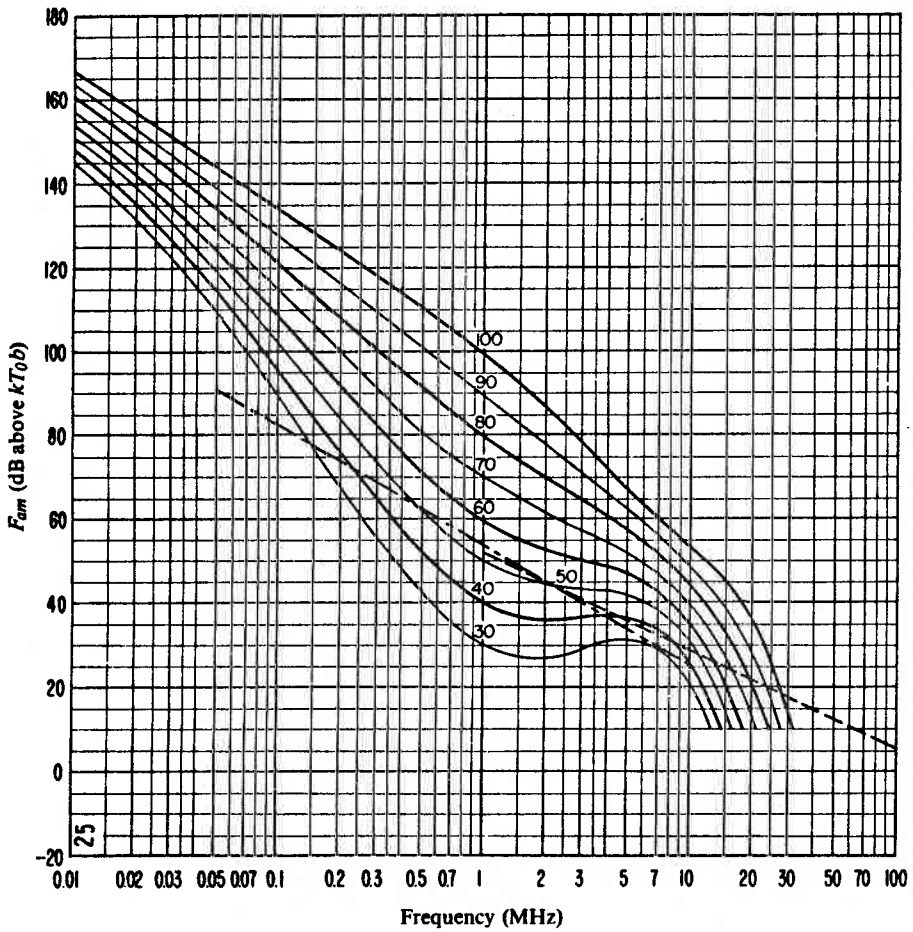

FIGURE 25b – *Variation of radio noise with frequency*
(Autumn; 2000-2400 h)

——— Expected values of atmospheric noise

— · — · — · — Expected values of man-made noise at a quiet receiving location

— — — — — Expected values of galactic noise

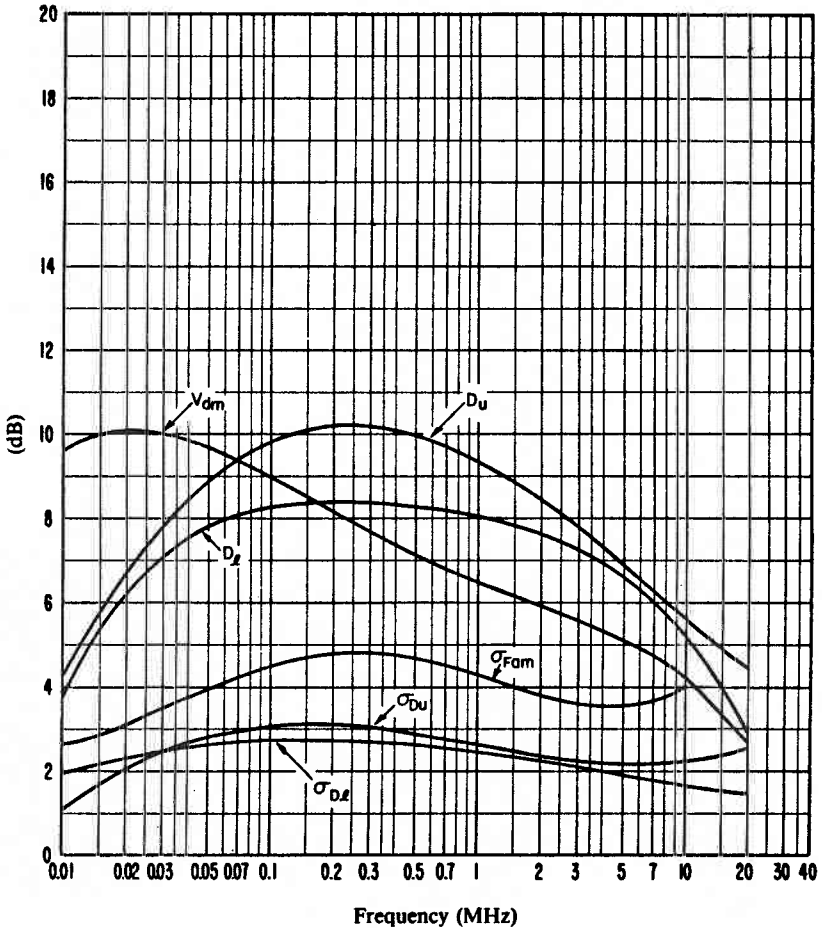

FIGURE 25c – *Data on noise variability and character*
(Autumn; 2000-2400 h)

σ_{Fam} : Standard deviation of values of F_{am}
D_u : Ratio of upper decile to median value, F_{am}
σ_{Du} : Standard deviation of values of D_u
D_l : Ratio of median value, F_{am}, to lower decile
σ_{Dl} : Standard deviation of value of D_l
V_{dm} : Expected value of median deviation of average voltage. The values shown are for a bandwidth of 200 Hz.

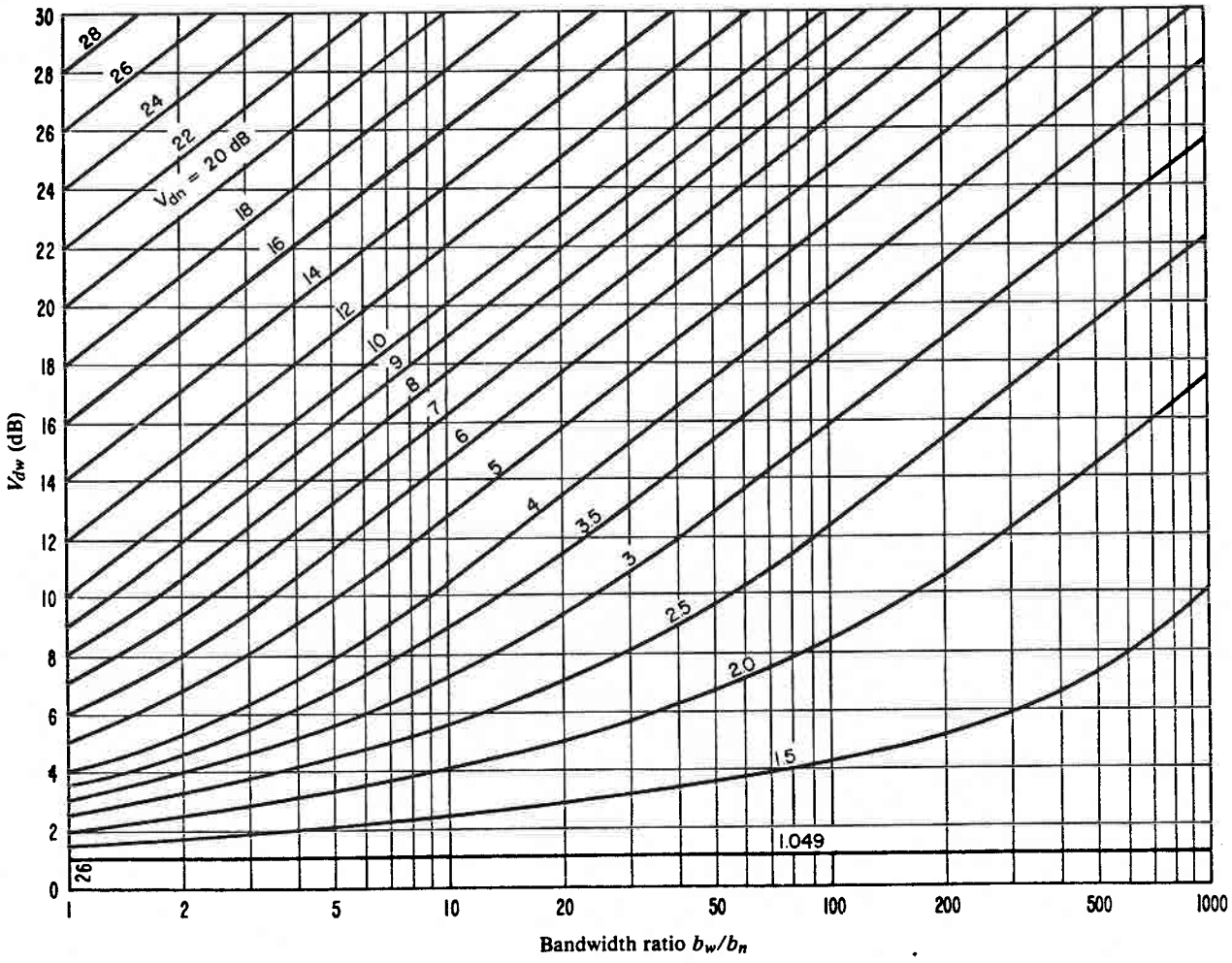

FIGURE 26 – *Conversion of V_d in one bandwidth to V_d in another bandwidth*

b_w : wider bandwidth
b_n : narrower bandwidth

Corresponding values of V_{dw} and V_{dn} are read along the appropriate line for the bandwidth ratio

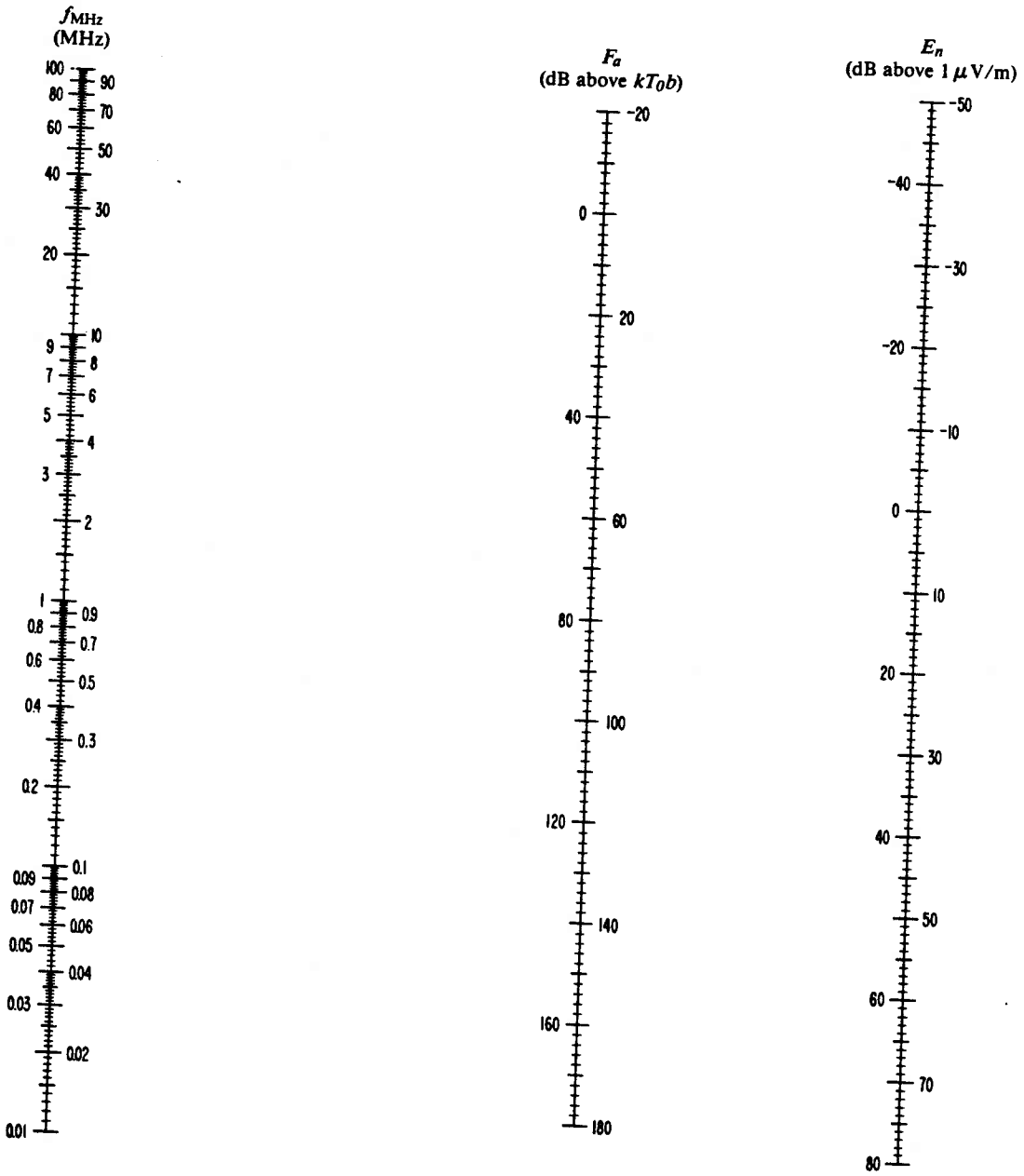

FIGURE 29 – *Nomogram for transforming effective antenna noise factor to noise field-strength as a function of frequency*

$$E_n = F_a + 20 \log_{10} f_{MHz} - 65.5$$

(E_n, F_a and f_{MHz} are defined in the list of symbols)

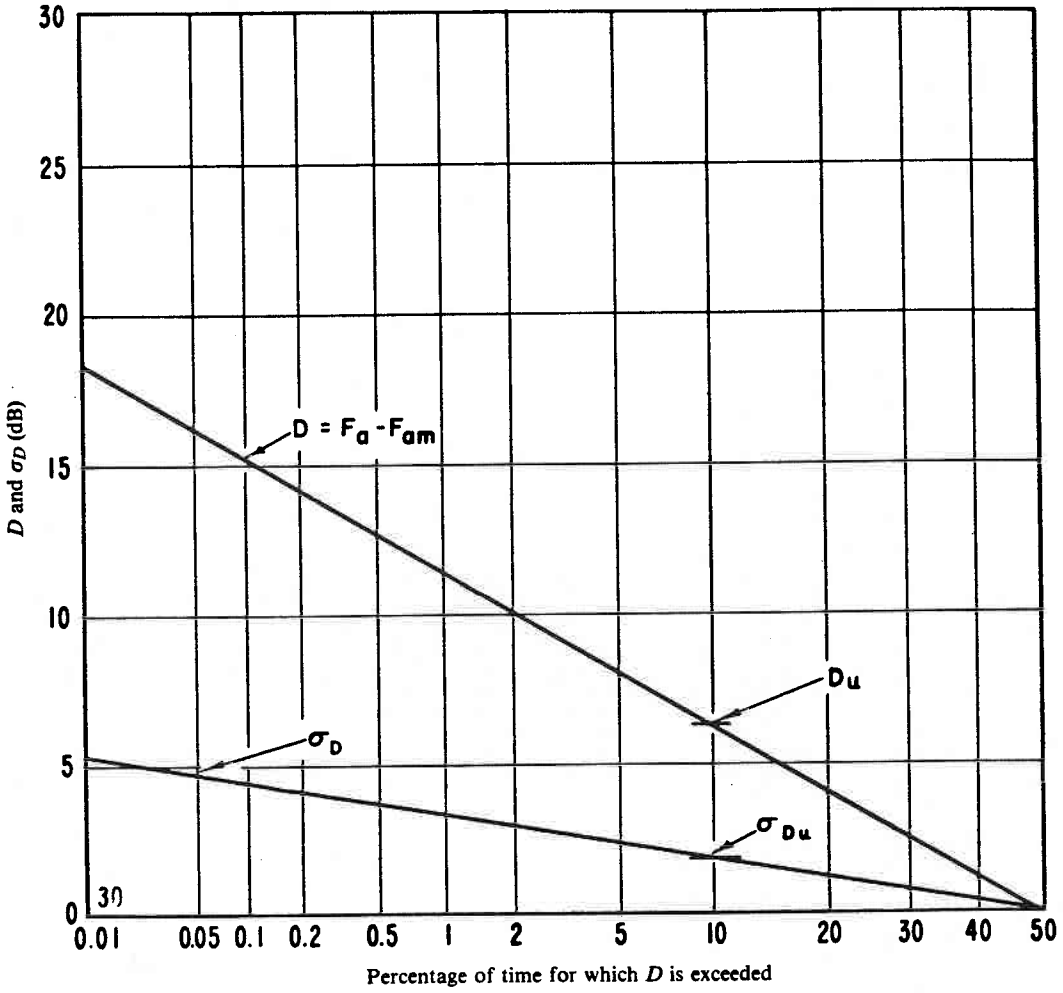

FIGURE 30 – *Expected values of D and their standard deviations* σ_D

Summer season; 2000-2400 h
Frequency: 50 kHz

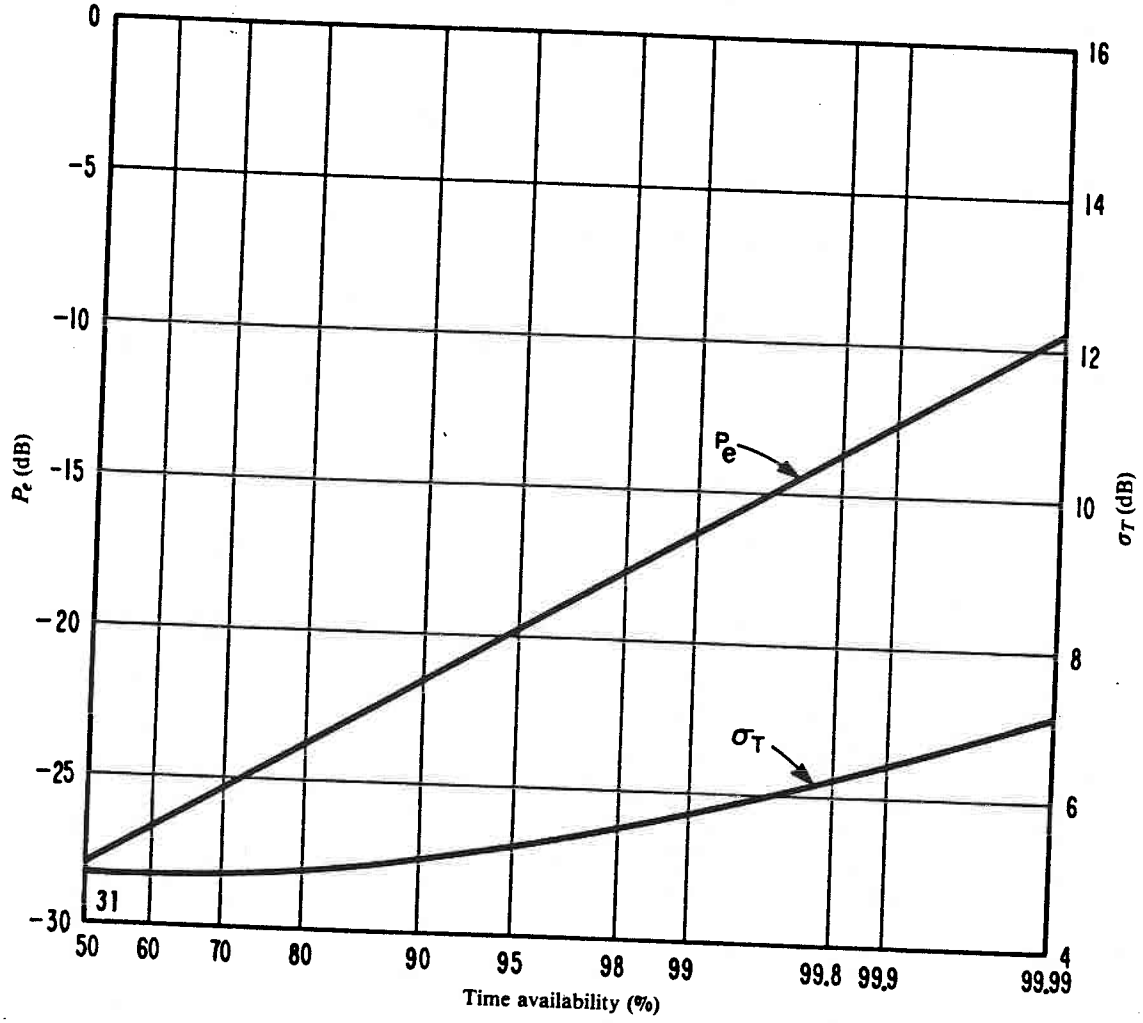

FIGURE 31 – *Expected values of P_e and their standard deviations σ_T*

Geneva, Switzerland
Summer season; 2000-2400 h
Frequency: 50 kHz
Bandwidth: 100 Hz
Binary errors: 0.05%
Type of service: FSK

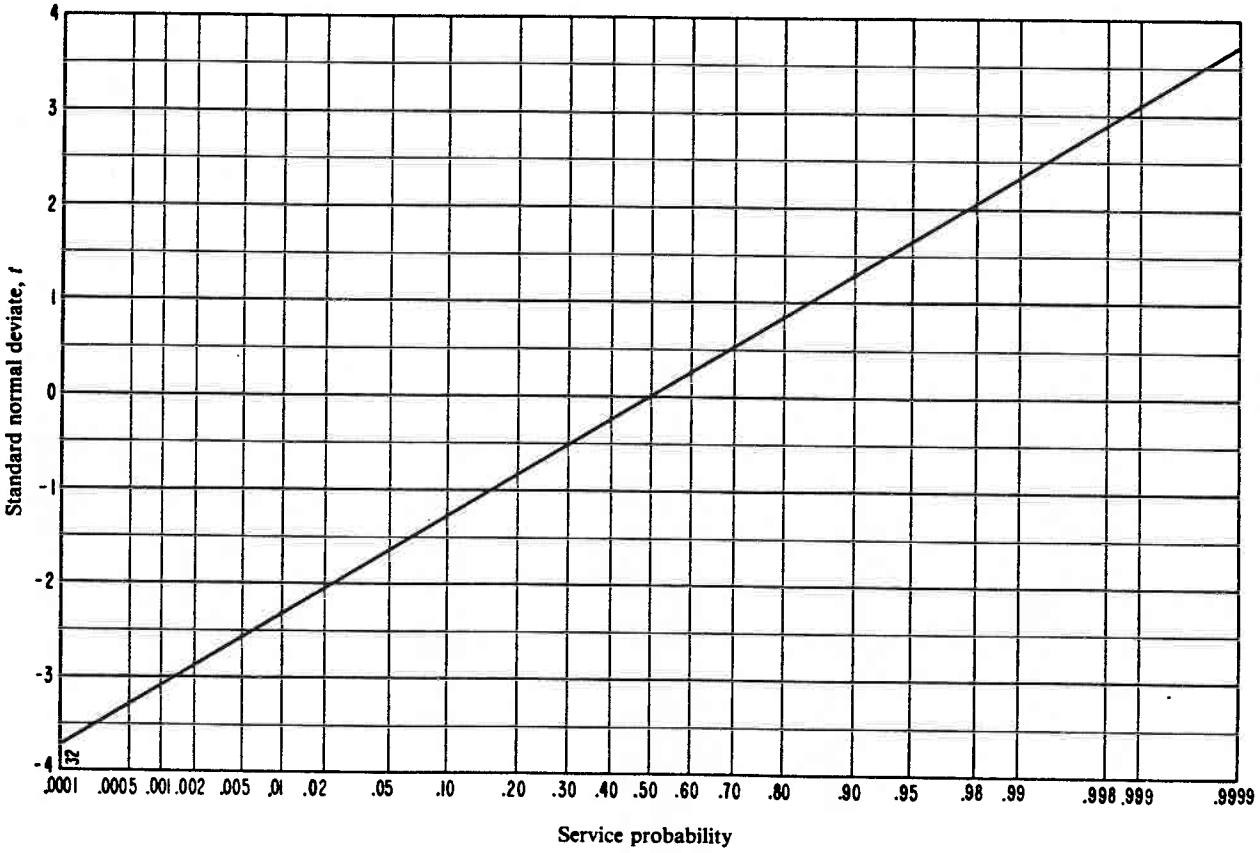

FIGURE 32 – *Service probability as a function of the standard normal deviate t*

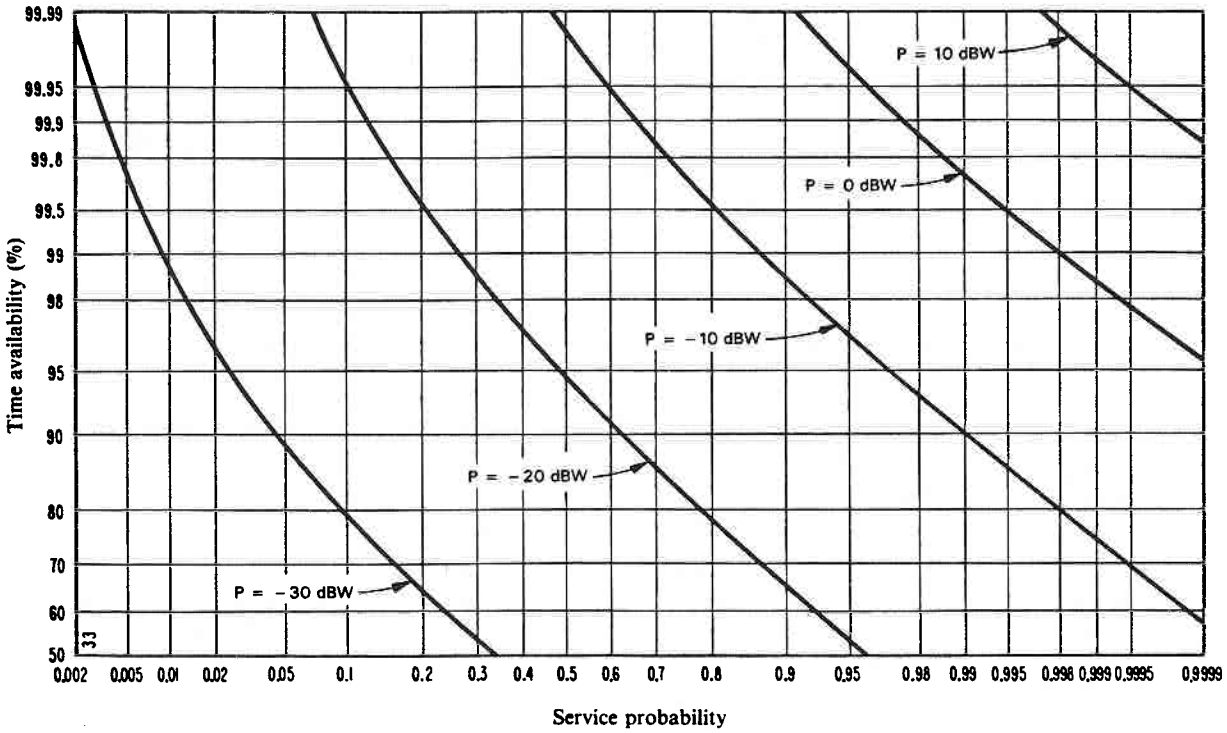

FIGURE 33 – *Time availability as a function of service probability*

Geneva, Switzerland
Summer season; 2000-2400 h
Frequency: 50 kHz
Bandwidth: 100 Hz
Binary errors: 0.05%
Type of service: FSK

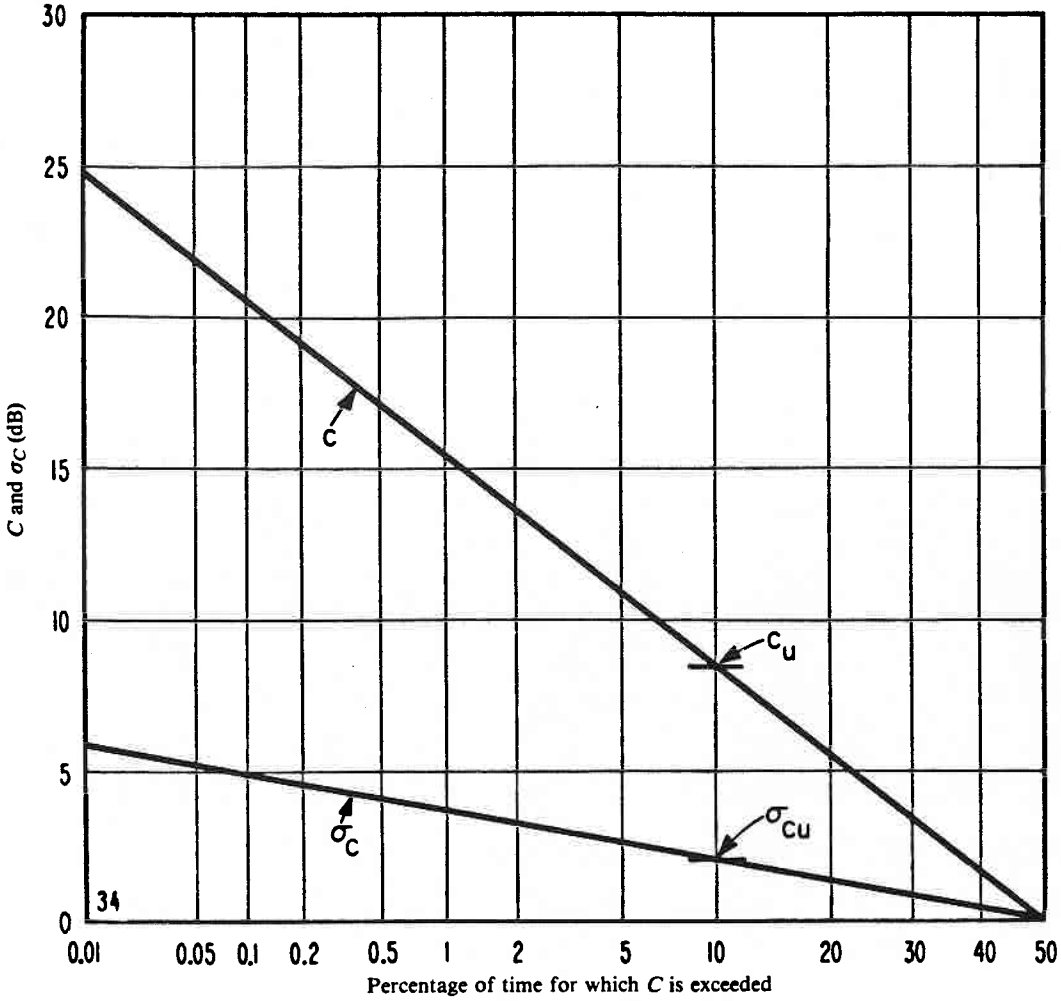

FIGURE 34 – *Expected values of C and their standard deviations* σ_C

Summer season; 2000-2400 h
Frequency: 5 MHz

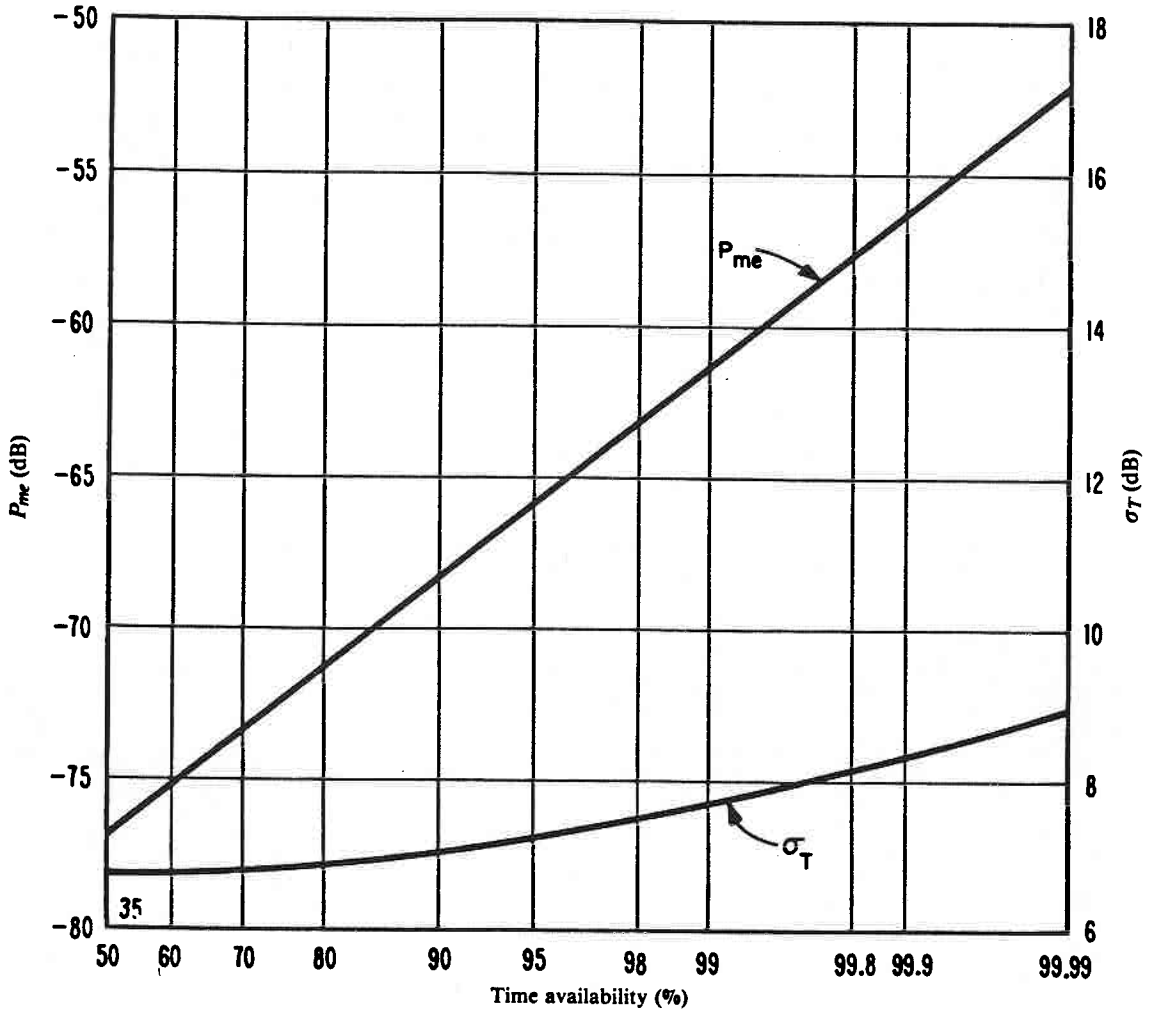

FIGURE 35 – *Expected values of P_{me} and their standard deviations σ_T*

Geneva, Switzerland
Summer season; 2000-2400 h
Frequency: 5 MHz
Bandwidth: 6 kHz
A3E JN telephony, marginally commercial service

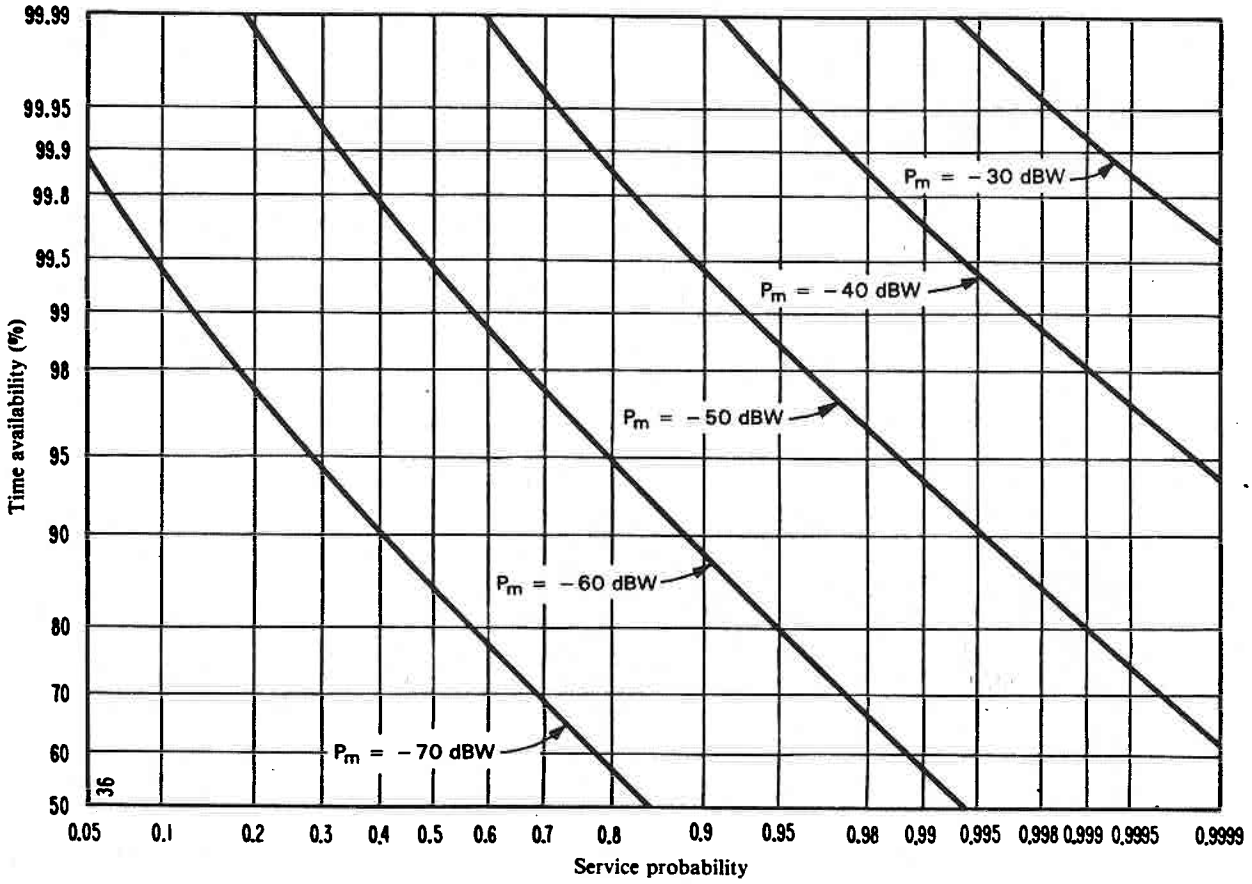

FIGURE 36 – *Time availability as a function of service probability*

Geneva, Switzerland
Summer season; 2000-2400 h
Frequency: 5 MHz
Bandwidth: 6 kHz
A3E JN telephony, marginally commercial service

REFERENCES

AUSTIN, L. W. [1932] Solar activity and radiotelegraphy. *Proc. IRE*, Vol. 20, 280.

BARSIS, A. P., NORTON, K. A., RICE, P. L. and ELDER, P. H. [1961] Performance predictions for single tropospheric communication links and for several links in tandem. NBS Tech. Note 102.

CLARKE, C. [1962] Atmospheric radio noise studies based on amplitude probability measurements at Slough, England, during the International Geophysical Year. *Proc. IEE*, Vol. 109B, 393.

COTTONY, H. V. and JOHLER, J. R. [1952] Cosmic radio noise intensities in the VHF band. *Proc. IRE*, Vol. 40, 1053.

CRICHLOW, W. Q., SMITH, D. F., MORTON, R. N. and CORLISS, W. R. [1955] World-wide radio noise levels expected in the frequency band 10 kc/s to 100 Mc/s. NBS Circular 557.

CRICHLOW, W. Q., DISNEY, R. T. and JENKINS, M. A. [1959-1962] Quarterly radio noise data. NBS Tech. Note Nos. 18 to 18-13.

CRICHLOW, W. Q., ROUBIQUE, C. J., SPAULDING, A. D. and BEERY, W. M. [1960a] Determination of the amplitude-probability distribution of atmospheric radio noise from statistical moments. *NBS J. Res.*, Vol. 64D, 49.

CRICHLOW, W. Q., SPAULDING, A. D., ROUBIQUE, C. J. and DISNEY, R. T. [1960b] Amplitude-probability distributions for atmospheric radio noise. NBS Monograph 23.

HAGN, G. H. [1981] Man-made electromagnetic noise. *Handbook of Atmospherics*, Chapter 7. Ed. H. Volland, CRC Press, Boca Raton, FL, USA.

KRONJÄGER, W. and VOGT, K. [1959] Über das Aussengeräusch kommerzieller Antennenanlagen (On the external noise of commercial antenna installations). *NTZ*, 12, 371.

LICHTER, Ya. I. and TERINA, G. J. [1960] Some results of the investigations of atmospheric radio noise at Moscow. *Some Ionospheric Results Obtained During the IGY*. Ed. Beynon, Elsevier, London, UK.

LUCAS, D. L. and HARPER, J. D. [1965] A numerical representation of CCIR Report 322: high frequency (3-30 Mc/s) atmospheric radio noise data. NBS Tech. Note 318, US Dept. of Commerce, Washington DC.

MONTGOMERY, G. F. [1954] A comparison of amplitude and angle modulation for narrow-band communication of binary-coded messages in fluctuation noise. *Proc. IRE*, Vol. 42, 447.

SCIENCE COUNCIL OF JAPAN [1960] Compilation of data in Japan for atmospheric radio noise during the IGY, 1957/58. Japanese National Committee for IGY.

SPAULDING, A. D. [1981] Atmospheric radio noise and its effects on telecommunication systems. *Handbook of Atmospherics*, Chapter 6. Ed. H. Volland, CRC Press, Boca Raton, FL, USA.

SPAULDING, A. D., ROUBIQUE, C. J. and CRICHLOW, W. Q. [1962] Conversion of the amplitude-probability distribution function for atmospheric radio noise from one bandwidth to another. *NBS J. Res.*, Vol. 66D, 713.

URSI [1962] The measurement of characteristics of terrestrial radio noise. Special Report No. 7. Elsevier, London, UK.

URSI [1981] *Review of Radio Science 1978-1980*, EM noise and interference, E1-E13. International Union of Radio Science, Brussels, Belgium.

WATT, A. D., COON, R. M., MAXWELL, E. L. and PLUSH, R. W. [1958] Performance of some radio systems in the presence of thermal and atmospheric noise. *Proc. IRE*, Vol. 46, 1914.

ZACHARISEN, D. H. and JONES, W. B. [1970] World maps of atmospheric radio noise in universal time by numerical mapping. Telecommunications Research Report OT/ITS/TRR2, US Dept. of Commerce, Washington DC.